ORNL/TM-2009/163
SNS107000000-TR0007-R01

Report from SNS Second Target Station Instrumentation Workshop, Feb. 20–22, 2007

2nd Target Station

NEUTRON SCIENCES

SNS

HFIR

June 2009

This report was prepared as an account of work sponsored by an agency of the United States government. Neither the United States government nor any agency thereof, nor any of their employees, makes any warranty, express or implied, or assumes any legal liability or responsibility for the accuracy, completeness, or usefulness of any information, apparatus, product, or process disclosed, or represents that its use would not infringe privately owned rights. Reference herein to any specific commercial product, process, or service by trade name, trademark, manufacturer, or otherwise, does not necessarily constitute or imply its endorsement, recommendation, or favoring by the United States government or any agency thereof. The views and opinions of authors expressed herein do not necessarily state or reflect those of the United States government or any agency thereof.

ORNL/TM-2009/163
SNS107000000-TR0007-R01

SNS Second Target Station Instrumentation Workshop
Feb. 20–22, 2007

Report

R. K. Crawford, G. S. Smith, J. F. Ankner, B. C. Chakoumakos,
J. Hodges, G. Ehlers, G. E. Granroth, L. Robertson, G. L. Greene

Rev. 01 June 2009

Prepared by
OAK RIDGE NATIONAL LABORATORY
P.O. Box 2008
Oak Ridge, Tennessee 37831-6285
managed by
UT-Battelle, LLC
for the
U.S. DEPARTMENT OF ENERGY
under contract DE-AC05-00OR22725

CONTENTS

Figures vii
Tables ix
Acronyms, Abbreviations, and Initialisms xi
Preface xiii

1.0 Executive Summary 1
1.1 Background and Workshop Goals 1
1.2 Workshop Outcomes 1

2.0 Overview 5
2.1 Background 5
2.2 Plenary Presentations 6
2.2.1 Overview and highlights of August 2006 scoping workshop 6
2.2.2 Accelerator systems for STS 6
2.2.3 Summary of December 2006 neutronics workshop 6
2.2.4 Neutronics model and performance for STS 7
2.2.5 Basis assumptions for instrumentation working groups 7
2.3 Instrumentation Workshop Goals 7
2.4 Workshop Results 8
2.4.1 Instruments considered 8
2.4.2 Candidate instruments for reference instrument suite 17
2.4.3 Science 24
2.4.4 Research and development needs 28
2.5 References 30
2.6 Other Useful Resources 30

3.0 Small-Angle Neutron Scattering 31
3.1 General Discussion 31
3.1.1 Instruments and length scales 31
3.1.2 Science 31
3.1.3 Source characteristics 32
3.1.4 Figure of merit for SANS 32
3.2 Straw Man Designs 34
3.2.1 High-resolution small-angle neutron diffractometer 34
3.2.2 High-throughput SANS 35
3.2.3 High-resolution SANS 35
3.2.4 USANS 36
3.2.5 SESANS 36
3.3 Developmental Work 37
3.3.1 Optics 37
3.3.2 Other 38
3.4 Conclusions 38
3.5 References 39

4.0 Reflectometry 40
4.1 Scientific Justification 40
4.2 Reflectometer Performance at STS 41
4.3 Commonalities 41
4.4 Instrument Concepts 44
4.4.1 SERGIS 44
4.4.2 GISANS and GID 45
4.4.3 Inelastic reflectometer 45
4.4.4 Generalized polarization-analysis reflectometer 45
4.4.5 Special-environment, small-sample, or kinetics reflectometer 46
4.5 References 46

5.0 Single Crystal Diffraction 47
5.1 Scientific Case 47
5.2 Instruments 48
5.2.1 HiMaNDi (high-throughput MaNDi instrument) 48
5.2.2 Polarized sample diffractometer (polarized proteins) 50
5.2.3 High-resolution, high-intensity, polarized small-molecule diffractometer 51
5.2.4 Diffuse scattering diffractometer 52
5.2.5 "Neutron microscope" for topography, magnetic domains, texture, and depth profiling 53
5.2.6 Quasi-Laue single-crystal diffractometer 55
5.3 References 57

6.0 Powder Diffraction 58
6.1 Overview 58
6.1.1 General 58
6.1.2 Desired capabilities 58
6.1.3 Proposed instruments 59
6.2 Comparative Performance of Several Proposed Materials Diffractometers 60
6.2.1 Basis for comparison 60
6.2.2 Very fast powder diffractometers (three instruments: small sampling volume, very high magnetic field, very high pressure) 61
6.2.3 Very-high-resolution powder diffractometers 62
6.2.4 Long-range pair distribution function diffractometer 63
6.2.5 SWANS—Simultaneous wide- and small-angle neutron scattering 64
6.3 Preliminary Conclusions 65
6.4 Preliminary Instruments 66
6.5 R&D Needs 66
6.6 References 66

7.0 Inelastic Scattering Using Neutron Spin Precession Techniques 67
7.1 Scientific Case 67
7.2 Instrumental Details 68
7.3 Conclusions: High Level Findings 70

7.4 Proposed Beam Lines 71
7.5 Anticipated Performance 71
7.6 References 73

8.0 "Conventional" Spectrometry 74
8.1 Scientific Case 74
8.2 General Comments 75
8.3 Backscattering Spectrometers 75
8.3.1 Fine-resolution backscattering spectrometer 75
8.3.2 Ultra-fine-resolution backscattering spectrometer 76
8.4 Chopper Spectrometers 76
8.4.1 High-resolution cold chopper spectrometer 76
8.4.2 High-intensity chopper spectrometer 78
8.4.3 Extreme sample environment spectrometer 79
8.5 Crystal Monochromator Instrument 79
8.6 Needed Technical Development 80
8.7 References 81

9.0 Imaging, Tomography, Microprobes, Microscopy, and Special Topics 82
9.1 Specific Instruments 82
9.1.1 Neutron imaging beam line 82
9.1.2 Three-dimensional imaging of large objects 82
9.1.3 Research and development beam line 83
9.1.4 Microprobe instrument 83
9.1.5 Holography instrument 83

10.0 Fundamental Neutron Physics 85
10.1 Introduction 85
10.2 Science Program at the Fundamental Neutron Physics Beamline 86
10.3 Opportunities at STS 86
10.4 Summary 87
10.5 References 87

Appendix—Workshop Participants 88

FIGURES

Figure **Page**

3.1 The resolution $\delta\lambda/\lambda$ of a SANS instrument as a function of instrument length and wavelength 32
3.2 Bandwidth versus the moderator-to-detector distance....35

4.1 Modeled and measured vertical divergence distributions of the SNS liquids reflectometer 43
4.2 Isometric design drawing and installation picture of the SNS liquids reflectometer guide system....43
4.3 Sample stages and optical tables for SNS vertical-sample magnetism reflectometer and horizontal-sample liquids reflectometer....44

5.1 Estimated experiment duration as a function of protein cell unit size for the MaNDi instrument 48
5.2 Neutron diffraction topography—schematic 54
5.3 Turnkey quasi-Laue instrument—schematic 56

6.1 Long-range pair distribution functions—Au nanoparticles 64
6.2 Long-range pair distribution functions—domains in $LiNiO_2$ 65

7.1 Range covered in a TOF NSE spectrometer 692
7.2 Ranges in the spatial and temporal variables covered by the three proposed instruments 72

8.1 Timing diagram showing possible RRM scheme for a cold neutron chopper spectrometer with E_i = 2, 1.36, and 0.94 meV 77
8.2 Timing diagram showing possible RRM scheme for a cold neutron chopper spectrometer with E_i = 10, 6.6, 4.4, 2.9, and 1.9 meV 78

TABLES

Table		Page
2.1	Instruments considered.	9
2.2	Candidate instruments for reference instrument suite	17
3.1	SANS-based instruments ordered by length scales	31
3.2	Science with SANS instruments	33
3.3	Performance characteristics and gains for a high-throughput SANS instrument	35
3.4	Performance characteristics and gains for a high-resolution SANS instrument	36
5.1	Performance of HiMaNDi	49
6.1	Performance of a very fast powder diffractometer	62
6.2	Performance of a very-high-resolution diffractometer	63

ACRONYMS, ABBREVIATIONS, and INITIALISMS

ANL	Argonne National Laboratory
BL	beam line
CMR	colossal magnetoresistance
CNCS	Cold Neutron Chopper Spectrometer (instrument at FTS)
CORELLI	diffuse scattering spectrometer at FTS
EDM	Electric dipole moment (of the neutron)
EIGER/CAMERA	Enhanced Intensity and Greater Energy Range / Continuous Angle Multiple Energy Readout Analysis (instrument at PSI)
EQSANS	Extended-Q Small Angle Neutron Scattering (instrument at FTS)
ESS	European Spallation Source
FNP	fundamental neutron physics
FNPB	Fundamental Neutron Physics Beamline (beam line at FTS)
FOM	figure of merit
FTS	SNS First Target Station
FZ Jülich	Forschungszentrum Jülich (research center in Germany)
GID	grazing incidence diffraction
GISANS	grazing incidence small-angle neutron scattering
GMR	giant magnetoresistance
GUI	graphical user interface
HFIR	High Flux Isotope Reactor (at ORNL)
HiMaNDi	High-throughput Macromolecular Neutron Diffractometer
HIPPO	High-Pressure Preferred-Orientation (instrument at LANL)
HiQSCD	High-Q Single Crystal Diffractometer
HMI	Hahn-Meitner Institute (reactor-based neutron scattering facility in Germany)
ILL	Institut Laue-Langevin (reactor-based neutron scattering facility in France)
IMAGINE	quasi-Laue macromolecular neutron diffractometer
ISIS	pulsed spallation neutron source in Great Britain
ITU	Institute for Transuranium Elements (institute in Germany)
J-PARC	spallation neutron source facility being built in Japan
K-B	Kirkpatrick-Baez
LADI III	quasi-Laue macromolecular neutron diffractometer at ILL
LANL	Los Alamos National Laboratory
LANSCE	Los Alamos Neutron Science Center (at LANL)
MACS	Multi-Axis Crystal Spectrometer (instrument at NIST)
MaNDi	Macromolecular Neutron Diffractometer (instrument at FTS)
MBE	molecular beam epitaxy
MC	Monte Carlo techniques
MIEZE	modulation of intensity by zero effort
MISANS	modulated-intensity small-angle neutron scattering
MIT	Massachusetts Institute of Technology
MOKE	magneto-optic Kerr effect
NCNR	NIST Center for Neutron Research

NIST	National Institute of Standards and Technology
NMI3	Integrated Infrastructure Initiative for Neutron Scattering and Muon Spectroscopy (European initiative)
NMR	nuclear magnetic resonance
NOMAD	Nanoscale Ordered Materials Diffractometer (instrument at FTS)
NPDF	Neutron Powder Diffractometer (instrument at LANL)
NSE	Neutron Spin-Echo
NSF	National Science Foundation
NSLS	National Synchrotron Light Source
ORNL	Oak Ridge National Laboratory
PCS	Protein Crystallography Station (instrument at LANL)
POWGEN3	high-resolution powder diffractometer at FTS
PR	precession regions
PSI	Paul Scherrer Institute (continuous spallation neutron source in Switzerland)
PUP	Power Upgrade Project (at SNS)
R&D	research and development
RAL	Rutherford-Appleton Laboratory
RITA	Re-Invented Triple-Axis spectrometer (RITA II is at PSI)
RRM	repetition-rate multiplication
SANS	small angle neutron scattering
SERGIS	spin-echo-resolved grazing incidence scattering
SESANS	spin-echo small angle neutron scattering
SMARTS	Spectrometer for Materials Research at Temperature and Stress (instrument at LANL)
SNAP	high-pressure diffractometer at FTS
SNS	Spallation Neutron Source (at ORNL)
SPINS	Spin-polarized triple-axis Spectrometer (instrument at NIST)
STS	SNS Second Target Station
SWANS	Simultaneous Wide-Angle Neutron Spectrometer
TAS	Triple-Axis Spectrometer
TISANE	time-resolved small angle neutron experiments
TOF	time-of-flight
TOPAZ	single-crystal neutron diffractometer at FTS
UCN	ultracold neutrons
USANS	Ultra Small Angle Neutron Scattering (instrument at FTS)
VCNS	Very Cold Neutron Source
VFD	Very Fast Powder Diffractometer
VHRD	Very High Resolution Powder Diffractometer
VULCAN	engineering diffractometer at FTS

PREFACE

This document provides the record of the SNS Second Target Station Instrumentation Workshop held at ORNL in February 2007. Much of it is in the form of reports from the various working group breakout sessions that comprised the bulk of the workshop, along with a section that roughly summarizes the results from the working groups. Therefore, this report should be viewed as a set of notes resulting from two days of work by the working groups, with some results remaining very sketchy because of the lack of time for further exploration at the workshop. Only minimal further refinements of these notes have been made for this report.

The workshop was very successful in meeting its goal of defining a number of neutron beam instruments that would be appropriate for the SNS Second Target Station and in evaluating the performance anticipated from these instruments. Part of the credit for this goes to the chairs of the working groups who guided the discussions and prepared the final reports. However, most of the credit goes to the workshop participants, who represented many different points of view and provided spirited discussions leading to many insights and some novel instrumentation ideas. The workshop could not have been a success without these efforts.

RKC—July 2007

SNS Second Target Station Instrumentation Workshop, Feb. 20–22, 2007

1.0 EXECUTIVE SUMMARY

1.1 Background and Workshop Goals

The Neutron Sciences Directorate at Oak Ridge National Laboratory (ORNL) is engaged in a process to define what new scientific capabilities could be made available if a second target station (STS) were built at the Spallation Neutron Source (SNS). A scoping workshop, held August 3–4, 2006 at the SNS, kicked off this planning effort to develop the SNS STS by defining some of the basic performance parameters for this target station. It was followed with a study to define the capabilities and options offered for STS by the SNS accelerator systems, and by a workshop December 14–15, 2006, to clarify the neutronic design of the STS target station. This STS instrumentation workshop, held February 20–22, 2007, at SNS, focused on instrumentation suitable for the source neutronic performance outlined at the first workshop and further developed in subsequent workshops and analyses. The ultimate goal of this series of workshops was to develop a preliminary facility concept with estimates of capabilities for the STS, including initial instrument concepts, by fall 2007.

The Instrumentation Workshop had ~70 attendees, representing a diverse range of expertise from the national and international neutron scattering communities. The goal specified for this instrumentation workshop was to suggest and evaluate a number of instruments (or other beam line uses) for STS. The important physical parameters should be specified for each instrument, and a rough estimate of performance and an indication of likely scientific potential should be provided. A further aim was to select from this set of instruments candidates to become part of the reference instrument suite for STS. Instruments so selected should have significant scientific potential and should require the unique source characteristics of the STS.

1.2 Workshop Outcomes

To set the stage for this workshop, there were presentations covering assessments of the level of performance expected from the SNS accelerator systems and from an optimized STS.

The SNS accelerator systems team presented an assessment of how the SNS accelerator systems could interface to both the first and second target stations, what would be needed to do so, and what performance could be expected for each of the stations. The SNS Power Upgrade Project (PUP) is expected to provide 2–3 MW of proton beam power. This could be split between the two target stations as desired, although the SNS first target station (FTS) cannot accommodate more than ~2 MW. The SNS accelerator systems currently are designed to use the accumulator ring to operate in a short-proton-pulse mode (proton pulse width < 1 μs). However, with relatively minor modifications, the systems could also send some of the pulses directly from the linac to the one of the target stations in a long-proton-pulse mode (proton pulse width ~1 ms or more). The SNS accelerator systems currently are designed to provide proton pulses at a 60 Hz repetition rate. Some of these pulses could be redirected to an STS in a “pulse stealing” mode. However, with additional modifications, these systems could operate at 120 Hz, in which

case the preferred operating mode would be to provide pulses at a steady 60 Hz rate to FTS while directing additional pulses to STS. With further additional modifications, the SNS accelerator systems should be able to deliver more than 3 MW, provided that some of it was in a long-proton-pulse mode. ***For the purposes of the present workshop, it was assumed that 1 MW would be delivered to STS at 20 Hz in either the short-proton-pulse or long-proton-pulse mode.***

A preliminary study presented by the SNS neutronics group for a simple model of the moderator and reflector geometry for STS showed gains in time-averaged cold neutron flux per incident proton of about a factor of 3 relative to the brightest cold moderators at the FTS. This same study showed that for an STS operating at 20 Hz, the peak flux per megawatt of proton power delivered in short proton pulses would exceed that at the brightest cold moderators at FTS by about a factor of 8. If the STS proton beam were delivered in 1 ms long pulses at 20 Hz instead, the peak flux per megawatt at STS would exceed that at FTS by a factor of 2.5 at 5 meV, ranging to factors of 4 or more for energies below 1 meV. The results of this preliminary neutronics study served as a guide to the instrumentation working groups in evaluating the performance of the instruments proposed.

For several categories of instruments, the performance was found to depend only on the time-averaged neutron production, since the neutron pulse width did not dominate the resolution even in the long-proton-pulse mode. These categories include the small-angle neutron scattering (SANS) instruments, the reflectometers (for most experiments), the instruments based on neutron spin-echo (NSE), a general-purpose imaging beam line, and the ultra-cold neutron beam line for fundamental neutron physics studies. These instruments would function equally well in either the short-proton-pulse or long-proton-pulse mode (at the same time-averaged power), with the same instrument designs being appropriate for either source mode. These comprise about half of the candidate instruments for STS.

For the remaining instruments, the performance was found to depend to a varying extent on the peak flux in the pulse, which is a factor of ~3 higher in the short-proton-pulse mode than in the long-proton-pulse (1 ms) mode at equal power. These instruments required a higher timing resolution than would be provided by the neutron pulses in the long-proton-pulse mode and, in some cases, needed even higher timing resolution than would be provided by the neutron pulses in the short-proton-pulse mode. Such instruments would need to shorten the neutron pulse by using neutron choppers (thus throwing away many of the neutrons produced by the source) if the source operated in the long-proton-pulse mode. Some of them might even have to use neutron choppers to shorten the neutron pulse in the short-proton-pulse mode, but the fraction of neutrons thus discarded would be smaller than if these instruments were operated in long-proton-pulse mode.

Instruments falling into this category include all of the diffraction instruments, high-resolution measurements on the reflectometers, the conventional inelastic scattering instruments (chopper spectrometers and crystal analyzer spectrometers), and imaging experiments using Bragg-edge contrast enhancement. Some of these instruments could take advantage of sophisticated data-rate-enhancement techniques such as repetition rate multiplication (RRM) or other neutron-chopper-based pulse-multiplexing techniques, so the real differential in performance between the short-proton-pulse and long-proton-pulse versions of the source will not be fully understood until detailed analyses are performed for optimized instrument configurations in both cases.

Based on these assessments, it is clear that if the total proton beam power delivered to STS were the same in both cases, and the target-moderator-reflector configuration were the same in both cases, then from a neutronic perspective the short-proton-pulse mode of delivery would always be preferred. However, it is likely that the proton beam power that ultimately can be delivered to STS by the SNS accelerator system will be significantly higher in the long-proton-pulse mode than in the short-proton-pulse mode. Furthermore, it is likely that the engineering constraints on the target-moderator-reflector system could be relaxed to permit the system to be optimized to provide more neutrons per proton in the long-proton-pulse mode. Target lifetime and reliability are also likely to be higher in the long-proton-pulse mode. All of these possibilities require further quantitative evaluation, but they argue strongly for further consideration of the long-proton-pulse mode.

Some of the instruments evaluated require or would benefit from shorter-wavelength neutrons in addition to the long-wavelength neutrons for which the STS model was optimized. In some other cases, the instrument performance would be significantly enhanced if even longer wavelengths could be provided (i.e., neutronically "colder" source configuration). ***Both possibilities should be investigated as part of the further optimization of the design of the STS target-moderator-reflector configuration.***

The workshop demonstrated that for a large number of the instruments considered, the gains at STS could be significant (at least a factor of 3) relative to comparably optimized instruments at FTS. For some of these instruments, these gains could be an order of magnitude or more. These rough estimates were based on the assumption that 1 MW of proton beam power would be delivered to STS at 20 Hz, and on the neutronic production calculated for the preliminary model described at the workshop. Even higher gains might be realized with further optimization of the target-moderator-reflector configuration and/or with more beam power on target. ***For many of these instruments, the gains from the time structure of the pulsed source relative to a steady-state source are quite large (1–2 orders of magnitude), and the performance of those instruments at either FTS or STS will be much better than that of comparably optimized instruments at any steady state source. Even for instruments for which these time-structure gains are more modest, the performance of most of the instruments considered here for the 1 MW STS is comparable to or better than what could be achieved with instruments optimized for the same science at a high-flux reactor such as the High Flux Isotope Reactor (HFIR) or Institut Laue-Langevin (ILL)***.

Although the focus of this workshop was on understanding the performance gains and new capabilities that could be achieved at STS rather than specifically on science, the performance gains found would clearly translate into new scientific capabilities. Innovative designs for some of the instruments proposed would enable measurement of dynamic phenomena at lower energies than before and would extend high-resolution dynamic measurements to larger length scales, enabling, for example, studies of excitations on surfaces or in membranes. Furthermore, the higher data rates that would be available for all of the STS instruments would enable kinetic studies that would otherwise be impossible, would enable structural or even dynamic studies of many advanced materials or biological materials for which only very small amounts of sample are available, and would enable parametric exploration of material behavior under wide ranges of sample conditions, including a number of different types of extreme environments. ***The workshop showed that an STS optimized for cold neutrons at SNS should indeed be very***

welcome to the scientific community and would enable many new and exciting scientific opportunities.

2.0 OVERVIEW

2.1 Background

The Neutron Sciences Directorate at ORNL is engaged in a process of defining what new scientific capabilities could be made available if an STS were built at SNS. A scoping workshop to kick off the planning effort to develop the SNS STS was held August 3–4, 2006, at the SNS. The goal was to define some of the basic performance parameters for this target station. The workshop was followed with a study to define the capabilities and options offered for STS by the SNS accelerator systems, and by a workshop December 14–15, 2006, to clarify the neutronic design of the STS target station.

This STS instrumentation workshop, held February 20–22, 2007, at SNS,, focused on instrumentation suitable for the source neutronic performance outlined at the first workshop and further developed in subsequent workshops and analyses. There were ~70 attendees at this workshop, representing a diverse range of expertise from the national and international neutron scattering communities.

The first morning of this workshop was taken up with plenary presentations aimed at setting the stage for the breakout sessions that made up the remainder of the workshop. Section 2.2 of this report summarizes these plenary sessions.

The remainder of the workshop was organized into parallel breakout sessions with working groups in the following areas:

- Small-Angle Scattering (SANS; including USANS, SESANS, TISANE)
- Reflectometry (including GISANS and SERGIS)
- Single Crystal Diffraction (including membranes and protein crystallography)
- Powder Diffraction (including total scattering, large-d diffraction, engineering and materials applications)
- Inelastic scattering using neutron spin precession techniques (including "standard" NSE, MIEZE, inelastic SANS, inelastic reflectometry)
- "Conventional" direct and indirect geometry inelastic scattering
- Imaging (radiography, tomography, microscopy, other) and microprobes
- Fundamental Neutron Physics

Section 2.4 summarizes the results from the working group discussions; detailed reports from these working groups are in Chapters 3 through 10.

2.2 Plenary Presentations

2.2.1 Overview and highlights of August 2006 scoping workshop

Kent Crawford (ORNL) summarized the reasons for beginning STS planning at this time and summarized the outcomes from the STS scoping workshop that kicked off this process in August 2006. That workshop resulted in the strong support for the following recommendations:

- STS should focus on achieving the highest practical usable flux of cold neutrons by making all the moderators cold coupled moderators.
- STS should operate at no more than 20 Hz.
- Either short proton pulses or long proton pulses can be used for STS and both should be considered.
- A Very Cold Neutron Source (VCNS) moderator could be considered for one, but not all, of the moderators on STS.
- STS must be able to achieve highly reliable (90%) operation in order to be useful as a user-based facility.

Reference [1] gives the full report from this workshop.

2.2.2 Accelerator systems for STS

John Galambos (ORNL), the SNS Accelerator Physics Group Leader, presented the results of a study carried out by the SNS accelerator teams during the fall of 2006 to define how the SNS accelerator systems could interface to both the first and second target stations. This study included what accelerator modifications would be needed to do this and what performance could be expected for each of the stations. Some of the highlights of that presentation were as follows:

- The SNS PUP is expected to provide up to ~3 MW of power. This could be split between the two target stations as desired.
- The SNS accelerator systems are currently designed to use the accumulator ring to operate in a short-proton-pulse mode (proton pulse width < 1 μs). However, with relatively minor modifications, the systems could also provide some of the pulses in a long-proton-pulse mode, delivering beam directly from the linac to one of the target stations (proton pulse width pulse ~1 ms).
- The SNS accelerator systems are currently designed to provide proton pulses at a 60 Hz repetition rate. Some of these pulses could be redirected to an STS in a "pulse stealing" mode.
- With additional modifications, the SNS accelerator systems could operate at 120 Hz, in which case they could continue to provide pulses at a steady 60 Hz rate to FTS while directing additional pulses to STS.
- With further additional modifications the SNS accelerator systems should be able to deliver more than 3 MW, provided that some of it is in a long-proton-pulse mode.

The full study is available as a report [2].

2.2.3 Summary of December 2006 neutronics workshop

Günter Bauer (FZ Jülich) summarized the STS neutronics workshop held in December 2006. This workshop took as a starting point the results of the STS scoping workshop and the anticipated accelerator characteristics (see Sect. 2.2.2). The outcomes from the neutronics workshop can be summarized as follows:

- We should focus on a coupled target-moderator-reflector system.

- We should plan on a 1 MW system with a capability to upgrade to ~3 MW (so bulk shield, nonupgradeable utilities, etc., must be planned for 3 MW).
- The short-proton-pulse versus long-proton-pulse issue is still open. There are advantages to running a coupled moderator system in short-pulse mode at 1 MW of beam power.
- Short-proton-pulse injection into a coupled system gives better overall performance at a constant number of protons per pulse.
- A 3 MW STS system might require long-proton-pulse operation because of limitations of the proton storage ring or of the target.

2.2.4 Neutronics model and performance for STS

Following the neutronics workshop the SNS neutronics group carried out performance calculations and optimizations for the target-moderator-reflector geometry recommended in the neutronics workshop. Franz Gallmeier (ORNL) presented the results of these calculations.

This model was a large fully-coupled parahydrogen moderator in wing geometry above the target and was viewed by multiple beam lines (possibly as many as 18 for one moderator). This model allows a similar moderator to be located below the target so the number of beam lines could possibly be increased to as many as 36. The calculated performance from this system was quite good, with time-averaged neutron intensities per proton about three times the corresponding quantities for the SNS FTS coupled parahydrogen moderators, and with even greater gains for peak intensities.

A draft report [3] provides greater detail concerning these calculations.

2.2.5 Basis assumptions for instrumentation working groups

Based on all this preparatory work, the instrumentation working groups were asked to use the following assumptions as the basis for their instrument designs and evaluations:

- Assume 2 MW to FTS and 1 MW to STS.
- Assume STS operates at 20 Hz, FTS at 60 Hz.
- Assume the coupled cryogenic parahydrogen moderator geometry and performance curves presented by the neutronics group (Sect. 2.2.4).
- Consider both short-proton-pulse and long-proton-pulse operation and look at which gives best performance for instrument.
- Bear in mind that options for further power upgrades almost certainly will require long-proton-pulse operation.

2.3 Instrumentation Workshop Goals

It is important to remember that the ultimate goal of this series of workshops is to develop a preliminary facility concept with estimates of capabilities for the STS, including initial instrument concepts, by fall 2007. The goal specified for this instrumentation workshop was to generate a straw man list of 20 or so instruments (or other beam line uses) for STS. This straw man list should include only instruments that have significant scientific potential and make use

of the unique source characteristics of this target station. For each instrument this list should define important instrument parameters (e.g., moderator needed, primary and secondary path lengths, rough instrument geometry, any other relevant instrument parameters such as specific instrument components) and provide a rough estimate of performance (e.g., flux on sample, data rate, resolution, range, from scaling or other means) and an indication of likely scientific potential. The estimated performance at STS may not be very good for some of the instruments considered, in which case the reasons this instrument should not be on STS should be documented.

2.4 Workshop Results

2.4.1 Instruments considered

Each working group produced a report discussing the instruments it considered, including instrument-specific information and any other supporting information. These individual working group reports are contained in Sects. 3 through 10 of this report. Table 2.1 summarizes the full range of instruments considered by the working groups.

The working groups considered 41 instruments, as indicated in Table 2.1. Many of these were evaluated in some detail, others were evaluated in much less detail, and some were left for future evaluation as a result of the time constraints of the workshop. In most cases the general scientific areas for which the specified instrument is intended were indicated, and for many of the instruments the desired performance parameters (Q, E range, resolution) were also indicated. For most of these instruments, there was also some indication of the desired source characteristics or "instrument figure-of-merit" (FOM); and in some cases, the instrument was felt to be better suited to FTS or to HFIR at ORNL than to STS. Table 2.1 summarizes all of this information.

It is important to bear in mind that the working group reports are the summary notes resulting from ~2 days of breakout sessions at the workshop. Little effort was made to further refine these notes for this workshop report.

Table 2.1. Instruments considered

Ref.	Instrument Description	Science Examples	FOM	L_1 (m)	L_2 (m)	λ_{min} (Å)	λ_{max} (Å)	Q-range ($Å^{-1}$)	E-range (meV)	Q-resol	E-resol	Perform.*	Notes
SANS													
3.2.1	High-resolution small-angle neutron diffractometer	High-resolution structure of membranes, low-resolution structure of membrane proteins, thin polymer composite films and 2D devices for biosensors and biotechnology	$\Phi_{TA}(\lambda)\Delta\lambda$	65	~5	2	6	0.01 - 5	—	0.015 – 0.02 $Å^{-1}$ $\delta\lambda/\lambda$ < 1%	—	2.5×FTS	
3.2.2	High-throughput SANS	Workhorse instrument for chemistry, biology, complex fluids, metallurgy, vortex lattice in superconductors	$\Phi_{TA}(\lambda)\Delta\lambda$	20	1.5–12	2	15	0.001 - 1.4	—	$\delta\lambda/\lambda$ < 5%	—	1.5-4.5 ×HFIR 9×FTS	
3.2.3a	High-resolution SANS—optical	Ordering in colloids, 2-dim structure in aligned polymers, strained materials, polymer crystallization, polyelectrolyte structures, viruses, pharmaceuticals	$\Phi_{TA}(\lambda)\Delta\lambda$	26	6–18	3	20	$3x10^{-4}$ – 0.23	—	$\delta\lambda/\lambda$ < 5%	—	0.8-3.1 ×HFIR 9×FTS	
3.2.3b	High-resolution SANS—magnetic	Ordering in colloids, 2-dim structure in aligned polymers, strained materials, polymer crystallization, polyelectrolyte structures, viruses, pharmaceuticals, vortex lattice in superconductors	$\Phi_{TA}(\lambda)\Delta\lambda$	26	6–18	3	20	$3x10^{-4}$ – 0.23	—	$\delta\lambda/\lambda$ < 5%	—	0.8-3.1 ×HFIR 9×FTS	
3.2.4	Ultra SANS	Stacking in composites, agglomerates, powders and colloids; phase transitions nucleation in ferrites, austenites; geology, transport in soil, carbon sequestration, environmental science; time-dependent nucleation of bubbles, cavitation damage; large-scale magnetic domains, fluids, colloids; artificial structures (magnetic versus nuclear)	$\Phi_{TA}(\lambda)$			0.5	4	2×10^{-6}	—	$\delta\lambda/\lambda$ < 5%	—		*a*

Ref.	Instrument Description	Science Examples	FOM	L_1 (m)	L_2 (m)	λ_{min} (Å)	λ_{max} (Å)	Q-range ($Å^{-1}$)	E-range (meV)	Q-resol	E-resol	Perform.*	Notes
SANS (cont.)													
3.2.5	Spin-echo SANS (SESANS)	Stacking in composites, agglomerates, powders and colloids; phase transition nucleation in ferrites, austenites; geology, transport in soil, carbon sequestration, environmental science; time-dependent nucleation of bubbles, cavitation damage; large-scale magnetic domains, fluids, colloids; artificial structures (magnetic versus nuclear)						6×10^{-5} – 0.3	—	$\delta\lambda/\lambda$ < 5%	—		
Reflectometry													
4.4.1	SERGIS	In-plane structures at surfaces and in thin films and membranes			2				—		—		
4.4.2	GISANS and GID	In-plane structures at surfaces and in thin films and membranes						0.01 – 1	—		—		
4.4.3	Inelastic reflectometer	Dynamics of motions associated with surfaces or interfaces							—		—		
4.4.4	Generalized polarization-analysis reflectometer	Magnetic structures in layered systems							—		—		
4.4.5	Special-environment, small-sample, or kinetics reflectometer	Rapid measurement of surface structures, with capability for simultaneous measurements with complementary probes							—		—		
Single Crystal Diffraction													
5.2.1a	High-resolution high-throughput MaNDi instrument	Higher data rates, enabling measurement of protein structures from smaller weakly diffracting protein crystals (<0.1 mm^3), thus greatly expanding the range of proteins that can be studied	$\Phi_P(\lambda)$	288	1	2.6	3.2		—	Unit cell dim ≤150 Å	—	3.6×FTS	*b*

Ref.	Instrument Description	Science Examples	FOM	L_1 (m)	L_2 (m)	λ_{min} (Å)	λ_{max} (Å)	Q-range ($Å^{-1}$)	E-range (meV)	Q-resol	E-resol	Perform.*	Notes
Single Crystal Diffraction (cont.)													
5.2.1b	Lower-resolution high-throughput MaNDi instrument	Higher data rates, enabling measurement of protein structures from smaller weakly diffracting protein crystals (<0.1 mm^3), thus greatly expanding the range of proteins that can be studied	$\Phi_P(\lambda)$	200	1	2.4	3.3		—	Unit cell dim ≤100 Å	—	5.2×FTS	*c*
5.2.2	Polarized sample diffractometer (polarized proteins)	Higher signal/noise ratio enabling faster measurements, etc. Also provides tunable contrast capabilities to separate, e.g., protein from water							—		—		*d*
5.2.3	High-intensity, polarized (small molecule)	Order-disorder transitions, displacive transitions, anharmonic motion, critical scattering, Huang scattering, domain structures, incommensurate satellite peaks, hydrogen bonding, magnetostriction		100					—		—		*e*
5.2.4	Diffuse scattering diffractometer	Defects and disorder in crystals							—		—		*f*
5.2.5	Neutron diffraction topography	3D mapping within large single crystals, image magnetic domains in magnetic crystals, visualization of defects							—		—		*g*
5.2.6	Quasi-Laue single crystal diffractometer	Structures of small proteins, pharmaceuticals, minerals and other inorganic crystals, small-molecules, molecular organometallic crystals, metal organic frameworks							—		—		*h*

Ref.	Instrument Description	Science Examples	FOM	L_1 (m)	L_2 (m)	λ_{min} (Å)	λ_{max} (Å)	Q-range ($Å^{-1}$)	E-range (meV)	Q-resol	E-resol	Perform.*	Notes
Powder Diffraction													
6.2.2a	Very Fast Powder Diffractometer	For small sampling volume crystallography and engineering studies; moderate complexity crystallography, kinetics, phase transitions, spin structures, engineering materials, and mapping of orientation distribution functions Best for d > 1 Å	$\Phi_P(\lambda)$	130					—	$\delta d/d = 5\times10^{-3}$ @ 90°	—	9 × FTS	*i*
6.2.2b	High Magnetic Field Diffractometer	Polarized sample, beam and analysis; spin-lattice coupling phenomena and phase mapping Best for d > 1 Å	$\Phi_P(\lambda)$	130					—	$\delta d/d = 5\times10^{-3}$ @ 90°	—	9 × FTS	*i*
6.2.2c	Ultrahigh Pressure Diffractometer	Smaller sample volumes than SNAP, high flux for total scattering measurements Best for d > 1 Å	$\Phi_P(\lambda)$	130					—	$\delta d/d = 5\times10^{-3}$ @ 90°	—	9× FTS	*i*
6.2.3	Very High Resolution Powder Diffractometer	Ab-inito structure determination, incommensurate systems, microstructure through peak shape analysis							—	$\delta d/d = 3\times10^{-4}$ @ 140°	—		*j,a*
6.2.4	Long-Range Pair Distribution Function Diffractometer	Very high data rates at good resolution for disordered solids with high Q resolution and energy selection, complement NOMAD							—	$\delta d/d = 10^{-3}$	—		*j,a*
6.2.5	SWANS	Combined wide and small angle instrument, quasielastic–inelastic capability, high-temperature metallurgy, hydrogen and oxygen diffusion and location							ΔE = 200		20 μeV		

Ref.	Instrument Description	Science Examples	FOM	L_1 (m)	L_2 (m)	λ_{min} (Å)	λ_{max} (Å)	Q-range ($Å^{-1}$)	E-range (meV)	Q-resol	E-resol	Perform.*	Notes
Inelastic Scattering using Spin Precession													
7.4a	Solids (vertical sample, resonance NSE)—wide angle	Excitation lifetimes with much greater resolution than currently possible, relevant now for superconductors and quantum liquids but later for study of propagating modes in biophysics and biology	$\Phi_{TA}(\lambda)\Delta\lambda$	40	2	2 7	7 12				$< 10^{-5} \times E_{inc}$	Flux 2×10^9 Flux 4×10^8 $n\cdot cm^{-2}\cdot s^{-1}$	*k*
7.4b	Liquids (horizontal sample, resonance SE)	Excitations of liquid surfaces or of membranes at very low Q, inelastic reflectometry and inelastic SANS particularly important for the range of length and time scales involved in biophysics and biology	$\Phi_{TA}(\lambda)\Delta\lambda$	40	2	2 7	7 12				$< 10^{-5}$ x E_{inc}	Flux 2×10^9 Flux 4×10^8 $n\cdot cm^{-2}\cdot s^{-1}$	*k*
7.4c	Wide angle	Reaction kinetics and kinetics of biological processes	$\Phi_{TA}(\lambda)\Delta\lambda$	40	3	2 7	7 12				$< 10^{-5} \times E_{inc}$	Flux 7×10^8 Flux 4×10^7 $n\cdot cm^{-2}\cdot s^{-1}$	*k*
7.1	Very long Fourier times	Complex systems such as polymers and biological molecules	$\Phi_{TA}(\lambda)\Delta\lambda$										*l*
7.2	NSE with depolarizing sample	Standard NSE from superconductors and ferromagnets, H/D contrast methods	$\Phi_{TA}(\lambda)\Delta\lambda$										*m*
Conventional Inelastic Scattering													
8.3.1	Fine resolution backscattering spectrometer	Interfacial dynamics, biological samples, absorbent behavior, confinement, tunneling, glassy systems, diffusive processes, ionic and proton conductors, quantum magnetism, molecular magnetism, frustrated magnets, relaxor ferroelectrics, energy storage	$\Phi_P(\lambda)$	200	4			< 1.9	± 0.1 about elastic line		800 neV	Flux 3×10^6 $n\cdot cm^{-2}\cdot s^{-1}$	*i*

Ref.	Instrument Description	Science Examples	FOM	L_1 (m)	L_2 (m)	λ_{min} (Å)	λ_{max} (Å)	Q-range ($Å^{-1}$)	E-range (meV)	Q-resol	E-resol	Perform.*	Notes
Conventional Inelastic Scattering (cont.)													
8.3.2	Ultra-fine-resolution backscattering spectrometer	Interfacial dynamics, biological samples, absorbent behavior, confinement, tunneling, glassy systems, diffusive processes, ionic and proton conductors, quantum magnetism, molecular magnetism, frustrated magnets, relaxor ferroelectrics, energy storage, dynamic critical scattering, ferroelectrics	$\Phi_P(\lambda)$	30	4				~ 2		500 neV	Flux 1×10^5 $n\cdot cm^{-2}\cdot s^{-1}$	*i*
8.4.1	High-resolution cold chopper spectrometer	Interfacial dynamics, biological samples, absorbent behavior, confinement, tunneling, glassy systems, diffusive processes, ionic and proton conductors, quantum magnetism, molecular magnetism, frustrated magnets, relaxor ferroelectrics, energy storage, dynamic critical scattering, ferroelectrics, membrane protein collective dynamics, ferro-elastic modes, shape memory alloys	$\Phi_P(\lambda)$	36	4				2-80		1% of E_{inc}	6–15×FTS	*i,n*
8.4.2	High-intensity chopper spectrometer	Interfacial dynamics, biological samples, absorbent behavior, confinement, tunneling, glassy systems, diffusive processes, ionic and proton conductors, quantum magnetism, molecular magnetism, frustrated magnets, relaxor ferroelectrics, energy storage, membrane protein collective dynamics, ferro-elastic modes, shape memory alloys, kinetic experiments, stroboscopic measurements	$\Phi_P(\lambda)$	36	4				2–80		5% of E_{inc}	10–100 ×FTS	*o*
8.4.3	Extreme sample environment spectrometer	Extreme sample environments, parametric studies	$\Phi_P(\lambda)$	36	4				2–80		5% of E_{inc}		*p*

Ref.	Instrument Description	Science Examples	FOM	L_1 (m)	L_2 (m)	λ_{min} (Å)	λ_{max} (Å)	Q-range ($Å^{-1}$)	E-range (meV)	Q-resol	E-resol	Perform. *	Notes
Conventional Inelastic Scattering (cont.)													
8.5	Crystal monochromator instrument	Interfacial dynamics, biological samples, absorbent behavior, confinement, tunneling, glassy systems, diffusive processes, ionic and proton conductors, quantum magnetism, molecular magnetism, frustrated magnets, relaxor ferroelectrics, energy storage, membrane protein collective dynamics, ferro-elastic modes, shape memory alloys	$\Phi_{TA}(\lambda)$						2–80			0.2×HFIR	*q*
Imaging													
9.1.1	Neutron imaging beam line	Better sensitivity to composition and thickness, higher spatial resolution than is currently available, separation of contributions from different wavelengths for sharper images, Bragg edge imaging techniques for phase identification and enhanced contrast		>30									
9.1.2	3D imaging of large objects	Large field tomography with the ability to "zoom in" and do more discrete measurements at higher resolution		>30				$\delta\lambda/\lambda <$ 1%					
9.1.3	Research and development beam line	Support for R&D on neutron detectors, new neutron optical concepts, more accurate computer modeling of instrument performance											
9.1.4	Microprobe instrument	Extremely high spatial resolution to study interfaces, inclusions, precipitants, grain boundaries, intra-granular strain.				1	4						
9.1.5	Holography instrument	Scientific use not clear											

Ref.	Instrument Description	Science Examples	FOM	L_1 (m)	L_2 (m)	λ_{min} (Å)	λ_{max} (Å)	Q-range ($Å^{-1}$)	E-range (meV)	Q-resol	E-resol	Perform.*	Notes
Fundamental Neutron Physics													
10.3	Ultracold neutrons beam line											20–40 ×FTS	

Notes: L_1 = source-to-sample distance; L_2 = sample-to-detector distance; λ_{min} = minimum wavelength used; λ_{min} = maximum wavelength used; Q = wavevector transfer; E = energy transfer; $\mathbf{\Phi_P(\lambda)}$ is the peak flux at the wavelengths of interest; $\mathbf{\Phi_{TA}(\lambda)}$ is the time-averaged flux at the wavelengths of interest; $\mathbf{\Phi_{TA}(\lambda)\Delta\lambda}$ is the time-averaged flux times the usable wavelength band.

* Based on Gallmeier and Iverson—performance is based on a per-proton basis (for 2 MW on FTS and 1 MW on STS, divide the comparison with FTS by a factor of 2)

a. Best at FTS.
b. For 150 Å unit cell, short proton pulse.
c. For 100 Å unit cell, short proton pulse.
d. Needs shorter-wavelength neutrons to determine high-resolution crystal structures for proteins.
e. Needs shorter-wavelength neutrons to determine high-resolution crystal structures for smaller unit cells. Needs polarized beam.
f. TOPAZ and CORELLI at FTS fill this need for now.
g. Some experiments could be done at the residual stress diffractometer HB-2B at HFIR or at VULCAN at FTS. Could also consider development of unit to "drop in" to existing instruments.
h. Best at HFIR.
i. Needs short proton pulse.
j. Needs chopper and shorter wavelengths too.
k. Include standard time-of-flight capability to increase range.
l. Current NSE at FTS meets need (better at STS?).
m. Needs R&D (MIEZE, intensity-modulated NSE).
n. Would like up to 80 meV incident.
o. Part of gain depends on focusing.
p. Built-in sample environment equipment and focusing for very small samples.
q. Standard new-generation cold triple axis.

2.4.2 Candidate instruments for reference instrument suite

Table 2.2 shows a subset of these instruments tentatively selected as candidates for the reference or straw man instrument suite. This selection of 28 instruments emphasizes those proposed during the workshop that benefit most from the intense cold beams at STS. However, the performance of some of these instruments depends on other source characteristics beyond just the intense cold beams (e.g., availability of shorter-wavelength neutrons, whether the proton pulse is short or long, how many beams are available, maximum available beam length). Therefore, the final selection of a reference suite of instruments for STS will depend on refinement of the details of the source configuration and performance.

Table 2.2. Candidate instruments for reference instrument suite

Ref.	Instrument Description	Science Examples	FOM	L_1 (m)	L_2 (m)	λ_{min} (Å)	λ_{max} (Å)	Q-range ($Å^{-1}$)	E-range (meV)	Q-resol	E-resol	Perform.*	Notes
SANS													
3.2.1	High-resolution small-angle neutron diffractometer	High-resolution structure of membranes, low-resolution structure of membrane proteins, thin polymer composite films and 2D devices for biosensors and biotechnology	$\Phi_{TA}(\lambda)\Delta\lambda$	65	~5	2	6	0.01–5	—	0.015 – 0.02 $Å^{-1}$ $\delta\lambda/\lambda$ < 1%	—	2.5×FTS	
3.2.2	High-throughput SANS	Workhorse instrument for chemistry, biology, complex fluids, metallurgy; vortex lattice in superconductors	$\Phi_{TA}(\lambda)\Delta\lambda$	20	1.5–12	2	15	0.001–1.4	—	$\delta\lambda/\lambda$ < 5%	—	1.5–4.5 ×HFIR 9×FTS	
3.2.3a	High-resolution SANS—optical	Ordering in colloids, 2-dim structure in aligned polymers, strained materials, polymer crystallization, polyelectrolyte structures, viruses, pharmaceuticals	$\Phi_{TA}(\lambda)\Delta\lambda$	26	6–18	3	20	3×10^{-4} – 0.23	—	$\delta\lambda/\lambda$ < 5%	—	0.8–3.1 ×HFIR 9×FTS	
3.2.3b	High-resolution SANS—magnetic	Ordering in colloids, 2-dim structure in aligned polymers, strained materials, polymer crystallization, polyelectrolyte structures, viruses, pharmaceuticals, vortex lattice in superconductors	$\Phi_{TA}(\lambda)\Delta\lambda$	26	6–18	3	20	3×10^{-4} – 0.23	—	$\delta\lambda/\lambda$ < 5%	—	0.8–3.1 ×HFIR 9×FTS	
3.2.5	Spin-echo SANS (SESANS)	Stacking in composites, agglomerates, powders and colloids; phase transition nucleation in ferrites, austenites; geology, transport in soil, carbon sequestration, environmental science; time-dependent nucleation of bubbles, cavitation damage; large-scale magnetic domains, fluids, colloids; artificial structures (magnetic versus nuclear)						6×10^{-5} – 0.3	—	$\delta\lambda/\lambda$ < 5%	—		

Ref.	Instrument Description	Science Examples	FOM	L_1 (m)	L_2 (m)	λ_{min} (Å)	λ_{max} (Å)	Q-range ($Å^{-1}$)	E-range (meV)	Q-resol	E-resol	Perform.*	Notes
Reflectometry													
4.4.1	SERGIS	In-plane structures at surfaces and in thin films and membranes			2				—		—		
4.4.2	GISANS and GID	In-plane structures at surfaces and in thin films and membranes						0.01–	—		—		
4.4.3	Inelastic reflectometer	Dynamics of motions associated with surfaces or interfaces							—		—		
4.4.4	Generalized polarization-analysis reflectometer	Magnetic structures in layered systems							—		—		
4.4.5	Special-environment, small-sample, or kinetics reflectometer	Rapid measurement of surface structures, with capability for simultaneous measurements with complementary probes							—		—		
Single Crystal Diffraction													
5.2.1b	Lower-resolution high-throughput MaNDi instrument	Higher data rates, enabling measurement of protein structures from smaller weakly diffracting protein crystals (<0.1 mm^3), thus greatly expanding the range of proteins that can be studied	$\Phi_P(\lambda)$	200	1	2.4	3.3		—	Unit cell dim ≤100 Å	—	5.2×FTS	*a*
5.2.2	Polarized sample diffractometer (polarized proteins)	Higher signal/noise ratio enabling faster measurements, etc. Also provides tunable contrast capabilities to separate, e.g., protein from water							—		—		*b*
5.2.3	High-intensity, polarized (small molecule)	Order-disorder transitions, displacive transitions, anharmonic motion, critical scattering, Huang scattering, domain structures, incommensurate satellite peaks, hydrogen bonding, magnetostriction		100					—		—		*c*

Ref.	Instrument Description	Science Examples	FOM	L_1 (m)	L_2 (m)	λ_{min} (Å)	λ_{max} (Å)	Q-range ($Å^{-1}$)	E-range (meV)	Q-resol	E-resol	Perform.*	Notes
Powder Diffraction													
6.2.2a	Very Fast Powder Diffractometer	For small sampling volume crystallography and engineering studies; moderate complexity crystallography, kinetics, phase transitions, spin structures, engineering materials, and mapping of orientation distribution functions Best for d > 1 Å	$\Phi_P(\lambda)$	130					—	$\delta d/d = 5x10^{-3}$ @ 90°	—	9 × FTS	*a*
6.2.2b	High Magnetic Field Diffractometer	Polarized sample, beam and analysis; spin-lattice coupling phenomena and phase mapping Best for d > 1 Å	$\Phi_P(\lambda)$	130					—	$\delta d/d = 5\times10^{-3}$ @ 90°	—	9 × FTS	*a*
6.2.2c	Ultrahigh Pressure Diffractometer	Smaller sample volumes than SNAP, high flux for total scattering measurements Best for d > 1 Å	$\Phi_P(\lambda)$	130					—	$\delta d/d = 5\times10^{-3}$ @ 90°	—	9 × FTS	*a*
Inelastic Scattering using Spin Precession													
7.4.1	Solids (vertical sample, resonance SE)—wide angle	Excitation lifetimes with much greater resolution than currently possible, relevant now for superconductors and quantum liquids but later for study of propagating modes in biophysics and biology	$\Phi_{TA}(\lambda)\Delta\lambda$	40	2	2 7	7 12				$< 10^{-5} \times E_{inc}$	Flux 2×10^9 Flux 4×10^8 $n\cdot cm^{-2}\cdot s^{-1}$	*d*
7.4.2	Liquids (horizontal sample, resonance NSE)	Excitations of liquid surfaces or of membranes at very low Q, inelastic reflectometry and inelastic SANS particularly important for the range of length and time scales involved in biophysics and biology	$\Phi_{TA}(\lambda)\Delta\lambda$	40	2	2 7	7 12				$< 10^{-5} \times E_{inc}$	Flux 2×10^9 Flux 4×10^8 $n\cdot cm^{-2}\cdot s^{-1}$	*d*
7.4.3	Wide angle	Reaction kinetics and kinetics of biological processes	$\Phi_{TA}(\lambda)\Delta\lambda$	40	3	2 7	7 12				$< 10^{-5}$ x E_{inc}	Flux 7×10^8 Flux 4×10^7 $n\cdot cm^{-2}\cdot s^{-1}$	*d*

Ref.	Instrument Description	Science Examples	FOM	L_1 (m)	L_2 (m)	λ_{min} (Å)	λ_{max} (Å)	Q-range ($Å^{-1}$)	E-range (meV)	Q-resol	E-resol	Perform.*	Notes
Conventional Inelastic Scattering													
8.3.1	Fine-resolution backscattering spectrometer	Interfacial dynamics, biological samples, absorbent behavior, confinement, tunneling, glassy systems, diffusive processes, ionic and proton conductors, quantum magnetism, molecular magnetism, frustrated magnets, relaxor ferroelectrics, energy storage	$\Phi_P(\lambda)$	200	4			< 1.9	± μeV about elastic		800 neV	Flux 3×10^6 $n\cdot cm^{-2}\cdot s^{-1}$	*a*
8.3.2	Ultra-fine-resolution backscattering spectrometer	Interfacial dynamics, biological samples, absorbent behavior, confinement, tunneling, glassy systems, diffusive processes, ionic and proton conductors, quantum magnetism, molecular magnetism, frustrated magnets, relaxor ferroelectrics, energy storage, dynamic critical scattering, ferroelectrics	$\Phi_P(\lambda)$	30	4				~ 2		500 neV	Flux 1×10^5 $n\cdot cm^{-2}\cdot s^{-1}$	*a*
8.4.1	High-resolution cold chopper spectrometer	Interfacial dynamics, biological samples, absorbent behavior, confinement, tunneling, glassy systems, diffusive processes, ionic and proton conductors, quantum magnetism, molecular magnetism, frustrated magnets, relaxor ferroelectrics, energy storage, dynamic critical scattering, ferroelectrics, membrane protein collective dynamics, ferro-elastic modes, shape memory alloys	$\Phi_P(\lambda)$	36	4						1% of E_{inc}	6–15×FTS	*a,e*

Ref.	Instrument Description	Science Examples	FOM	L_1 (m)	L_2 (m)	λ_{min} (Å)	λ_{max} (Å)	Q-range ($Å^{-1}$)	E-range (meV)	Q-resol	E-resol	Perform.*	Notes
Conventional Inelastic Scattering (cont.)													
8.4.2	High-intensity chopper spectrometer	Interfacial dynamics, biological samples, absorbent behavior, confinement, tunneling, glassy systems, diffusive processes, ionic and proton conductors, quantum magnetism, molecular magnetism, frustrated magnets, relaxor ferroelectrics, energy storage, membrane protein collective dynamics, ferro-elastic modes, shape memory alloys, kinetic experiments, stroboscopic measurements	$\Phi_P(\lambda)$	36	4						5% of E_{inc}	10–100 ×FTS	*f*
8.4.3	Extreme sample environment spectrometer	Extreme sample environments, parametric studies	$\Phi_P(\lambda)$	36	4						5% of E_{inc}		*g*
Imaging													
9.1.1	Neutron imaging beam line	Better sensitivity to composition and thickness, higher spatial resolution than is currently available, separation of contributions from different wavelengths for sharper images, Bragg edge imaging techniques for phase identification and enhanced contrast		>30									
9.1.2	3D imaging of large objects	Large field tomography with the ability to "zoom in" and do more discrete measurements at higher resolution		>30				$\delta\lambda/\lambda <$ 1%					
9.1.3	Research and development beam line	Support for R&D on neutron detectors, new neutron optical concepts, more accurate computer modeling of instrument performance											
Fundamental Neutron Physics													
10.3	Ultracold neutrons beam line											20–40 ×FTS	

Notes: L_1 = source-to-sample distance; L_2 = sample-to-detector distance; λ_{min} = minimum wavelength used; λ_{min} = maximum wavelength used; Q = wavevector transfer; E = energy transfer; $\mathbf{\Phi_P(\lambda)}$ is the peak flux at the wavelengths of interest; $\mathbf{\Phi_{TA}(\lambda)}$ is the time-averaged flux at the wavelengths of interest; $\mathbf{\Phi_{TA}(\lambda)\Delta\lambda}$ is the time-averaged flux times the usable wavelength band.

* Based on Gallmeier and Iverson—performance is based on a per-proton basis (for 2 MW on FTS and 1 MW on STS, divide the comparison with FTS by a factor of 2).

a. Short proton pulse.
b. Needs shorter-wavelength neutrons to determine high-resolution crystal structures for proteins.
c. Needs shorter-wavelength neutrons to determine high-resolution crystal structures for smaller unit cells. Needs polarized beam.
d. Include standard time-of-flight capability to increase range.
e. Would like up to 80 meV incident.
f. Part of gain depends on focusing.
g. Built-in sample environment equipment and focusing for very small samples.

2.4.3 Science

2.4.3.1 SANS and small Q diffraction

SANS studies benefit research in areas ranging from physics, chemistry, and materials science to biology and environmental science. Some of these types of studies are listed here, ordered in terms of length scales to be probed ranging from 600 μm down to 0.1 nm with the longest length scales on top. The set of SANS instruments proposed for the STS reference suite together will provide complete coverage of this continuous range of length scales to address important scientific problems in all of these areas.

- Stacking in composites, agglomerates, powders and colloids
- Phase transition nucleation in ferrites, austenites
- Geology, transport in soil, carbon sequestration, environmental science
- Time dependent nucleation of bubbles, cavitation damage
- Large-scale magnetic domains, fluids, colloids
- Artificial structures (magnetic versus nuclear)
- Ordering in colloids
- 2-dim structure in aligned polymers**,** strained materials**,** polymer crystallization**,** polyelectrolyte structures**,** viruses**,** pharmaceuticals
- Chemistry**,** biology**,** complex fluids**,** metallurgy
- Surface ordering, membranes and proteins
- In-plane structures of complex fluids, thin films, membranes, dynamic systems, block copolymers, proteins
- Vortex lattice in superconductors

2.4.3.2 Reflectometry

Science areas in which the reflectometers proposed as reference instruments for STS can have a large impact include

- Phase separation in polymer films
- Inorganic templating at air/water interfaces
- Complex fluids under flow
- Vesicles and gels
- Reaction kinetics
- Surfactants at interfaces
- Interfacial structure in drug delivery systems
- Membranes and their intermolecular interaction
- Protein adsorption
- Critical phenomena in fluid systems
- Biocompatibility and sensors

- Multilayer materials (e.g., giant magnetoresistance [GMR])
- Depth-dependent domain imaging
- In-situ characterization of MBE-grown layers
- Magnetic monolayers
- Superparamagnetic nanoparticles
- Exchange-biased interfaces
- Magnetic tunnel junctions
- Hard/soft magnetic multilayer combinations

2.4.3.3 Single crystal diffraction

Crystallographic studies of single crystals ranging from small molecules to macromolecular systems are fundamental to understanding their physical properties and functional behavior in chemical systems. Much of this is done with X-ray diffraction, but neutron diffraction offers significant complementarity to X-ray diffraction studies; and for the general problem of hydrogen atom location, magnetic structural studies, and many specific crystallographic problems, neutron diffraction is superior to X-ray diffraction. Neutron diffraction studies using the time-of-flight (TOF) methods at spallation neutron sources generally can out-perform reactor-based instruments in data collection rates and signal-to-noise ratio.

The major limitation to the wider use of neutron diffraction for single-crystal studies has been and will continue to be the availability of crystals of sufficient size to provide the necessary diffracted intensity. Several next-generation single-crystal diffractometers being built at FTS promise to expand dramatically the range of feasible studies. Three single-crystal diffractometers are proposed for the reference suite for STS to expand and complement the capabilities of the FTS instruments. These are a workhorse protein crystallography instrument (up to 100 Å unit cells), a unique instrument using polarized samples to selectively enhance the contrast for portions of a sample, and a polarized-beam small-molecule diffractometer. These three instruments can provide significant new capabilities for studies in the following fields:

- Atomic-scale structural information from macromolecular crystals
- Huge gains in signal-to-background by decreasing the hydrogen incoherent scattering
- Ability to separate scattering of molecule and solvent
- Order-disorder transitions
- Displacive transitions (ferroelectrics, ionic conductors, colossally magnetoresistive [CMR] materials, and superconductors)
- Anharmonic motion (ferroelectrics, ionic conductors, CMR materials, and superconductors)
- Critical scattering (ferroelectrics, ionic conductors, CMR materials, and superconductors)
- Huang scattering
- Domain structures
- Incommensurate satellite peaks (high-T_c superconductors)
- Hydrogen bonding (minerals, proteins)

- Magnetostriction

2.4.3.4 Powder diffraction

The study of atomic structure and transformations spans engineering materials, chemistry, condensed matter physics, geoscience, and biology. Neutron powder diffraction has played and will continue to play a very important role in investigating complex crystal structures, kinetic transformations, and engineering and disordered (dominated by short-range atomic correlations) materials. Current trends include increasing complexity (e.g., spatial inhomogeneity, symmetry lowering, large unit cells, multiple structure-property couplings, new length and time scales, increasing interest in deviations from long-range order, complex spin systems, and more emphasis on organic and organic-containing materials.

The broad pulse widths inherent to the fully coupled moderators at STS do not lend themselves well to high-resolution TOF powder diffraction, which is much better done at FTS. However, STS will provide adequate resolution for many experiments in which d-spacings < 1 Å are not required; and for such experiments, STS will offer an order of magnitude gain relative to FTS, especially if these experiments require use of the longer wavelengths. This gain will enable measurements on much smaller samples (extremely important for many of the new advanced materials) or with shorter data collection times (important for kinetic or parametric studies). Therefore, we propose three moderate-resolution powder diffractometers as candidates for the reference instrument suite for STS; a general very-small-sample diffractometer, a similar diffractometer dedicated to ultra-high-pressure studies (pressure equipment incorporated into the instrument, and another similar instrument dedicated to very-high-magnetic-field studies (magnet or magnets incorporated into the instrument). These instruments will enable new science that includes the following types of studies on very small samples or with very rapid measurements on larger samples:

- Moderate complexity crystallography
- Kinetics
- Phase transitions
- Spin structures
- Engineering materials
- Mapping of orientation distribution functions
- Polarized sample, beam and analysis
- Spin-lattice coupling phenomena and magnetic phase mapping
- Smaller sample volumes (potentially higher pressures) than at the Spallation Neutrons and Pressure Diffractometer (the FTS high-pressure diffractometer)

2.4.3.5 Neutron spin-echo

NSE is the spectroscopic method with the highest resolution in quasielastic and inelastic neutron scattering, with energy resolution values typically better than 10^{-5} of the incident neutron energy. NSE is thus perfectly suited to investigate slow motions in hard and soft condensed matter, including biophysics and biology. Examples of areas where the three NSE instruments proposed as candidates for the STS reference suite could lead to new science include

- Excitations lifetimes with much greater resolution than currently possible—superconductors and quantum liquids
- Excitations lifetimes with much greater resolution than currently possible—processes in complex organic molecules, propagating modes in biophysics and biology and their importance for biological key functions
- Reflectometer geometry—surface excitations, dynamics on liquid surfaces or of the membranes at very low Q, inelastic reflectometry, and inelastic SANS
- Reaction kinetics and kinetics of biological processes

2.4.3.6 Conventional inelastic scattering

The conventional inelastic scattering instruments typically cover much more extensive energy ranges but with lower energy resolution than is the case for the NSE instruments. These instruments complement the NSE instruments, and both are needed to span the broad range of energies necessary to understand the dynamic processes. A number of conventional inelastic instruments have been built or are being built at FTS. However, the STS will provide much more intense beams of cold neutrons than are available at FTS, so the complementary instruments at STS will be focused on extending the capabilities for dynamic studies to probe lower-energy (slower) motions. Several conventional inelastic instruments are proposed to be included in the STS reference suite of instruments, and these will provide capabilities complementary to and in many cases well beyond those of the FTS instruments. Examples of areas in which these extended capabilities can enable new science include

- Interfacial dynamics—biological samples; absorbent behavior, confinement, tunneling—glassy systems; diffusive processes—ionic and proton conductors
- Quantum magnetism, molecular magnetism, frustrated magnets, relaxor ferroelectrics
- Energy storage
- Dynamic critical scattering—ferroelectrics
- Membrane protein collective dynamics, ferro-elastic modes, shape memory alloys
- Kinetic experiments—stroboscopic measurements
- Extreme sample environments (high magnetic fields, high pressure, levitated samples, often with low or high temperatures)—parametric studies

2.4.3.7 Imaging

Two imaging beam lines and one beam line for development of components and techniques utilizing the cold-neutron capabilities are proposed as part of the reference instrument suite for STS. New science that would be enabled with the imaging beam lines includes

- 3D and time-resolved imaging
- Longer-wavelength neutrons provide better sensitivity to composition and thickness
- Longer-wavelength neutrons facilitate optics to attain much higher spatial resolution than is currently available
- Use of TOF to separate the contributions from different wavelengths for sharper images

- Bragg edge imaging techniques to provide material-selective contrast
- Capability for large-field tomography with the ability to "zoom in" and do more discrete measurements at higher resolution

2.4.3.8 Fundamental neutron physics

Cold neutrons and ultracold neutrons (UCN) have been employed in a wide variety of investigations that shed light on important issues in nuclear, particle, and astrophysics in the determination of fundamental constants and in the study of the fundamental symmetries of nature. A beam line for Fundamental Neutron Physics is being instrumented to address a number of these issues. However, an optimized beam line at STS could provide as much as a 40-fold increase over FTS in the flux for UCN. This beam line, proposed as one of the STS reference suite of instruments, would provide significant new scientific capabilities in several areas, including

- The search for a neutron electric dipole moment
- Measurement of the neutron lifetime

2.4.4 Research and development needs

The working groups identified a wide variety of areas in which research and development (R&D) could improve the scientific capabilities of the source and neutron beam instrumentation. These are summarized here.

Moderators

- Tunable moderators
- Very cold moderator (more very-long-wavelength neutrons)
- Inclusion of shorter wavelengths without sacrificing cold neutron intensity (e.g., viewing thermal and cold moderator simultaneously on a few beams)

Techniques

- New techniques
  - TISANE
  - MIEZE
  - Longitudinal resonance spin-echo
- Multiplexing / multipulse /Fourier diffractometer
  - MC simulations, user-friendly software
  - Evaluate for complex structures
- Phase space transformation devices to trade Q resolution for energy resolution and increased flux
- A research effort to examine ways of multiplexing the beam line other than using a monochromator
- Use of TOF to separate the contributions from different wavelengths to improve image sharpness, use of epithermal neutrons for imaging very large (thick) materials, and the development of Bragg edge imaging techniques

Optics

- Variety of optical focusing capabilities and techniques for SANS
- Focusing optic techniques for the inelastic instruments
- Polarizers, analyzers, and polarization-handling components

Detectors

- Detectors with higher resolution and higher data rates for SANS
- Detectors with very high spatial resolution and TOF for imaging applications
- Detectors (data rate, cost, efficiency at high E)
- Detector with large dynamic range and high instantaneous count rate capability

Sample environment

- Pressure cells including 180° panoramic cell
- Equipment that allows low temperature, high magnetic field, and high pressure simultaneously (useful for both diffraction and inelastic studies
- Cryopad

Software

- Data reduction, refinement, analysis improvements for all instruments

Other components

- High-quality single crystals of a material with a d spacing in the range between Si and mica would provide added flexibility in the design of crystal analyzer spectrometers.
- Choppers
  - Pulse-shaping choppers
  - Optimized chopper systems for RRM
  - Higher-speed choppers
  - Advanced coating process for neutron-absorbing coatings
  - Simpler and more uniform coating process should be investigated

Most of these development efforts cannot be fully evaluated and refined without significant access time for testing in a neutron beam. Thus, central to a successful instrumentation R&D program will be the construction of one or more dedicated test beams at FTS, HFIR, or other facilities, and later at STS.

- R&D beam line(s) to develop and test
  - New types of neutron detectors
  - New neutron optical concepts
  - Low-energy cross sections for more accurate computer modeling of instrument performance
  - Concepts for new instrumental techniques
  - Other beam line component developments

2.5 References

[1] R. K. Crawford, G. S. Smith, G. Ehlers, L. Robertson, *SNS Second Target Station Scoping Workshop, Aug. 3–4, 2006, Final Report*, SNS 107000000-TR0006-R00.

[2] J. D. Galambos, "STS Accelerator Impacts," SNS 100000000-IN0001-R00.

[3] F. X. Gallmeier and E. B. Iverson, "Draft: A First Effort towards a Target Moderator Reflector Assembly for a SNS Second Target Station," February 2007.

2.6 Other Useful Resources

Useful sources for further information:

ESS reports	http://neutron.neutron-eu.net/n_documentation/n_reports/n_ess_reports_and_more/102
ISIS TS2 studies/plans	http://ts-2.isis.rl.ac.uk
NMI3 European road-mapping reports	http://neutron.neutron-eu.net/n_nmi3
LANL Long-Pulse workshop	*Proceedings of the Workshop on Neutron Instrumentation for a Long-Pulse Spallation Source*, LBL-37880, April 1995
ANL VCNS workshop	*Proceedings of the Workshop on Applications of a Very Cold Neutron Source*, ANL-05/42, December 2005
ANL-generated NSF Technical Study for SNS 2nd Target Station	*Technical Concepts for a Long-Wavelength Target Station for the Spallation Neutron Source*, ANL-02/16, ORNL/SNS-TM-2001/163, November 2002
National Nanotechnology Initiative Workshop report (DRAFT)	*X-Rays and Neutrons: Essential Tools for Nanoscience Research*, Report of the National Nanotechnology Initiative Workshop, June 16–18, 2005

3.0 SMALL-ANGLE NEUTRON SCATTERING: WORKING GROUP REPORT

Chair: G. Smith (ORNL)

Other Participants: J. Carpenter (ANL), K. Littrell (ORNL), D. Mildner (NIST), T. Rekveldt (TU Delft), P. Thiyagarajan (ANL), J. K. Zhao (ORNL)

3.1 General Discussion

3.1.1 Instruments and length scales

The SANS working group considered some of the instruments discussed at the August 2006 STS Scoping Workshop by the Large Scale Structures working group. The current working group discussed the real-space and Q-space ranges accessible by those instruments in order to arrange the instruments by the length scales required for various scientific problems. Table 3.1 lists the SANS-based instruments ordered by the length scales probed, from the largest to the smallest. It was noted that there is sufficient overlap in these techniques to cover the continuous range of length scales from hundreds of microns to a few Angstroms.

Table 3.1. SANS-based instruments ordered by length scales

Real space range	Q Range	Instrument type	Resolution ($\delta\lambda/\lambda$)
600 microns–600 Å	3×10^{-6} Å^{-1} < Q < 10^{-2} Å^{-1}	SESANS, USANS	<5%
25 microns (@ λ~2Å)–50 Å	N/A	SESANS	<5%
60,000–600 Å	10^{-4} Å^{-1} <Q< 10^{-2} Å^{-1}	SESANS, (Focused) Intermediate SANS	<5%
6000–6 Å	10^{-3} Å^{-1} < Q < 1 Å^{-1}	Workhorse SANS	<5%
600–6 Å	10^{-2} Å^{-1} < Q < 1 Å^{-1}	GISANS	<1%
600–1 Å	10^{-2} Å^{-1} < Q < 5 Å^{-1}	Small Q diffraction	<1%

Table 3.1 also lists the wavelength resolution required for the instruments proposed for the STS. The wavelength resolution, $\delta\lambda/\lambda$, is proportional to $\delta t/t$ (where t is the time of flight). A cold-coupled moderator on a short-pulse spallation source produces a neutron pulse a few hundred microseconds wide. This may be extended to approximately two milliseconds for a long-pulse source. The wavelength resolution due to the neutron pulse width is shown for a 1 ms wide pulse (the baseline case) in long-proton-pulse mode in Fig. 3.1. It is recognized that for reactor-based SANS, $\delta\lambda/\lambda$ (which is also the bandwidth $\Delta\lambda/\lambda$) typically varies from 5 to 30%. The wavelength resolution is required to be less than ~1% only for the diffraction instruments, and this would necessitate pulse shaping for a long-proton-pulse version of STS.

3.1.2 Science

Next, the group considered the scientific areas of study which would be covered by a suite of instruments such as those listed in Table 3.1. These areas are listed by the types of materials and/or the general areas that may be studied with the SANS instruments. As can be seen from Table 3.2, SANS studies benefit research in areas ranging from physics, chemistry, and materials

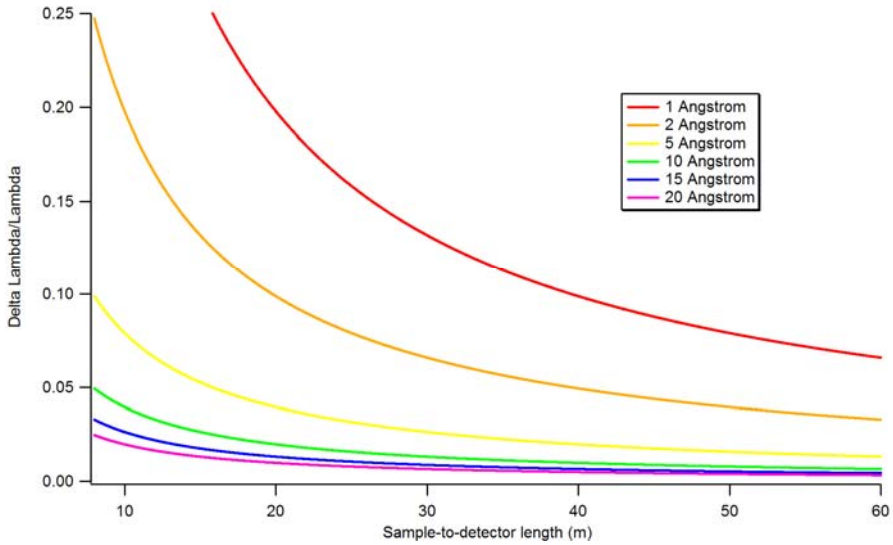

Fig. 3.1. The resolution δλ/λ of a SANS instrument as a function of instrument length and wavelength. The pulse width is assumed to be 1 ms.

science to biology and environmental science. Given this, we endorse a wide range of SANS instruments to address all of these areas.

3.1.3 Source characteristics

The assumption for either a long-proton-pulse or a short-proton-pulse version of STS is that 1 MW of average power will be delivered to the target at a rep rate of 20 Hz. In that case the time-averaged neutron flux is the same for both versions. For the large-length-scale instruments, which typically need resolution ~10% δλ/λ, either choice is just as good. The exception is for small Q diffraction, where better resolution is required for the smallest real space length scales.

3.1.4 Figure of merit for SANS

In order to compare the performance of various SANS instruments at a long-proton-pulse or short-proton-pulse STS, at FTS, or at the HFIR reactor source, we had to consider comparing an FOM for these types of sources. We considered the FOM for SANS instruments presented by Gunter Bauer [1] at the workshop:

$$\text{FOM} = \int_{\lambda_{\min}}^{\lambda_{\max}} I(\lambda)\lambda^4 d\lambda \ . \tag{3.1}$$

Here $I(\lambda)$ is the wavelength-dependent neutron intensity at the sample. To the first approximation, let us consider $I(\lambda)\lambda^4$ to be constant over the bandwidth $\Delta\lambda = \lambda_{max} - \lambda_{min}$. Therefore, in this approximation, the FOM $\propto \Phi_{avg}\Delta\lambda$, where Φ_{avg} is the time averaged flux for the source. From the draft calculations of the performance of the STS by Gallmeier and Iverson [2]:

$$\Phi_{ILL} \approx 3\times\Phi_{STS} \approx 9\times\Phi_{FTS} \ , \tag{3.2}$$

Table 3.2. Science with SANS instruments

Real space range	Science	Instrument type
600 microns—50 Å	Stacking in composites, agglomerates, powders and colloids; phase transition nucleation in ferrites, austenites; geology, transport in soil, carbon sequestration, environmental science; time-dependent nucleation of bubbles, cavitation damage; large-scale magnetic domains, fluids, colloids; artificial structures (magnetic versus nuclear); vortex lattice in superconductors	SESANS, USANS (including polarized option)
60,000—60 Å	Ordering in colloids, 2D structure in aligned polymers, strained materials, polymer crystallization, polyelectrolyte structures, viruses, pharmaceuticals, vortex lattice in superconductors	(Focused) Intermediate SANS— one magnetic instrument; one optical
6000—6 Å	Chemistry, biology, complex fluids, metallurgy, vortex lattice in superconductors	Workhorse SANS
600—6 Å	Surface ordering, membranes and proteins	GISANS (GID, reflectometry)
600—1 Å	In-plane structures of complex fluids, thin films, membranes, dynamic systems, block copolymers, proteins	Small Q diffraction

where Φ_{FTS} and Φ_{STS} are the time averaged fluxes for FTS and STS, respectively.

We assumed that the HFIR cold source flux is roughly equal to that of the ILL; therefore, we have used the value of the ILL time average flux for comparison, $\Phi_{HFIR} = \Phi_{ILL}$.

For a given instrument geometry:

$$FOM_{STS}/FOM_{HFIR} \text{ (at a given wavelength)} = (\Phi_{avg\ STS}/\Phi_{avg\ HFIR})\ (\Delta\lambda_{STS}/\Delta\lambda_{HFIR}) = (\Delta\lambda_{STS}/\Delta\lambda_{HFIR})/3\ .$$

Since the HFIR velocity selectors will produce $5\% < \Delta\lambda/\lambda < 30\%$, we assume a typical value of 10% so,

$$FOM_{STS}/FOM_{HFIR} \text{ (at a given wavelength)} \approx 3.3(\Delta\lambda_{STS}/\lambda)\ . \tag{3.4}$$

$\Delta\lambda = 3956/Lf$, where f is the source frequency in Hz, L is the length of the instrument in meters, and $\Delta\lambda$ is in Angstrom. As an example, for a 40 m long instrument and a 20 Hz source $\Delta\lambda = 5$ Å, then at a wavelength band of 5–10 Å,

$$FOM_{STS}/FOM_{HFIR} \text{ (centered at 7.5 Å)} \approx 2\ . \tag{3.5}$$

Similarly, for an instrument of the same length at STS or FTS,

$$FOM_{STS}/FOM_{FTS} \text{ (at a given wavelength)} = 3\ (\Delta\lambda_{STS}/\Delta\lambda_{FTS}) = 9\ . \qquad (3.6)$$

Clearly, more detailed Monte Carlo calculations are necessary to produce fully optimized instruments for STS, but this has given us a starting point for discussion.

3.2 Straw Man Designs

3.2.1 High-resolution small-angle neutron diffractometer

High-resolution neutron diffraction combined with targeted deuteration of specific groups in macromolecules in a Q region of $10^{-2} < Q < 5$ Å^{-1} offers a great deal to the field of high-resolution structure of membranes, low-resolution structure of membrane proteins, thin polymer composite films and 2D devices for biosensors and biotechnology. Successful development of an instrument to address these problems will lead to solutions for many important problems related to health and biotechnology and to the development of patterned arrays of biomimetic matrices for diagnostic purposes. Furthermore, such an instrument will enable the investigation of functional mechanisms of assembly and ordering of antimicrobial peptides in host membranes and self-assembly of nanoparticle arrays in block copolymer matrices for applications in nanotechnology. These systems have a wide length scale and ordering, and their investigations require high $\delta Q/Q$ resolution with ΔQ in the range of 0.015 to 0.02 Å^{-1} over the Q range of $10^{-2} < Q < 5$ Å^{-1}.

To achieve this $\delta Q/Q$ resolution, this instrument requires a wavelength resolution of $\delta\lambda/\lambda \sim 0.01$. With an appropriate goniometer and high-resolution position-sensitive detectors, this instrument can be developed to provide medium to high $\delta Q/Q$ resolution.

Employing monochromators to deliver neutrons with $\delta\lambda/\lambda \sim 0.01$ will result in the rejection of a substantial amount of neutron flux, so reactors are not viable for this application. Hence, we provide the instrument design parameters for FTS and the proposed STS target moderator system, both with a coupled hydrogen moderator and 1 MW proton beam. The 20 to 22 m flight path at EQ SANS (FTS—BL6) with an operating wavelength of 5 Å can obtain 1% $\delta\lambda/\lambda$. This wavelength resolution can be achieved with the long-proton-pulse option at the STS using 5 Å neutrons on a instrument with a flight path of ~70 m, resulting in a bandwidth $\Delta\lambda = 3955/(20\times70) = 2.8$ Å. Similar resolution can be achieved on FTS using 5 Å neutrons with a bandwidth $\Delta\lambda = 3955/(20\times60) = 3.3$ Å. The time-averaged flux at the STS = 3 times that at the FTS. Hence the overall gain at the STS when compared with FTS is $2.8\times3/3.3 = 2.5$

By using appropriate optics for efficient transport of cold neutrons within the wavelength range of 2 to 6 Å, the diffractometer at a long-proton-pulse-based target station at the STS will have superior performance. The long instrument also will have significantly smaller background compared with a short instrument at the FTS.

3.2.2 High-throughput SANS

As a straw man, for the un-optimized high-throughput SANS concept we have considered a traditional, movable detector SANS with a 1 m^2 detector with 5 mm^2 pixels. We assume a standard, symmetric geometry with a 1 cm diameter sample aperture and a wavelength that is tunable to select either a minimum wavelength of 2 Å or a maximum wavelength of 15 Å with the bandwidth determined by TOF (Fig. 3.2). There is taken to be an exclusion zone of 8 m from the source in which we assume no collimation elements are placed. The approximate performance parameters for such an instrument are given below. The gain over the same instrument at FTS would be about 9.

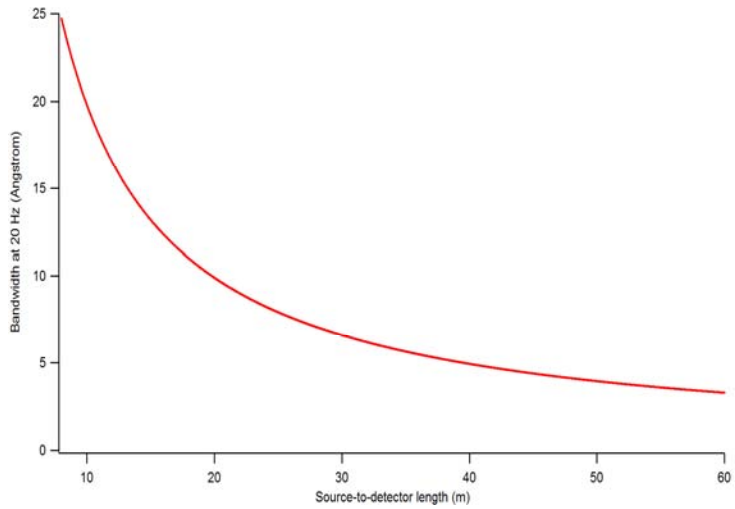

Fig. 3.2. Bandwidth versus the moderator-to-detector distance for the baseline 20 Hz pulsed source.

Table 3.3. Performance characteristics and gains for a high-throughput SANS instrument

L_1 (m)	L_2 (m)	λ_{min} (Å)	λ_{max} (Å)	Q_{min} ($Å^{-1}$)	Q_{max} ($Å^{-1}$)	Gain relative to HFIR or ILL
20	12	9	15	0.0010	0.039	1.5
20	6	8	15	0.0021	0.087	1.9
20	3	7	15	0.0042	0.20	2.1
20	1.5	7	15	0.0084	0.40	2.3
20	12	2	8	0.0020	0.17	3.7
20	6	2	9	0.0035	0.35	4.2
20	3	2	10	0.0063	0.70	4.3
20	1.5	2	10	0.013	1.4	4.5

L_1 = source-to-sample distance; L_2 = sample-to-detector distance; λ_{min} = minimum wavelength used; λ_{min} = maximum wavelength used; Q = wavevector transfer.

3.2.3 High-resolution SANS

For this instrument, we consider a traditional, symmetric long-baseline SANS with focusing. We again consider a 1 cm source aperture with the beam focused to 1 cm on the detector. This

instrument might perform the same or better on the HFIR cold source. The gains from increased resolution, even with the long-proton-pulse option, have not been quantified. Again, the same-instrument gain over FTS is about 9.

Table 3.4. Performance characteristics and gains for a high-resolution SANS instrument

L_1 (m)	L_2 (m)	λ_{min} (Å)	λ_{max} (Å)	Q_{min} (Å^{-1})	Q_{max} (Å^{-1})	Gain relative to HFIR or ILL
26	18	16	20	0.00026	0.015	0.8
26	12	9.5	14.5	0.00054	0.037	1.4
26	6	3	9	0.0017	0.23	3.1

L_1 = source-to-sample distance; L_2 = sample-to-detector distance; λ_{min} = minimum wavelength used; λ_{min} = maximum wavelength used; Q = wavevector transfer

3.2.4 USANS

The TOF Ultra-Small-Angle Neutron Scattering (USANS) instrument is now in the stage of detailed design and committed for construction at FTS beam line 1A. The instrument uses neutrons of up to about 0.3 eV (0.5 Å) to access a minimum Q of approximately 2×10^{-6} Å^{-1} (its unique feature), meanwhile using long-wavelength neutrons (~4 Å, 5 meV) for larger Q values. The instrument needs the highest possible fluxes of neutrons of both low and high energy. Good TOF resolution is not required as the basis for Q-resolution. High-order (n = 7) reflections need only be distinguished from the nearby orders ($\Delta t/t < 1/8$ at the detector, about 30 meters total flight path), which criterion should be considerably exceeded to provide the best signal-to-noise ratios.

For these reasons, the TOF USANS machine is best placed on a short-pulse source that provides the highest possible fluxes of both low-energy (5 meV) and high-energy (0.5 eV) neutrons. If all moderators of STS are optimized for low-energy neutrons at the expense of higher-energy ones, this feature excludes TOF USANS. At a long-pulse version of STS, TOF USANS would suffer a further disadvantage in signal-to-noise.

3.2.5 SESANS

The Spin-Echo Small-Angle Neutron Scattering (SESANS) arrangement consists in principle of two precession regions (PRs) with parallel inclination faces [3]. With opposite precession in the two regions, we have the spin-echo mode that is sensitive to small-angle changes of the beam between the two PRs. This mode, called the NSE mode, has three different applications that are discussed in A, B, C. The two PRs in parallel mode are applied in high-resolution diffraction that will be discussed in D.

A. This is the normal SESANS mode that enables one to measure the scattering density-density correlation of inhomogeneities. The range of sensitivity is proportional to the square of the wavelength, the magnetic field in the PRs, the lengths of the regions, and the inclination angle of the front faces of the regions. Depending on the instrumental details, spin-echo lengths from 5 nm to 100 μm are achievable.

B. The SESANS mode applied in reflectometry [4] with the Q analysis perpendicular to the reflecting plane enables one to measure directly the Q-dependence and spread in the Q

vector, independent of the collimation of the beam. The resolution in Q is only determined by the wavelength resolution of the beam. Also, the flatness of the sample does not affect the average Q vector measured, although it will contribute to the spread in Q, which adds to the off-specular reflection. To make high-resolution reflectometry possible, an optimized wavelength resolution is preferable. Scattering angles of 10^{-5} radian are achievable, without any collimation. Applying the SESANS analyzing direction parallel to the reflecting plane enables one to study density-density correlations from 5 nm to 100 μm as in A).

C. This application mirrors the inclination angles of the PR around the reflecting sample. That means that all specular reflection does not contribute to any depolarization of the beam, so the latter can only be attributed to the off-specular reflection. This option does not in principle deliver more information than in B.

D. In this option the inclined faces of the two PRs are set parallel to the reflecting planes of the sample under investigation. Because the total precession angle in the two PRs is proportional to 1/Q, the spread in Q leads to the depolarization of the beam. Because precession angles of 10^4 radians are achievable, lattice spacing variations of $\delta d/d$ better than 10^{-4} are measurable without any collimation of the beam and independent of the wavelength spread of the beam. Also, the line shape of the different Bragg reflections, scanned by the different wavelengths in the pulsed beam, are determined simultaneously from the field dependence of the measured polarization in each reflection. It is clear that wavelengths in the range of 1–4 Å are required for this option. [5]

3.3 Developmental Work

3.3.1 Optics

To reach the desired low value of Q in the general SANS instruments, focusing should be employed to reduce the direct-beam spot size at the detector. Focusing devices, both magnetic and optical, can be employed for this. Magnetic sextapole- based focusing devices are currently used at reactor sources and need to be developed for pulsed sources. One natural advantage of this focusing technology is that the beam is polarized by such a device, though only half the intensity is available. Similarly, transmission neutron focusing optics are in use at some reactor facilities, and further research needs to be done to apply them to a pulsed source.

Another area of development needed to reach small Q is the use of conical optics for neutron focusing. The optic requires a parallel or near-parallel beam incident on it. It can transmit and send to the focus only those neutrons within the critical angle θ_c. On the other hand, a simple aperture of the same outer radius will send to the focus those neutrons within the half-conical angle $\alpha = R/L$, where R is the radius of the optic and L is the focal length. The gain of the optic is therefore (α/θ_c), or $(\alpha/\theta_c)^2$ in two dimensions. This means that the gains may only be modest. Hence this optic is of no value for increasing the current density on sample. However, in SANS the collimation is usually provided by two pinhole apertures to produce a beam with small divergence onto the sample. The optimum condition is that the two apertures project to a point on the detector plane, giving a conical shape to the beam at the detector so that there is no umbra. The extent of the penumbra determines the minimum scattering vector. Reducing the size

of the apertures to obtain a lower value of Q_{min} results in a great decrease in intensity at the sample ($I \sim Q_{min}^4$).

The object of using converging optics is not to increase the intensity on sample but to decrease the extent of the penumbra, and hence reduce Q_{min}, without paying too great a price in the intensity on sample. With the focusing optic, the footprint of the beam on the detector plane is cylindrical with uniform density (complete umbra and no penumbra), with a radius equal to the source aperture radius. Hence the focusing optic can be used to attain lower values of the scattering vector. Whether nested cones can also be used in a similar fashion remains to be seen. The great advantage of reflective optics over refractive optics is that the focus is independent of wavelength. It seems that this should be a useful property to be exploited in TOF at pulsed sources.

3.3.2 Other

The group considered some other options for the instruments. For example, TISANE [6] was considered as an independent technique. In this technique, the beam is chopped at a high frequency, while the sample is "pumped" by an external field and the detector is gated at yet another frequency. Using this technique, dynamic measurements could be performed. The group discussed that this could possibly be added to the instruments described above to give increased flexibility, but more work needs to be done.

Also, in addition to the SESANS concepts, polarization and polarization analysis would be good options for many of the instruments described. This type of development requires TOF spin manipulation techniques (robust and user friendly) using wavelength-independent flippers, polarizers, precession devices, etc. Other general development ideas briefly discussed were continued supermirror development for these very long proposed instruments. For instrument lengths at which the neutrons bounce several times, a few percent increase in the reflectivity of the supermirrors over the entire wavelength band would enhance the flux at the sample position.

Detectors were also briefly discussed. SANS instruments could be enhanced in both flux and resolution if detector technology for large area detectors could simultaneously improve the dynamic range, efficiency, and resolution over today's technology. All of this also needs to accompany robust, long-lived detectors.

3.4 Conclusions

In the above discussions, the SANS working group presents a suite of instruments which cover a wide range of lengths scales of interest in many areas of science. Most of these instruments which require a wavelength resolution of <5% would be a good match for STS with modest gains over reactor-based sources. In most cases, the total number of neutrons on the sample in the wavelength range of interest is the important parameter, so either a long-proton-pulse or a short-proton-pulse version of STS delivering the most neutrons is a viable option. In the baseline case given, STS outperforms FTS for many of these types of instruments, including the general SANS and SESANS by a factor of 2 to 4. However, in the case of TOF USANS, we conclude that because of the need for high peak flux, the instrument would best be constructed on FTS (as is currently planned). We have based our discussions on a crude approximation to an FOM for the SANS instruments. The conclusions regarding which instruments to build and their

locations should serve as a good starting point. Detailed Monte Carlo analysis will be needed to optimize the instrument suite.

3.5 References

1. G. S. Bauer, *Report on the STS-2 Neutronics Workshop Held at SNS on Dec. 15 and 16, 2006*, presentation at the SNS Second Target Station Instrumentation Workshop, February 20–22, 2007.
2. F. X. Gallmeier and E. B. Iverson, *A First Effort Towards a Target Moderator Reflector Assembly for a SNS Second Target Station*, Spallation Neutron Source report, February 2007.
3. M. T. Rekveldt, J. Plomp, W. G. Bouwman, W. H. Kraan, S. Grigoriev, and M. Blaauw, *Rev. Sci. Instrum*. **76**, 033901 (2005).
4. M. T. Rekveldt, *J. Appl. Cryst.* **36**, 1301(2003).
5. M. T. Rekveldt, T. Keller, and R. Golub, *Europhys. Lett.* **54** (3), 342(2001).
6. A. Wiedenmann, U. Keiderling, K. Habicht, M. Russina, and R. Gahler, *Phys. Rev. Lett.* **97**, 057202(2006).

4.0 REFLECTOMETRY: WORKING GROUP REPORT

Chair: J. Ankner (ORNL)

Other Participants: J. Majewski (LANL), C. Majkrzak (NIST—participated by phone), R. Pynn (Indiana U.), T. van Vuure (ITU Karlsruhe)

4.1 Scientific Justification

Reflectometers probe boundaries between materials and measure nuclear and magnetic density profiles perpendicular to planar interfaces. The technique also gives information about interfacial roughness and provides information about the in-plane structures of thin films. Given the fundamental importance of interfacial phenomena in biology, chemistry, polymer science, structural materials, and artificially layered magnetic systems, reflectometry is expected to continue to play a crucial role in deepening our understanding of important scientific issues, many of which are technologically important. Neutron reflectometers are uniquely sensitive to vector magnetization and to isotopic substitution, most notably the use of deuterium (^{2}H) for contrast enhancement. The following is a partial list of past, current, and future fields of interest.

- Phase separation in polymer and copolymer films
- Inorganic templating at air/water interfaces
- Complex fluids under flow
- Vesicles and gels
- Reaction kinetics at surfaces
- Surfactants at interfaces
- Interfacial structure in drug delivery systems
- Membranes and their intermolecular interaction
- Protein adsorption to surfaces and membranes
- The effect of surfaces on critical phenomena in fluid systems
- Biocompatibility and sensors
- Multilayer materials (e.g. GMR) for magnetic recording
- Depth-dependent domain imaging
- In-situ characterization of MBE-grown layers
- Magnetic monolayers and multilayers
- Superparamagnetic nanoparticles
- Exchange-biased interfaces
- Magnetic tunnel junctions
- Hard/soft magnetic multilayer combinations

4.2 Reflectometer Performance at STS

Several detailed simulations of the performance of reflectometers at continuous and pulsed neutron sources have been carried out over the past decade. In a particularly thorough study, Fitzsimmons [1] concluded that (1) properly calibrated reflectometers at any neutron source can produce equally accurate and precise data; (2) reflectometers at pulsed sources are always faster than reflectometers that use monochromators at CW neutron sources of equal time-averaged neutron flux; (3) reflectometers at low-frequency sources are always faster than those at high-frequency sources of equal power, provided access to a large region of reciprocal space is required; (4) reflectometers at short-pulse sources perform marginally better than those at long-pulse sources of equal power, frequency, and resolution. Importantly, Fitzsimmons concluded on the basis of his simulations that the primary design criterion for a pulsed source as far as reflectometry measurements are concerned is the moderator brightness per pulse, and that a secondary criterion is reduction of source frequency.

From the point of view of the present study, past simulations imply that a reflectometer at STS would perform considerably better than at FTS. A large part of that gain (a factor of ~8×, assuming equal proton power were delivered to both targets) would come from moderator brightness, and an additional smaller factor (~2×) would derive from the reduced source frequency. This overall enhancement factor of ~15× for a short-proton-pulse version of STS would be reduced to a gain factor of ~ 10× for a long-proton-pulse option with equal proton beam power and equal frequency, assuming that the same Q resolution was achieved in both cases. Thus whichever choice in proton pulse length is made, reflectometry is a technique that would gain enormously from the installation of STS.

4.3 Commonalities

In considering the various reflectometers that might be constructed at STS, we noted a significant commonality in instrument configuration, particularly the neutron guides and choppers. The current SNS reflectometers use multi-channel curved guides to eliminate direct line-of-sight and deliver almost all of the available flux at the 2.5 Å peak of the coupled H_2 moderator in a 15–20 m moderator-detector distance. Figure 4.1 compares the vertical divergence spectrum measured at the current SNS liquids reflectometer with the design calculation, and Figure 4.2 shows the SNS liquids and magnetism reflectometer incident-beam transport (guides, disk choppers, and beam shutters) as an isometric design drawing (left) and photographed during installation (right) [2]. The guide performs two crucial functions: (1) A multi-channel bender rejects $\lambda < 1$ Å neutrons. (2) A tapered funnel produces a wide angular dispersion, providing a range of incident angles, shallower than the 4° centerline of the beam, for measuring reflections from liquid surfaces.

At STS, which will feature longer flight paths and a somewhat longer-wavelength neutron spectrum, guide performance should be even better. One may alternatively employ a cheaper and less technologically risky lower-index guide to achieve comparable performance. We can optimize curved, tapered guides to fit a wide range of beam divergence and wavelength requirements, but all of the instruments discussed below may be built using similar guide systems.

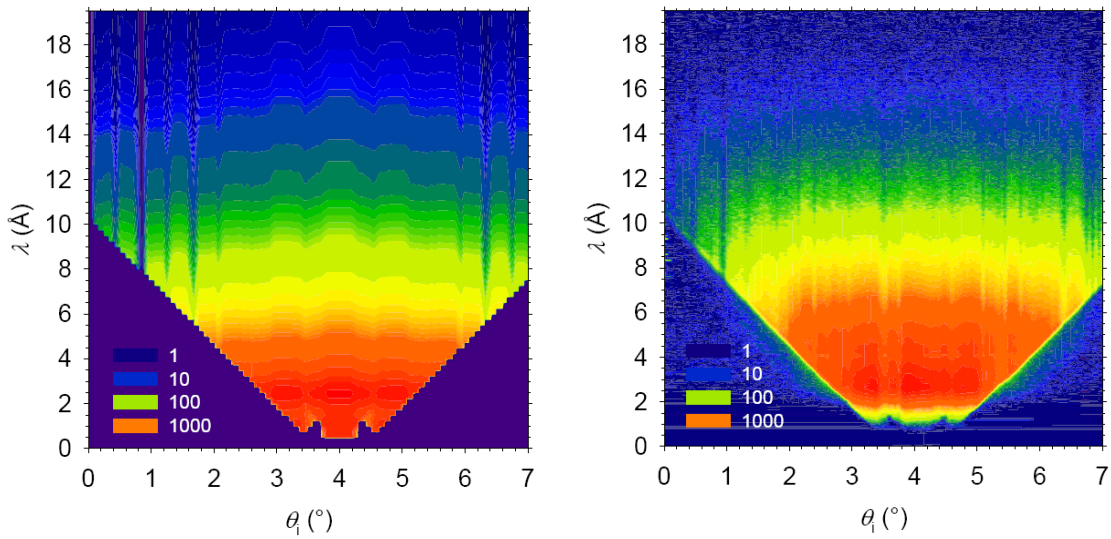

Fig. 4.1. Modeled (left) and measured (right) vertical divergence distributions of the SNS liquids reflectometer guide system.

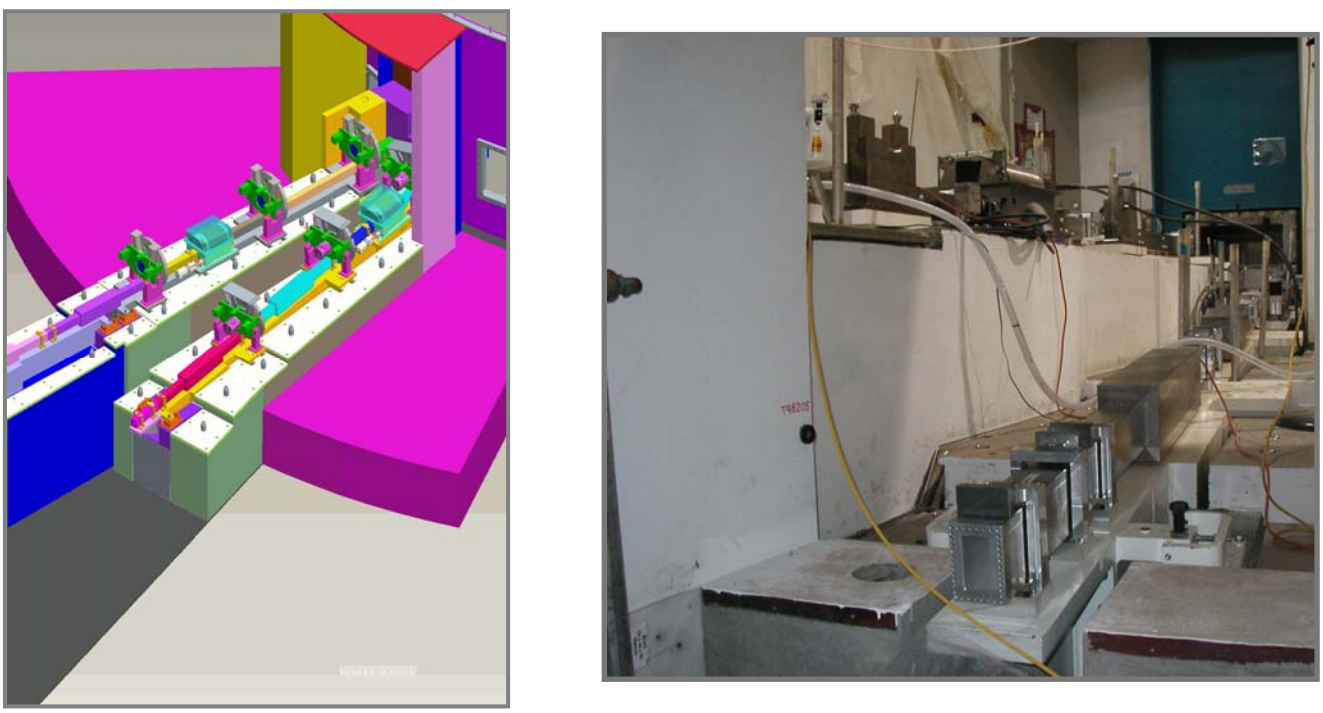

Fig. 4.2. Isometric design drawing (left) and installation picture (right) of the SNS liquids reflectometer guide system.

The existing SNS liquids and magnetism reflectometers utilize three disk choppers to eliminate frame overlap at the 60-Hz source frequency of FTS. Instruments built at STS should require only two frame-overlap choppers because of the slower 20 Hz proposed repetition rate, a feature again shared in common with all of the concepts described below.

Sample positioning and alignment is extremely important in reflectivity measurements. Reflectometers are generally built to study either horizontally or vertically mounted samples. Horizontal sample mounting is necessary to study free-liquid surfaces, while vertical mounting schemes are generally more compatible with standard sample environment equipment, such as superconducting magnets or cryostats. At FTS, the magnetism reflectometer features a vertical sample geometry and can accommodate massive sample environment gear (up to 1000 kg), whereas the liquids reflectometer is more compact and is designed for equipment no heavier than 300 kg (see Figure 4.3). Positioning systems for the instruments described below will generally conform to one or another of these schemes.

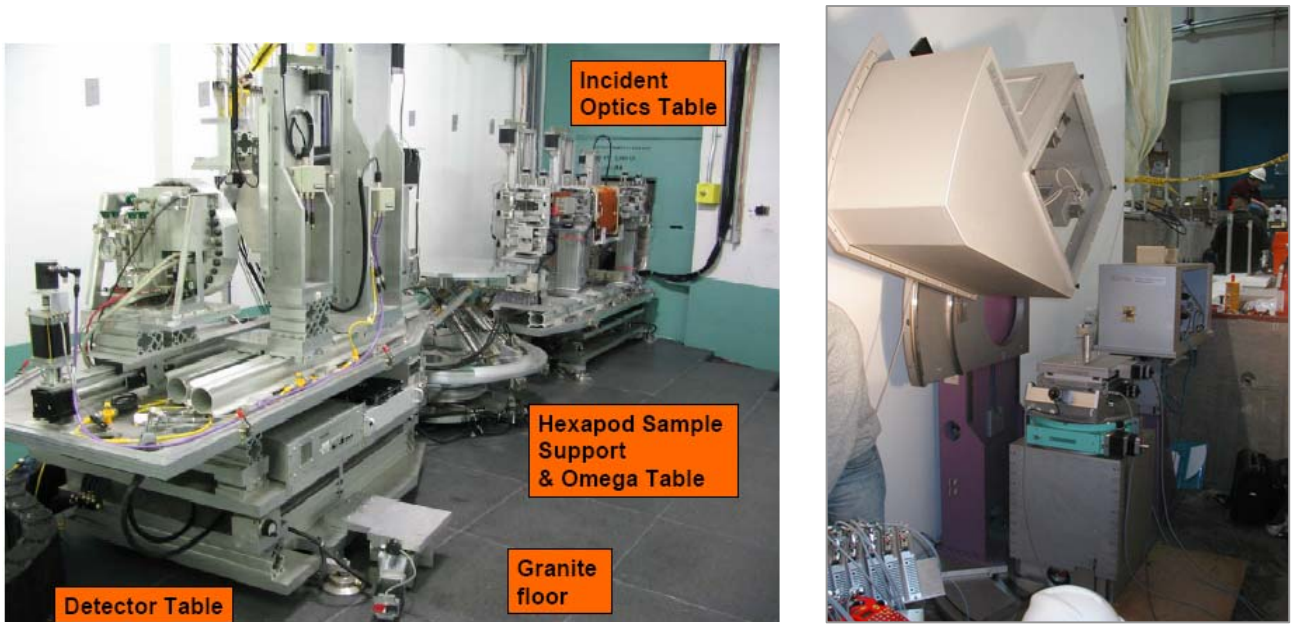

Fig. 4.3. **Sample stages and optical tables for SNS vertical-sample magnetism reflectometer (left) and horizontal-sample liquids reflectometer (right).**

Specularly reflected neutron beams are generally quite compact , so reflectometer detectors are normally small (< 20×20 cm^2), featuring moderate (1 mm one-dimensional or 1 mm^2 pixel resolution two-dimensional position-sensitive detectors) or coarse (^{3}He tubes) spatial resolution. These small detectors may either be positioned to catch scattered neutron beams (see Figure 4.3 above) or remain fixed on an optical bench. The spatially diffuse nature of off-specular reflectivity and grazing-incidence scattering may more profitably be measured using larger fixed banks of detectors.

4.4 Instrument Concepts

4.4.1 SERGIS

While neutron specular reflectometry has been very successfully employed to probe layered structures, it has been less often used to probe the in-plane structures of thin films and membranes, essentially because the scattering from such low-volume systems is very weak. This problem is exacerbated by the fact that the typical sizes of interesting structures (1–100 nm) require rather well-collimated neutron beams. To overcome this problem, the technique of Spin Echo-Resolved Grazing Incidence Scattering (SERGIS) has been proposed [3] in which scattering angles of a broadly divergent beam are coded by the Larmor precession of neutron spins in a magnetic field in a variant of the well-known NSE method. A team of U.S. and European researchers at the ILL has recently successfully tested this technique. The SERGIS technique does not require either good neutron wavelength resolution or precise definition of the neutron trajectories with respect to the plane of specular reflection. Within the specular reflection plane, good beam collimation, as provided by adjustable slits that are traditionally used, is required to separate specular from diffuse scattering on the detector. Thus high-index neutron guides can be used to provide broad divergence, at least in one dimension. The only other difference between a SERGIS instrument and a traditional polarized-neutron reflectometer involves the installation of specially designed spin flippers that ensure the Larmor coding of neutron trajectories. Magnetic and magnetizable materials need to be avoided in the construction of the instrument since these can disturb neutron spin precession.

SERGIS is a technique that measures spatial correlations directly in real space rather than in reciprocal space. The technique yields a measure of the projection of the Patterson correlation function along one direction, chosen in the SERGIS case to be in the plane of the reflecting sample. Correlation lengths of up to 300 nm have been measured in the SERGIS geometry in a preliminary experiment at the ILL, while distances of up to 20 microns have been measured by the SESANS technique in bulk samples. There appears to be no inherent reason why such distances should not be achievable in the SERGIS case. By the time STS is built there are likely to be several possible solutions to the problem of designing suitable spin flippers for pulsed-source applications of SERGIS. Currently several designs have been proposed and are awaiting thorough testing. It appears likely that the SERGIS and SESANS techniques (Sect. 3.2.5) will be developed considerably over the next few years at less powerful neutron sources both in the United States and in Europe.

4.4.2 GISANS and GID

Grazing incidence small-angle neutron scattering (GISANS) and grazing incidence diffraction (GID) are traditional methods of measuring in-plane structures of surface layers and films. GID is used to measure short-range structure (length scales of a few tenths of a nanometer), whereas GISANS measures large length scales (~5 nm to 100 nm).

While several reflectometers (including both reflectometers at FTS) have been designed to measure GID, none, to our knowledge, has yet been constructed to measure GISANS. Doing so would probably require a converging beam geometry perpendicular to the specular reflection plane. Sophisticated converging-beam SANS instruments are beginning to appear (e.g., at HMI

in Germany) and we expect that these will provide the R&D platform required for the successful design of a GISANS instrument.

Because both GID and GISANS are severely intensity-limited by the small volumes of the samples they probe, STS would be a great step forward for both of these techniques.

4.4.3 Inelastic reflectometer

So far, very little work on the dynamics of motions associated with surfaces or interfaces has been done with neutrons, essentially because sample volumes are small and inelastic scattering signals are very weak. For example, in order to probe the out-of-plane dynamics of lipid membranes, Rheinstädter [4] was obliged to deposit several thousand bilayers on each of a stack of ~20 silicon wafers to obtain a total sample weight of 500 mg, sufficient for experiments with various spectrometers (triple-axis, back scattering and spin echo) at the ILL.

A fair amount of R&D would be needed to optimize the design of a reflectometer aimed at measuring inelastic scattering from surfaces and films. Various techniques, including chopper-based TOF, NSE, and modulated-intensity small-angle neutron scattering (MISANS) are plausible. Whichever technique is used, the principal design criterion is quite clear, namely to compensate for the low signal intensity by relaxing the instrumental resolution in all dimensions that are not essential for the measurement. There is no doubt that this type of measurement, which can provide important information about molecular interactions in membranes and films, can only be done at the world's most intense neutron sources such as STS.

4.4.4 Generalized polarization-analysis reflectometer

Full neutron polarization analysis is not always used in neutron reflectometry experiments. Often it is sufficient to polarize the incident neutron beam and to measure the specular reflectivity for incident neutrons polarized both parallel and antiparallel to a (usually saturating) magnetic field applied to the sample. More information can be obtained by analyzing both the Q-dependence and the neutron spin dependence of diffusely scattered neutrons. In particular, this technique has been used to obtain unique information about helical and fan-like magnetic structures in layered systems. Until now, however, these types of measurements have involved measuring only one component of the spin of the reflected neutrons. Even more information about the vector magnetization within a layered structure could be obtained by measuring the full tensor dependence of the polarized neutron scattering cross section. In this type of measurement, often known as generalized polarization analysis, the direction of the polarization of incident neutrons is controlled and the polarization direction of the scattered neutrons is accurately determined. Experiments at ILL (the only place where this technique has been extensively developed) have shown that, with bulk samples, exquisite information about magnetic structure can be obtained. We expect that the same improvement in the quality of information would also be available if the technique were applied to neutron reflectometry.

An instrument designed for generalized polarization analysis would follow traditional design principles for a polarization neutron reflectometer and would also need to be equipped with devices (like the ILL cryopad) to manipulate the polarization of neutrons incident on and scattered from the sample. It is likely that such a device could be mounted as needed on a polarized neutron reflectometer, which could otherwise function in the traditional manner already implemented at FTS. We expect the STS would be superior to FTS for generalized

polarization analysis measurements, essentially because the diffuse scattering that is measured arises from small scattering volumes and is therefore inherently weak.

4.4.5 Special-environment, small-sample, or kinetics reflectometer

Most existing neutron reflectometers occupy comparatively cramped quarters and so have limited capability to accommodate exotic sample environments or to allow extensive incident beam line modification. There has been a great deal of interest recently in carrying out complementary measurements, such as X-ray reflectivity, Brewster-angle microscopy, magneto-optic Kerr effect (MOKE), thin-film deposition, or gamma-ray spectroscopy simultaneously with neutron reflectivity measurements. Likewise, one would like to measure very small samples or to use high-intensity, low-resolution beams for kinetic studies. Both of these applications would benefit greatly from several meters of configurable front-end optics.

We therefore propose a beam line composed of a conventional front-end guide and chopper arrangement, followed by a configurable section capable of accommodating different focusing optics (significant R&D would be required to design these). The beam would then pass into a sample area large enough to install equipment for one or more complementary probes.

The low repetition rate of STS allows one to move farther away from the target monolith to claim more floor space. The longer-wavelength neutron spectrum, particularly that of an ultra-cold moderator, will greatly facilitate neutron focusing, making possible significantly smaller beams.

4.5 References

1. M. R. Fitzsimmons, " Reflectometry at continuous wave and pulsed-neutron sources," *Nuclear Instruments and Methods in Physics Research Section A*, **383**, 549–565, (1996).
2. J. F. Ankner, private communication (2007).
3. G. P. Felcher, S. G. E. te Velthuis, J. Major, H. Dosch, C. Anderson, K. Habicht, and T. Keller, "Spin-echo resolved grazing incidence scattering (SERGIS) of cold neutrons," *Proceedings of SPIE—Volume 4785, Advances in Neutron Scattering Instrumentation*, eds. Ian S. Anderson and Bruno Guerard, 164–173, November 2002.
4. M. C. Rheinstädter, C. Ollinger, T. Salditt, G. Fragneto, and F. Demmel, "Collective dynamics of lipid membranes studied by inelastic neutron scattering," *ILL Annual Report—2003*, Institute Laue-Langévin, 74–75.

5.0 SINGLE CRYSTAL DIFFRACTION: WORKING GROUP REPORT

Chair: B. Chakoumakos (ORNL)

Other Participants: L. Coates (LANL), C. Hoffmann (ORNL), D. Myles (ORNL), A. Schultz (ANL)

5.1 Scientific Case

Crystallographic studies of single crystals ranging from small molecules to macromolecular systems are fundamental to understanding their physical properties and functional behavior in chemical systems. In the case of newly synthesized crystals, crystallographic studies are among the first characterizations undertaken to determine the atomic arrangement. Generally, this is done with X-ray diffraction, using either laboratory-style diffractometers or synchrotron-based instruments. However, neutron diffraction offers significant complementarity to X-ray diffraction studies; and for the general problem of hydrogen atom location, magnetic structural studies, and many specific crystallographic problems, neutron diffraction is superior to the use of X-ray diffraction.

The major limitation to the wider use of neutron diffraction for single-crystal studies has been and will continue to be the availability of crystals of sufficient size to provide the necessary diffracted intensity. Although the feasible crystal size has continued to decrease with the advent of more powerful neutron sources such as ISIS, SNS, and J-PARC, for many materials, especially proteins, it is not possible to grow crystals with dimensions beyond a few hundred microns in volume with our current understanding and technology. The next-generation diffractometers, such as TOPAZ and MaNDi at the SNS, do promise to expand dramatically the range of feasible studies; and the need for additional single-crystal diffractometers at the SNS should be anticipated, although limitations imposed by current neutron detector technologies will become more apparent on these instruments. Diffraction studies using TOF methods at spallation neutron sources generally can out-perform reactor-based instruments in data collection rates and signal-to-noise ratio. The STS project offers the opportunity to expand and complement the existing instrument suite for doing single-crystal diffraction studies.

The existing suite of single-crystal diffraction instruments under construction and already planned for the FTS are (in order of expected completion) SNAP, TOPAZ, MaNDi, and CORELLI. SNAP is a dual-purpose instrument in that both powder and single-crystal studies can be undertaken, and its main purpose is to optimally support the use of high-pressure sample environments (e.g., Paris-Edinburgh pressure cells). TOPAZ is to be a workhorse small-molecule diffractometer, where “small” means less than about 50 Å average cell dimensions. MaNDi will be dedicated to larger unit cell sizes, 150 Å on average, and thus will mainly address the needs of the protein crystallography community. CORELLI will be dedicated to studies of diffuse scattering.

5.2 Instruments

5.2.1 HiMaNDi (high-throughput MaNDi instrument)

An instrument analogous to MaNDi on STS could possibly have more intensity and thereby alleviate the expected burden that will be placed on MaNDi from the biological macromolecular community. Given that existing neutron diffractometers for protein crystallography are currently over-subscribed, and the anticipated growth in this area over the several-year construction period for MaNDi, it is reasonable to assume that MaNDi will have a huge over-subscription the instant it is ready for users. In part this is likely to be caused by the increased number of protein systems suitable for neutron diffraction studies, arising from a reduction in the required crystal volume and advances in protein perdeuteration that improve the signal-to-noise ratio. These experiments are likely to form the cutting edge of neutron macromolecular crystallography utilizing small crystals with large unit cell repeats.

If we call such an instrument the high-throughput macromolecular neutron diffractometer (HiMaNDi), we can consider its performance in comparison with that simulated for MaNDi [1]. Situated on a decoupled hydrogen moderator, MaNDi is optimized to achieve 1.5 Å resolution from crystals 0.2–1 mm^3 with lattice dimensions of up to 150 Å (this includes 69% of the structures currently deposited in the Protein Data Bank). The performance, measured as experiment duration time, is shown for different moderators as a function of unit cell size in Fig. 5.1. For the coupled hydrogen case, which will be one of the moderators available on STS, HiMaNDi could shorten the experiment duration for unit cell sizes smaller than about 110 Å (this includes 48% of the structures currently deposited in the Protein Data Bank). For unit cells greater in size, MaNDi would be the instrument of choice.

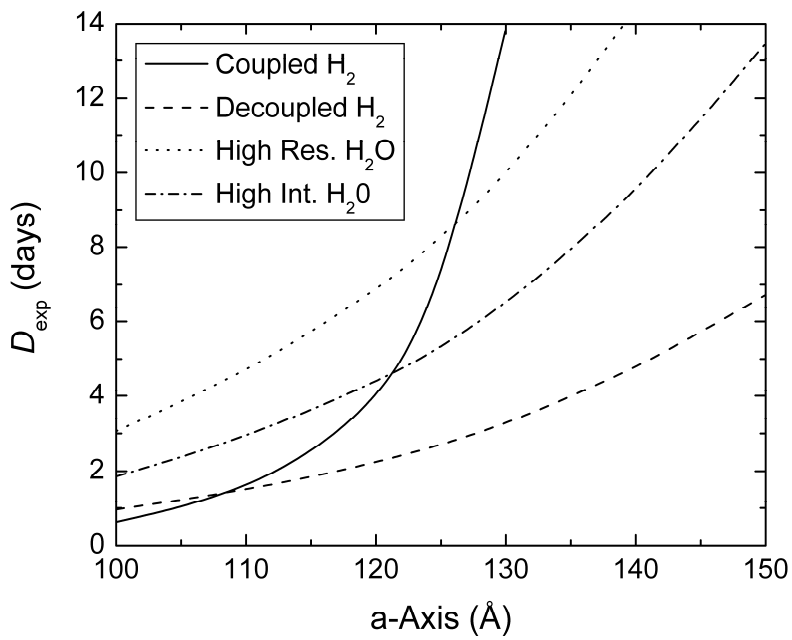

Fig. 5.1. Estimated experiment duration as a function of protein unit cell size for the MaNDi instrument [1]. Evaluated for a 98% perdeuterated crystal of volume 0.125 mm^3, d_{min} = 2 Å .

Again, if we use as a measure of performance the experiment duration time, we can compare the possible improvement of HiMaNDi situated on STS over that of MaNDi on FTS via a spreadsheet calculation [2]; see Table 5.1. In the table, four cases are compared. The first case (FTS-Dec-H_2) is for MaNDi at its home on FTS. The next three cases are HiMaNDi on STS, using a short proton pulse, a long proton pulse, and a long proton pulse with neutron pulse shaping provided by an "eye-of-the-needle" chopper system (long-pulse-EoN). The short-proton-pulse case offers possible gains of 3.5 times, but the primary flight path becomes long, nearly 300 m, to achieve the equivalent resolution. The two long-proton-pulse cases do not offer any gains. In particular, the eye-of-the-needle chopper system case does have higher raw flux, but this is all negated by the reduction in duty factors. Therefore, it is proposed that HiMaNDi on a short-proton-pulse version of STS should use a coupled moderator system and be optimized for protein crystals with unit cell dimensions of around 100 Å. Forty percent of the structures deposited into the protein data bank have all unit cell lengths less than 100 Å, and 62% (25861) have all unit cells lengths less than 150 Å. HiMaNDi would thus be complementary to the existing higher-resolution instrument MaNDi, enabling faster data collection for smaller unit cells but, perhaps more important, reducing the data collection times; this would enable the study of even smaller, weaker diffracting protein crystals less than 0.1 mm^3 in volume. This would make the study of many more protein systems feasible using neutron diffraction.

Table 5.1. Performance of HiMaNDi

	FTS_dec-H_2	**Short-pulse**	**Long-pulse**	**Long-pulse-EoN**	
	60	20	20	20	(Hz)
δt	25	300	1300	50	(μs) λ=2.86Å
L_1	24	288	1250	48	(m)
$\Delta\Theta_{inc,horiz}$	5.0	5.0	5.0	5.0	(mrad)
$\Delta\Theta_{inc,vert}$	5.0	5.0	5.0	5.0	(mrad)
Ω_{det}	2π	2π	2π	2π	(sr)
$\bar{\varphi}$	4.00E+06	5.83E+07	5.83E+07	1.79E+06	($n.s^{-1}.cm^{-2}.Å^{-1}$)
$\Delta\lambda_{BW}$	2.50	0.62	0.144	3.74	Å
V_s	1.25E-04	1.25E-04	1.25E-04	1.25E-04	(cm^3)
f_{sl}	0.10	0.10	0.10	0.10	(cm^{-1})
K	62.5	226	52.5	41.8	($n.s^{-1}$)
$t_{pattern}$	22	6	26	33	(hours)
FOM	1.00	3.65	0.84	0.67	cf. STS-1

EoN = 'Eye of Needle' pulse-defining chopper selecting and shaping a portion of the source pulse
$t_{pattern}$ = time to collect diffraction pattern containing 5,000,000 counts
FOM = figure of merit

5.2.2 Polarized sample diffractometer (polarized proteins) (J.K. Zhao)

As pointed out by Zhao [3], neutron scattering from dynamically polarized protons provides an effective way to study the structures of hydrogenous materials, particularly protein crystals. Hydrogen makes up about half of all the atoms in biological molecules. Its content in much other soft condensed matter is also high. Because the neutrons' interactions with hydrogen depend strongly on their spin states, polarized neutron scattering from polarized hydrogen atoms can both increase the coherent scattering signal and reduce the incoherent background. This approach obviates the need to deuterate samples and massively simplifies sample preparation. Many of the past applications of this method have focused on solution scattering from large biological complexes such as the ribosome.

High nuclear spin polarization in biological samples can be achieved by the technique of dynamic nuclear polarization [4–6]. It requires a high magnetic field (usually 2.5 T or higher), low temperature (1 K or lower), the presence of paramagnetic centers (free electron spins), and microwave irradiation. In biological molecules, the nuclear species important to polarized neutron diffraction/scattering are the proton and deuteron (if deuterated). Protons can be almost completely polarized under the condition of 2.5 T and ~500–600 mK. The maximal achievable polarization for deuterons is comparably smaller (~40%). Once the nuclear spins are polarized, they can be "frozen" at low temperature (~100 mK) and remain stable for the period of neutron diffraction measurement. The nuclear spin polarization can also be monitored and manipulated by nuclear magnetic resonance (NMR). Saturation of the proton or deuteron NMR signal will depolarize either of them completely while leaving the other untouched. This provides simplicity and clarity for the neutron diffraction/scattering experiment.

For biological macromolecular crystallography, the most useful aspects of using polarized neutrons are the huge increase in coherent and huge decrease in incoherent cross section of the proton–neutron interaction, which means higher diffraction peaks and lower background and thus a higher signal-to-noise ratio. Hydrogen strongly scatters neutrons, but mainly incoherently, as a result of the nuclear spin misorientation. The incoherent background scattering of hydrogen is a major obstacle to increasing the signal-to-noise ratio in neutron protein crystallography and other neutron experiments using hydrogen-rich samples. In a spin-aligned sample and with incident neutron spins parallel to the nuclear spin, the coherent scattering length of the protons varies from –3.74 fm (0% nuclear polarization) to 10.82 fm (100% polarization). The corresponding increase in total coherent cross section is from 1.8 barns to 14.7 barns, while the cross section for incoherent scattering decreases from 80 barns to zero. If these numbers were translated into diffraction from a typical protein, the increase in diffraction intensity would exceed 10-fold while the background would be reduced nearly to zero. Tremendous gain in signal-to-noise ratio can thus be obtained.

Further benefits of using polarized neutrons arise from the ability to have only one nuclear species polarized at a time, which will enable us to separate the diffraction from the protein molecule and from the solvent, if the solvent is deuterated. Of course, we must consider that the deuterated solvent will promote exchange of the labile hydrogens in the protein. Nevertheless, this approach should provide a way to study the protein–solvent interaction and hydrogen exchange on the protein surface, which is important to many enzyme functions.

Polarized neutrons also hold the hope of solving the phase problem ab initio for neutron protein crystallography. Many macromolecules have known structures of a subdomain/subunit (like ribosome). If the macromolecule is crystallized with this subdomain/subunit deuterated, the

diffraction from this part of the molecule can be separated from the rest of the molecule and be used as the initial phase to solve the structure of the whole macromolecule. Another possibility is to use "polarized proton spin clusters" surrounding the paramagnetic centers that are fixed on a protein [3,7] as the initial phase. The diffraction of such a spin cluster can also be extracted and the structure of it should be solvable by direct methods. The advantage is that no specific deuteration is required. For molecules whose structures are difficult to solve by isomorphous replacement or other techniques of X-ray crystallography, polarized neutron protein crystallography will provide a powerful alternative approach to resolving their structures ab initio.

The polarized neutron option would require an ~5 Tesla magnet, a ^{3}He/^{4}He dilution refrigerator with large cooling power and capable of achieving temperatures of ~50–100 mK, a microwave generator (140 GHz for a 5T field) and an NMR system. The higher magnetic field and large cooling power of the cryostat are both needed to achieve high nuclear polarization, which in turn is essential to maximize the benefit of increasing diffraction intensity and decreasing background incoherent scattering. For optimal nuclear polarization, the desirable temperature in the sample should be ~500 mK or lower during dynamic polarization, i.e., while microwaves are irradiating the sample. The lowest achievable temperature (~100 mK, without microwave irradiation) is needed to keep the proton/deuteron spins frozen with minimal loss in polarization during the neutron diffraction measurement. The polarized neutron option would also require a polarized incident beam.

This concept could be implemented in a dedicated instrument, and given today's technology, the required ancillary equipment probably could be accommodated only in a dedicated instrument. However, given some advances over the next few years in high-field magnet designs, NMR systems, dilution refrigerators, and neutron polarization filters, it is conceivable that the ability to spin polarize the sample could be provided by a complex ancillary equipment system, which could be mounted on an existing instrument.

The best location of such a system or instrument will likely be determined by the need to determine high-resolution crystal structures. This suggests the use of a water moderator on STS, or use of FTS or an unallocated location. Other design aspects to consider are that the use of the high-field magnet will limit the scattering view to a few degrees above and below the scattering plane.

5.2.3 High-resolution, high-intensity, polarized small-molecule diffractometer

For many studies of materials and their properties, obtaining information at length scales to a few hundredths or less of an Angstrom is crucial. The following is a partial list of the types of phenomena for which resolving small d-spacings is important:

- order-disorder transitions
- displacive transitions
- anharmonic motion
- critical scattering
- Huang scattering
- domain structures
- incommensurate satellite peaks
- hydrogen bonding

- magnetostriction

The properties of materials are most clearly related to their underlying crystal structures. Atomic displacement parameters, or Debye-Waller factors, are usually treated as harmonic motion, although anhamonic motion is critical in understanding the properties of many materials and phenomena, such as ionic conductors and ferroelectric transitions. The treatment of anharmonic motion requires accurate diffraction data on small d-spacings. Only neutron diffraction data can do this unambiguously, since X-ray data include the nonspherical electron deformation density.

Some of the other issues in the above list—displacive transitions, anharmonic motions, and critical scattering—are all important to materials such as ferroelectrics, ionic conductors, CMR materials, and superconductors. Critical scattering is particularly applicable to CMR and superconducting materials. Anharmonic motion and the transition between single and double well potentials are important properties of many hydrogen bonds, which are essential to understanding materials from minerals to proteins. The characterization of incommensurate satellite peaks from high-T_c superconductors is essential to understanding the oxygen ordering in those materials. In addition, anomalously low thermal conductivity in crystals is intimately linked to rattling and positionally disordered atoms and molecules positioned in oversized atomic cages. Two important examples are the clathrate hydrates and clathrate semiconductors. Optimizing low thermal conductivity in thermoelectric materials such as the clathrate semiconductors can greatly improve their overall efficiency, making them viable for refrigeration and power generation devices.

A high-Q single-crystal diffractometer (HiQSCD), situated on a 20 Hz source with a room-temperature water moderator, would complement TOPAZ (60 Hz, cold hydrogen moderator). HiQSCD would require only a small bandwidth of short-wavelength neutrons. A beam line of 100 m on STS would have a bandwidth of 1.5 Å and very good $\delta t/t$ resolution. A segmented tapered guide should provide a good balance of flux and incident beam divergence. In addition, neutron polarization capabilities would permit magnet studies and take some of the demand from TOPAZ for this type of experiment.

5.2.4 Diffuse scattering diffractometer

Defects and disorder in crystals are central to the useful properties of many technologically functional materials. Not surprisingly, there is a consensus among experienced X-ray and neutron diffraction users that diffuse scattering from crystals has the potential to offer great insights to understand disorder and defects in a full range of materials from alloys to biological macromolecular structures. Indeed, coherent diffuse scattering from single crystals may be the most powerful probe of complex disorder because it is the measure of both the local distortions around defects and the length scale and spatial distribution of defect–defect correlations. Although more powerful X-ray and neutron sources, better area detectors, and more powerful computers make it possible to record and model the diffuse scattering distributions from crystals, it is also recognized that instruments optimized to study diffuse scattering and the tools to fully analyze diffuse scattering are underdeveloped. As a statement of interest from the user community, the American Crystallographic Association has devoted its transactions symposium this year to the subject of diffuse scattering.

One of the challenges to measuring diffuse scattering is that the intensity is generally orders of magnitude weaker than Bragg scattering, yet it is generally desirable to record both. TOF methods offer a great advantage, compared with quasi-Laue methods at reactor sources, in being able to clearly separate the Q-dependence. Most diffractometers with large area detectors obviously can and do record the diffuse along with the Bragg scattering from a single crystal; however, the design of these instruments has not been optimized with diffuse scattering as the primary goal. One of the main problems is that the diffraction experiment includes no energy analysis, so the static diffuse scattering is included with that arising from vibrational and other dynamic processes in the sample. The proposed instrument, CORELLI, aims to solve this problem by combining the high efficiency of white-beam Laue diffraction with energy discrimination produced by the use of a statistical chopper. CORELLI is included in the SING II instrument suite and will be located on the FTS.

There are formidable difficulties in using the diffuse scattering distribution to construct 3-dimensional models of defect structures. Given that large volumes of reciprocal space can be mapped efficiently, the immense data sets that result are difficult to analyze. In contrast to average-structure determination problems, where only Bragg peaks are integrated, one needs to simultaneously fit a defect structural model against every voxel in the dataset.

Will CORELLI be able to satisfy the needs of the diffuse scattering user community, which is expected to grow significantly over the next few years? Are there benefits to locating a diffuse scattering instrument on STS compared with FTS? These questions are difficult to answer because the effectiveness of the cross-correlation method to be employed in CORELLI has not been fully tested yet. Experiments later this year at ANL are specifically designed to field test the Monte Carlo simulations of the cross-correlation principle. The CORELLI instrument at SNS is not scheduled for completion until 2013. Generally speaking, the higher resolution afforded by shorter wavelengths and a large Q-range is necessary to elucidate the local short-range order in materials. Along with energy discrimination, because the diffuse scattering is often weak, background scattering from extraneous sources must be reduced as much as possible.

5.2.5 "Neutron microscope" for topography, magnetic domains, texture, and depth profiling

Neutron diffraction topography is an imaging technique based on Bragg diffraction. It provides a 3-dimensional intensity mapping of the beam(s) diffracted by a crystal. This method was originally developed for X-ray diffraction, where only the defects within the penetration depth (near-surface) of the X rays could be imaged, and the detector that could provide sufficient spatial resolution was film. This has restricted spatial resolutions to greater than a micrometer, although it has been recently suggested that sub-100 nm resolutions are possible using a technique exploiting both diffraction and absorption contrasts with the use of focusing X-ray optics [8]. Some beam lines at synchrotrons, such as X-19C at NSLS, are dedicated to this purpose of X-ray topography. A practical guide for recording and analyzing X-ray topographs is given by Black and Long [9]. Given the large penetration depth of neutrons in most materials, it is possible to imagine using this approach for 3-dimensional mapping within large single crystals, where the gauge volume is defined by incident and diffracted beam collimation. Moreover, with a polarized neutron beam, it is possible to image magnetic domains in a wide range of magnetic crystals. Neutron topography has been variously demonstrated since the early

1970s [10–12], but the number of papers published utilizing this method since then has remained small, ~20 [13–15].

Topography is used for the visualization of defects (e.g., dislocations, twins, domain walls, inclusions, impurity distribution) present in the crystal volume. More exactly, it records the long-range distortion fields and/or the strain fields associated with a macroscopic crystal deformation. Their observation becomes possible because these distortion fields can affect the diffracted intensity, so as to give "contrast" (non-homogeneous intensity distribution) in the image. In this way, topography is a study of the fine structure of a Bragg spot, which contains the information about the departures from the perfect crystal structure, i.e., the defect structure. The principle of this method is illustrated in Fig. 5.2.

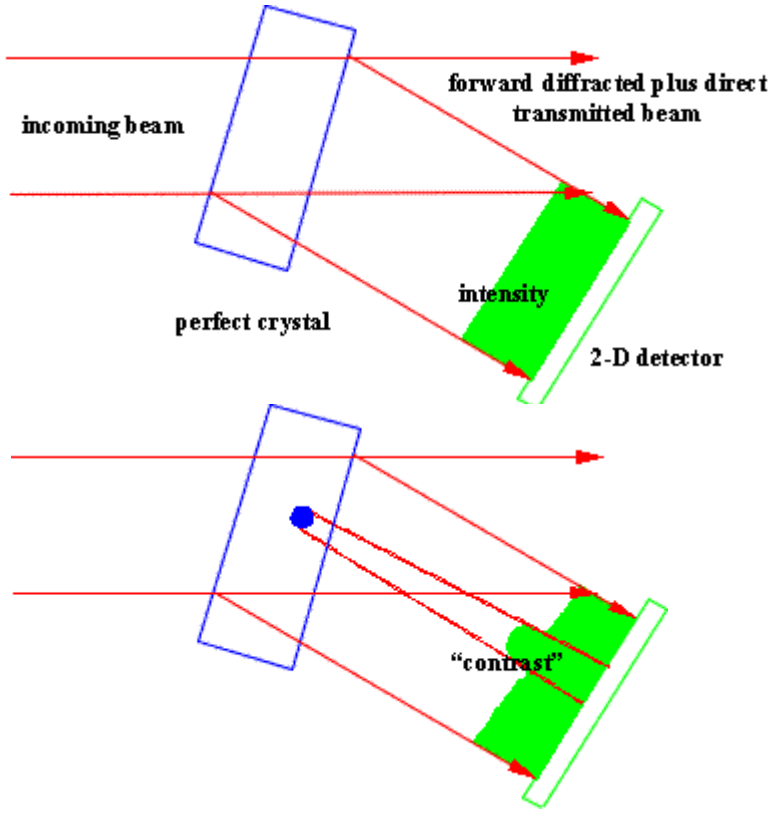

Fig. 5.2. Neutron diffraction topography—schematic.

Neutron topography previously has been done at reactor sources, and the detector has been film with a suitable converter, such as ^{157}Gd. To make use of the white beam from a spallation source, the detector would have to have time and space resolution. The latter would require some R&D over the next few years to achieve a spatial resolution like that of film in a scintillation detector. Meanwhile, some types of neutron topographic studies could be done at the HFIR using the existing HB-2B residual stress diffractometer. A more efficient, dedicated instrument could be considered for the HFIR cold-guide hall, because such an instrument would greatly benefit from having low background. Alternatively, one could think of having a portable high-resolution detector and sample positioning stage that could be viewed as ancillary equipment for performing neutron diffraction topography on an existing instrument. With more expansive

detector coverage, one can envision a different mode of operation to retrieve grain orientations from a polycrystalline aggregate consisting of greater than mm-sized crystals, and thereby determine the preferred orientation or texture of the overall aggregate. Actual examples of such problems exist in the geological sciences. For instance, determining the texture of mantle-derived peridotite nodules (composed of olivine and pyroxene crystals) brought up by volcanic eruptions could provide insight into the texture and, hence, flow structure of the source region. This has great implications for understanding the geodynamics of the upper mantle and lower crust of the earth.

5.2.6 Quasi-Laue single-crystal diffractometer

A quasi-Laue diffractometer, which we are calling IMAGINE for the purposes of this report, could be quickly installed on the CG-4 end-station in the HFIR Cold Guide Hall. IMAGINE would be designed to rapidly collect diffraction data from single crystals, even of small dimensions (< 0.1 mm). The instrument would employ a vertically oriented cylindrical detector with neutron-sensitive image plates. This geometry, in principle, would allow the instrument to accommodate a wide range of sample environment equipment, including furnaces, high-pressure cells, and cryomagnets. The user community targeted would be as diverse as the single-crystal diffraction community, including researchers studying small protein structures, pharmaceuticals, minerals and other inorganic crystals, small molecules, molecular organometallic crystals, and metal organic frameworks, etc. This kind of system can readily be purchased complete and is effectively a turnkey system, fully automated with a user-friendly GUI, ready to operate upon installation (see Fig. 5.3 below).

The image plates are erasable and reusable and cover a large area of reciprocal space enabling rapid data collection. They have sensitive areas of 400×800 to 450×1250 mm^2. The integrated reading system provides pixel resolution down to 100 μm. Additional advantages include a compact design, 2×1×1 m, which provides for a small instrument footprint. Built-in sample rotation about the vertical axis has a precision of 0.1°. The major drawback to image plate detectors is that they do not offer real-time readout. Several minutes are required to read and erase a detector bank paneled with image plates. A better detector system would employ either gas-filled, scintillation, or solid-state detector modules, which can have greater efficiency and provide the capability for real-time data collection. In addition, these alternatives could provide better gamma discrimination, reducing the level of background on the diffraction image. Real-time detectors are essential for many parametric studies. This advanced quasi-Laue instrument concept has been proposed by the ILL [16].

Implementation of the commercially available instrument with the image plate detector system can be done on a short time scale, because the complete turnkey system can be purchased for less than $800K. LADI III, a quasi Laue protein diffractometer based at the Instituit Laue-Langevin, was purchased as a turnkey system and installed during 2005 and is now in operation collecting data.

The impact of such an accelerated timeline (less than 2 years) for installation of such an instrument would be significant, because it could come online several years prior to MaNDi on FTS and thereby immediately begin building a protein crystallography user community for MaNDi and any further protein crystallography instruments built at the SNS.

This is important, as the production of the large protein crystals needed for neutron diffraction is time consuming and can take several months. Such samples are not always stable indefinitely; thus once large crystals are produced, data collection should proceed as quickly as possible. The only dedicated protein crystallography instrument in North America currently is the Protein Crystallography Station (PCS) based at LANSCE at LANL. That instrument is highly oversubscribed and is unable to meet the data collection needs of the current user community, let alone the needs of the community in several years.

R&D on a real-time detector system could begin at the same time and run in parallel with the operation of IMAGINE, so that at a future date IMAGINE could undergo an upgrade to replace the image plate system with the real-time detector system. The HFIR guide hall is a good location for IMAGINE because of the ample space, low background, and guide characteristics. One drawback would be having the planned U.S.–Japan Program triple-axis spectrometer upstream, which would reduce various energies of the incident spectrum when it was operating at the same time as IMAGINE. In addition, there are two additional instrument positions upstream on CG-4 that are presently not allocated.

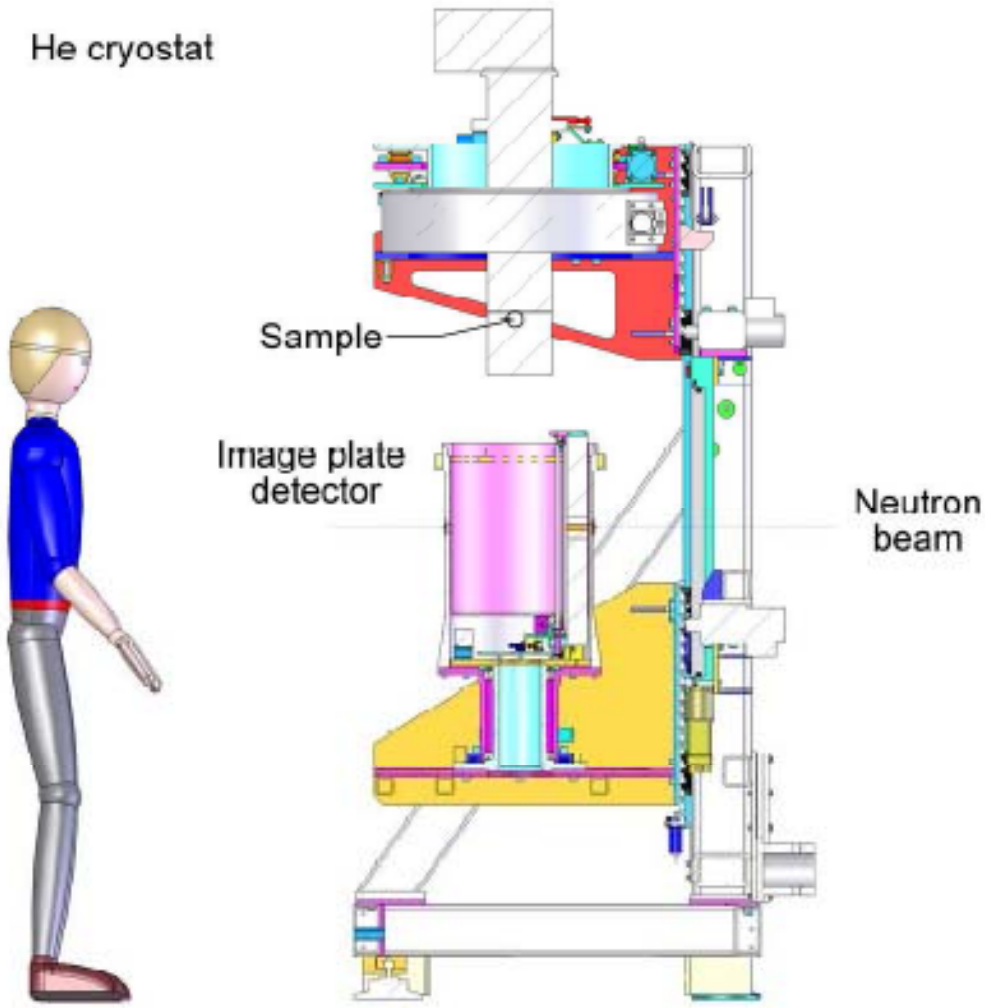

Fig. 5.3. Turnkey quasi-Laue instrument—schematic.

5.3 References

1. A.J. Schultz, P. Thiyagarajan, J. P. Hodges, C. Rehm, D. A. A. Myles, P. Langan, and A. D. Mesecar, "Conceptual design of a macromolecular neutron diffractometer (MaNDi) for the SNS," *J. Appl. Cryst.* **38**, 964–974 (2005).
2. J. Hodges, private communication (2007).
3. J. K. Zhao, "Dynamically polarized hydrogenous materials for neutron scattering," *Physica B* **356**, 168–173 (2005) .
4. H. B. Stuhrmann, O. Schärpf, M. Kumpolc, T. O. Niinikoski, M. Rieuland, and A. Rijllart, *European Biophysics Journal* **14**, 1–6 (1986**).**
5. W. Knop, M. Hirai, H.-J. Schink, H. B. Stuhrmann, J. Zhao, O. Schärpf, R. R. Crichton, M. Krumpolc, K. H., Nierhaus, A. Rijllart, and T. Niinikoski, *J. Appl. Cryst.* **25**, 155–165 (1992**)**.
6. J. K. Zhao, W. Meerwinck, T. Niinikoski, A. Rijllart, M. Schmitt, R. Willumeit, and H. Stuhrmann, *Nuclear Instruments and Methods A* **356**, 133–13 (1995).
7. J. K. Zhao, "Protein Crystallography with Polarized Neutrons," unpublished (1998).
8. Y. Chu, "Bright field x-ray topography with sub-100-nm spatial resolution," APS March Meeting, abstract S6.00002, 2007, http://meetings.aps.org/Meeting/MAR07/Event/61159.
9. D. R. Black and G. G. Long, *X-ray Topography*, NIST Special Publication 960-10, 64 pp. (2004).
10. K. Doi, N. Minakawa, H. Motohashi, and N. Masaki, "Trial of neutron diffraction topography," *J. Appl. Cryst.* **4**, 528 (1971) .
11. M. Ando and S. Hosoya, "Q-Switch and polarization domains in antiferromagnetic chromium observed with neutron-diffraction topography," *Phys. Rev. Lett.* **29**, 281–285 (1972).
12. M. Schlenker and C. G. Shull, *J. App. Phys.* **44**, 4181 (1973).
13. M. Schlenker and J. Baruchel, "Observation of magnetic domains by neutron diffraction topography," *IEEE Transactions on Magnetics* **MAG-17**(6), 3085–3089 (1981).
14. Y. G. Abov, N. O. Elyutin, and A. N. Tyulyusov, "Dynamical neutron diffraction on perfect crystals," *Physics of Atomic Nuclei* **65** (11), 1933–1979 (2002).
15. M. Dudley, J. Baruchel, and Jn. Sherwood, "Neutron topography as a tool for studying reactive organic-crystals—A feasibility study," *J. Appl. Cryst.* **23**, 186–198 (1990).
16. A. W. Hewat, B. Ouladdiaf, G. J. McIntyre, M-H. Lemee-Cailleau, D. Brau, and S. York, "CYCLOPS, A proposed high flux CCD neutron diffractometer," proposal to the ILL Millennium Programme Symposium, 4 pp. (2006)

6.0 POWDER DIFFRACTION: WORKING GROUP REPORT

Chair: J. Hodges (ORNL)

Other Participants: A. Huq (ORNL), R. McGreevy (RAL), T. Proffen (LANL), J. Richardson (ANL), A. Stoica (ORNL), X.-L. Wang (ORNL), A. Wilkinson (Georgia Tech)

6.1 Overview

6.1.1 General

The study of atomic structure and transformations spans engineering materials, chemistry, condensed matter physics, geoscience, and biology. Regardless of whether a material is ordered crystalline or disordered, quantitative atomic short- and long-range correlations (structure) can be obtained from a measured S(Q). Ideally a materials diffractometer would measure $S(Q)$ over a very broad Q range, with extreme $\delta Q/Q$ resolution over a minute sample volume in next to zero time. Neutron source limitations and sample size aspects, however, mean that neutron diffractometers are generally optimized to match one of these features to a chosen science area. For example high $\delta Q/Q$ resolution, high neutron flux, large sample capability and wide Q range are appropriate for investigating complex crystal structures, kinetic transformations, engineering and disordered materials (dominated by short-range atomic correlations), respectively.

Powder neutron diffractometers at pulsed spallation sources have been particularly successful, primarily because the TOF aspect that comes from the pulsed nature of the source can effectively be used in the place of a monochrometer, which would normally reject 97–99% of the incoming neutron beam.

6.1.2 Desired capabilities

The inability to build an *ideal* materials diffractometer, combined with the broad science base to which diffraction can be applied, means that a diverse suite of neutron diffractometers is required in the United States for materials science. An idea of the complete diffractometer suite required can be generated from considering recent trends in materials science and from a differential analysis of types of boundary-pushing diffraction experiments with respect to a generic powder diffraction experiment. Current trends include increasing complexity (spatial inhomogeneity, symmetry lowering, large unit cells, multiple structure-property couplings, …), new length and time scales, increasing interest in deviations from long-range order, complex spin systems, and more emphasis on organic and organic-containing materials. The beyond generic experimental characteristics that come from these considerations are

- High reciprocal space resolution
  - $\delta d/d \sim 3\times10^{-4}$ at d = 1 Å
- High spatial resolution
  - Ideally ~10 μm, but 100 μm still good
- Fine time resolution

- High data rate for mapping
- Parametric studies
- Real time transformations, nucleation, crystallization, grain growth …
- Measurements in seconds at $\delta d/d = 10^{-3}$ resolution

- Wide *Q*-range
  - Access to $Q > 40$ Å^{-1} for total scattering on well ordered materials
- Simultaneous access to large d-spacings
  - Self-assembled ordered nanomaterials
  - At minimum 0.5 Å < d < 50 Å
- Multiple structural length scales
  - Combined SANS and diffraction
  - Continuous coverage down to $Q_{min} = 0.003$ Å^{-1}
- Suppression of incoherent scattering
  - Facilitation of studies of organic materials
- Energy discrimination
  - Separate elastic and inelastic diffuse components
- Polarized neutron beam and analysis
  - Complex spin structures
  - Spin pair distribution function determination

6.1.3 Proposed instruments

The United States has a number of world-class neutron materials diffractometers in operation or under construction. At the LANSCE, there is SMARTS, NPDF and HIPPO. At NCNR, there is BT-1, a high-resolution powder diffractometer. At SNS are POWGEN3, VULCAN, and NOMAD. At HFIR, the powder diffractometer is undergoing an upgrade that will be completed shortly. These instruments together form a core suite of materials diffractometers with some overlap of capabilities and a certain degree of redundancy across the suite.

The current suite of U.S. materials diffractometers have or are expected to have good performance for the most sought-after types of characterization experiments, but many of the boundary-pushing experimental characteristics listed above cannot be met. To fulfill these unmet instrument needs, the following materials diffractometers are proposed for consideration to be included in a suite of STS instruments.

- Very High Resolution Powder Diffractometer
  - ab-inito structure determination
  - incommensurate systems
  - microstructure through peak shape analysis
- Very Fast Powder Diffractometer
  - for small sampling volume (crystallography and engineering studies)
- Long-distance G(r) Diffractometer
  - very high data rates at good resolution for disordered solids with high Q resolution and energy selection
  - should complement NOMAD

- High Magnetic Field Diffractometer
  - polarized sample, beam and analysis
  - spin-lattice coupling phenomena and phase mapping
- Ultrahigh-Pressure Diffractometer
  - smaller sample volumes than SNAP
  - high flux for total scattering measurements
- Simultaneous Wide Angle Neutron Spectrometer (SWANS)
  - a combined wide and small angle instrument
  - quasielastic–inelastic capability
  - high-temperature metallurgy, hydrogen, and oxygen diffusion and location

6.2 Comparative Performance of Several Proposed Materials Diffractometers

6.2.1 Basis for comparison

In this section we present quantitative performance estimates for several of the proposed diffractometers on both a short-proton-pulse and a long-proton-pulse version of STS. Ideally performance of a diffractometer can be estimated from the integrated Bragg intensity function:

$$II_\tau = \sum_{pixels} \Omega_{\text{pixel}} \varphi(\lambda) \varepsilon(\lambda) \frac{d_\tau^4 \sin\theta}{2\pi} \frac{N_s}{\upsilon_{uc}} j_\tau |F_\tau|^2 \tag{6.1}$$

where $\varphi(\lambda)$ = incident neutron flux at the sample position, $\varepsilon(\lambda)$ = detector efficiency, N_s = number of unit cells in sample, υ_{uc} = unit cell volume, j_τ = reflection multiplicity and F_τ = structure factor for reflection τ.

$$II_\tau = F_{eff} \frac{N_s}{\upsilon_{uc}} j_\tau |F_\tau|^2 \tag{6.2}$$

$$F_{eff} = \sum_{pixels} \Omega_{\text{pixel}} \varphi(\lambda) \varepsilon(\lambda) \frac{d_\tau^4 \sin\theta}{2\pi} \tag{6.3}$$

where $F_{eff}(d)$ is a function that effectively represents the counting performance for a specific configuration of the instrument. With some loss of accuracy, the sum of all pixels in Eq. (6.3) can be avoided by the following instrument performance approximation

$$K = \frac{\Omega_{\text{det}}}{4\pi} \overline{\varphi} \Delta\lambda_{\text{BW}} \overline{\varepsilon} V_s f_{\text{sl}} \tag{6.4}$$

where K = experiment count rate ($n.s^{-1}$), Ω_{det} = total detector coverage (sr), $\overline{\varphi}$ = average incident neutron flux at the sample position ($n.s^{-1}.cm^{-2}.Å^{-1}$), $\overline{\varepsilon}$ = average detector efficiency, $\Delta\lambda_{BW}$ = incident neutron wavelength bandwidth (Å), V_s = sample volume (cm^3) and f_{sl} = fraction of incident neutrons scattered by sample per unit thickness (cm^{-1}). The average incident neutron flux at sample must account for any guide gain; vertical guide gain is denoted g_v below. The fractional scattering length used in these calculations has been 10% for 1 cm thickness of sample.

6.2.2 Very fast powder diffractometers (three instruments: small sampling volume, very high magnetic field, very high pressure)

A sample gauge volume of $V_s = 2\times2\times2$ mm^3 has been assumed; this represents 32 mg for a sample density $\rho = 4$ g.cm^{-3}. The resolution required is $\delta d/d = 5\times10^{-3}$ at d ~ 2 Å, and since geometric sample contribution to resolution will be negligible, this sets $\delta\lambda/\lambda = 3.2\times10^{-3}$. This can be combined with moderator pulse width, δt, calculations (a representative wavelength λ = 2.86 Å is used here) to determine L_1 the moderator to sample flight path distance by

$$L_1 = v_\lambda t \text{ and since } \frac{\delta t}{t} = \frac{\delta\lambda}{\lambda} \tag{6.5}$$

$$L_1 = v_\lambda \delta t \left(\frac{\delta\lambda}{\lambda}\right)^{-1} \tag{6.6}$$

where $v_\lambda = 3956/\lambda$ is the velocity of λ wavelength neutrons (m.s^{-1}) and t is time of flight from moderator to sample. The geometric contribution to instrument resolution at $2\theta = 90^\circ$ is matched to the pulse width contribution by

$$\frac{\delta\lambda}{\lambda} = \Delta\Theta_{inc} \cot 2\theta \tag{6.7}$$

Regardless of whether the incident neutrons are transported by evacuated collimator, supermirror guide system, or some other optic device, the beam divergence has been assumed to be symmetric; the horizontal and vertical beam divergences are equal.

Based on the above considerations, the performance of a very fast powder diffractometer on various beam lines can be estimated for comparison. This has been done for FTS dec-H_2, and for short-proton-pulse and long-proton-pulse versions at STS in Table 6.1.

For many experiments where d-spacings < 1 Å are not required—including moderate complexity crystallography, kinetics, phase transitions, spin structures, engineering materials, and mapping of orientation distribution functions—a very fast powder diffractometer situated on the short-proton-pulse version of STS offers almost an order of magnitude gain. The long flight path distance, L_1 = 130 m, of this instrument is a drawback, but perhaps some of this can be overcome by a frame multiplication method.

The performance merit above applies equally to the special-environment diffractometers proposed—High Magnetic Field Diffractometer and Ultrahigh Pressure Diffractometer. In the case of the High Magnetic Field Diffractometer, the long L_1 distance is perfectly fine, since such an instrument also needs to be situated far out to provide adequate lateral space to accommodate the magnet and to minimize stray magnetic field interference with other instruments.

Table 6.1. Performance of a very fast powder diffractometer

	FTS dec-H_2	Short-pulse	Long-pulse	Short-pulse FM	Long-pulse FM	
	60	20	20	20	20	(Hz)
δt	25	300	1300	100	100	(μs) λ=2.86Å
L_1	10.8	130	562	43	43	(m)
$\Delta\Theta_{inc}$	3.75	3.75	3.75	3.75	3.75	(mrad)
L_{FMC}	–	–	–	2	6	(m)
FM	–	–	–	×8	×x6	
Ω_{det}	2π	2π	2π	2π	2π	(sr)
$\bar{\varphi}$	8.96E+05	3.27E+07	3.27E+07	3.48E+07	6.03E+06	($n.s^{-1}.cm^{-2}.Å^{-1}$)
$\Delta\lambda_{BW}$	5.55	1.39	0.32	0.52	0.67	Å
V_s	0.008	0.008	0.008	0.008	0.008	(cm^3)
f_{sl}	0.10	0.10	0.10	0.10	0.10	(cm^{-1})
K	1990	18200	4190	7180	1620	($n.s^{-1}$)
$t_{pattern}$	50	6	24	14	62	(s)
FOM	1.00	9.11	2.10	3.61	0.81	cf. STS-1

FM = frame multiplication technique / factor
L_{FMC} = moderator to frame multiplication chopper distance
$t_{pattern}$ = time to collect diffraction pattern containing 100,000 counts
FOM = figure of merit
ε = 1 is assumed for this table

6.2.3 Very-high-resolution powder diffractometers

A sample volume of $V_s = 4\times12\times4$ mm^3 has been assumed; this represents 0.77 g for a sample density $\rho = 4$ $g.cm^{-3}$. With a resolution required of $\delta d/d = 3\times10^{-4}$ at $d \sim 2$ Å, and assuming approximately equal contributions to resolution by pulse width, incident beam divergence, and sample size, this sets $\delta\lambda/\lambda = 1.6\times10^{-4}$ at a representative wavelength $\lambda = 2.86$ Å. The incident beam divergence is assumed to be asymmetric with $\Delta\Theta_{vert}/\Delta\Theta_{horiz} = 4$, and the $\Delta\Theta_{horiz}$ contribution is matched to the pulse width contribution at a backscattering angle of $2\theta = 140°$.

From the above considerations, the performance of a very-high-resolution diffractometer on various beam lines can be estimated for comparison. This has been done for FTS dec-H_2, and short-proton-pulse and long-proton-pulse beam lines in Table 6.2.

Table 6.2. Performance of a very-high-resolution diffractometer

	FTS_dec-H_2	Short-pulse	Long-pulse	Long-pulse-EoN	
	60	20	20	20	(Hz)
δt	25	300	1300	15	(μs) λ=2.86Å
L_1	216	2594	11239	130	(m)
$\Delta\Theta_{inc,horiz}$	0.45	0.45	0.45	0.45	(mrad)
$\Delta\Theta_{inc,vert}$	1.80	1.80	1.80	1.80	(mrad)
Ω_{det}	2π	2π	2π	2π	(sr)
$\bar{\varphi}$	1.30E+05	1.89E+06	1.89E+06	1.74E+04	($n.s^{-1}.cm^{-2}.Å^{-1}$)
$\Delta\lambda_{BW}$	0.278	0.069	0.016	1.388	Å
V_s	0.192	0.192	0.192	0.192	(cm^3)
f_{sl}	0.10	0.10	0.10	0.10	(cm^{-1})
K	345	1260	291	232	($n.s^{-1}$)
$t_{pattern}$	24	7	29	36	(mins)
FOM	1.00	3.65	0.84	0.67	cf. STS-1

EoN = "Eye of needle" pulse-defining chopper selecting and shaping a portion of the source pulse
$t_{pattern}$ = time to collect diffraction pattern containing 500,000 counts
FOM = figure of merit

6.2.4 Long range pair distribution function diffractometer

This instrument is intended to study disordered complex materials (nanodomains) and nanoparticles and should complement NOMAD, the disordered materials diffractometer at FTS. It should at the same time provide a large accessible momentum transfer and a good momentum transfer resolution. While the accessible momentum transfer determines the real space resolution ($\delta r = \pi/Q_{max}$), the momentum transfer resolution determines the range over which atomic correlations can be determined. A nice demonstration of this principle has been achieved for gold nanoparticles of varying size (Fig. 6.1). High momentum transfer resolution therefore plays a role if the coherence length in the structure is on the order of several tens to a couple of hundreds of Å as in many new nanomaterials. It has been shown that a number of effects difficult to characterize with any other method exist, for example, in the frustrated magnetic system $LiNiO_2$, such as anomalous peak broadening, local Jahn Teller distortions, and inverted temperature dependence of medium-range correlation (Fig. 6.2). While a high momentum transfer resolution (~0.2%) is available in a limited angular range at NOMAD, an instrument optimized for that purpose could provide high resolution with much higher throughput, which is especially critical for novel materials that are usually available in small quantities only.

The instrument should provide the following characteristics:

- Wide Q range (0.4–40$Å^{-1}$), resolution ~0.1%

- Possibility to measure S(Q,ω=0).
- Sufficient flux at small d (<0.5Å) but also needs low-q
- Best suited for FTS, water moderator

6.2.5 SWANS—simultaneous wide- and small-angle neutron scattering

This instrument is designed to study diffusion-controlled problems in metallurgy, catalysis, and hydrogen-containing materials. The following are the desired characteristics:

- Optimized for compatible data rates (~10 s)
  - Use multi-slit choppers to select multiple bandwidths for wide- and small-angle scattering
- Quasielastic – inelastic capabilities
  - Inverse geometry with analyzer crystals
  - 20 μeV resolution
  - Up to 200 meV dynamic range
- Simultaneous characterization
  - Differential scanning calorimetry
  - Dilatometry
  - TGA

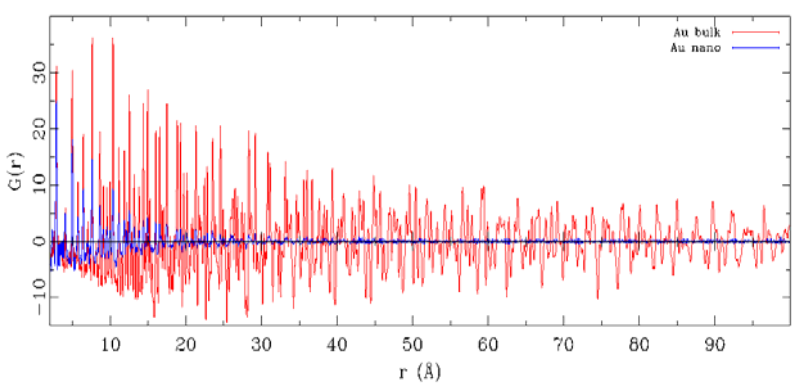

Fig. 6.1. Long-range pair distribution functions— Au nanoparticles [2].

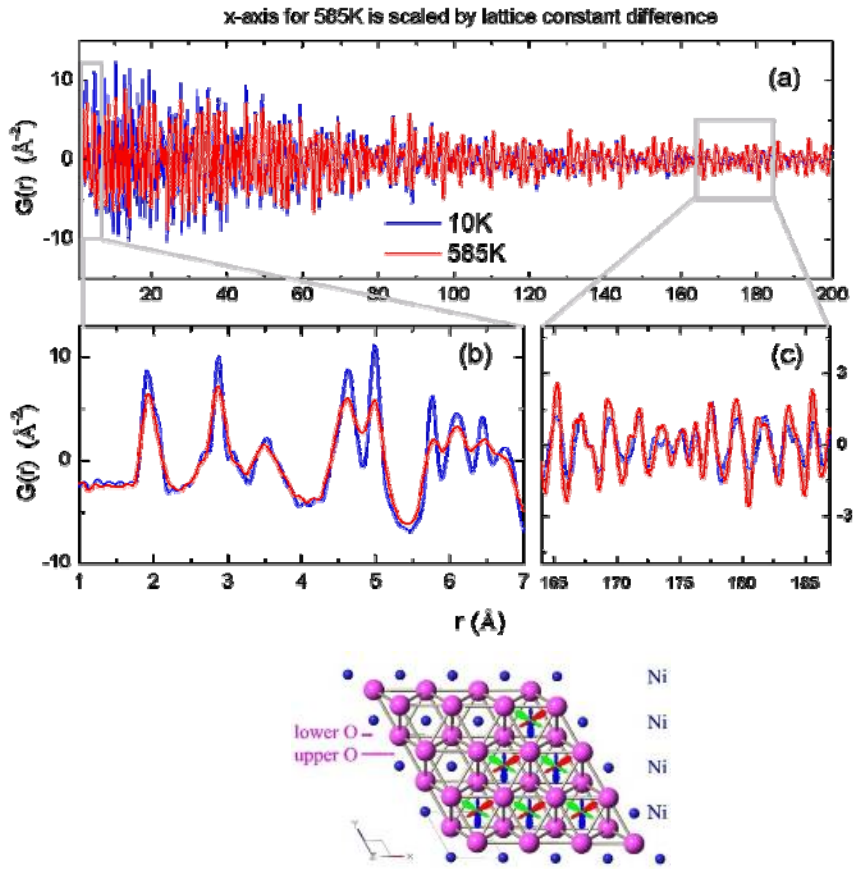

Fig. 6.2. Long-range pair distribution functions—domains in $LiNiO_2$ [3].

6.3 Preliminary Conclusions

- The broad pulse widths of both the short-proton-pulse and long-proton-pulse versions of STS lead to long, complex instruments for some gain over limited d-spacing range (longer d-spacing range).
- For crystallographic studies that require short d-spacings (~0.5 A) and high resolution (including strain mapping), there appears only to be great difficulty in overcoming the very broad pulses and lower epithermal flux
- For high flux medium resolution (small samples, texture mapping, special environment), there are significant gains at long d-spacings (d > 1.5 A) but gains disappear at shorter d-spacing.
  - Would be useful especially if instrument has to be far from target.
- Water moderator might help for short d-spacings, but broad pulse width at STS is still a problem.
- Very High Resolution Diffractometer complements the FTS workhorse POWGEN3 and should be located on dec-H_2 beam line on FTS.

6.4 Preliminary Instruments

- High Flux/Fast Mapping Diffractometer: short-proton-pulse STS—100 m
- High Magnetic Field Diffractometer: short-proton-pulse STS—100 m
- High-P Diffractometer (V reduced /10): short-proton-pulse STS—100 m
- High Resolution Large Q-range: FTS dec-H_20— ~50 m
- Very High Resolution Diffractometer: FTS dec-H_2 200 m
- SWANS

6.5 R&D needs

- Multiplexing / multipulse /Fourier diffractometer
  - MC simulations, user-friendly software
  - Does it work for complex structures ?
- Detectors (data rate, cost, efficiency at high E)
- Tunable moderators
- Sample environment
  - Pressure cells 180 panoramic cell
- Software (data reduction, refinement)
- Optics, focusing

6.6 References

1. J. A. Stride, F. Mezei, J.-J. Bleif, and C. Guy, "Powder diffraction using time-of-flight monochromatization", *Physica B* **234-236**, 1157–1159 (1997).
2. K. L. Page, Th. Proffen, H. Terrones, M. Terrones, L. Lee, Y. Yang, S. Stemmer, R. Seshadri ,and A. K. Cheetham, "Direct observation of the structure of gold nanoparticles by total scattering powder neutron diffraction," *Chem. Phys. Lett.* **393**, 385–388 (2004).
3. J.-H. Chung, Th. Proffen, S.-I. Shamoto, A. M. Ghorayeb, L. Croguennec, B. C. Sales, R. Jin, D. Mandrus and T. Egami, "Local structure of LiNiO2 studied by neutron diffraction," *Phys. Rev. B* **71**, 064410 (2005).

7.0 INELASTIC SCATTERING USING NEUTRON SPIN PRECESSION TECHNIQUES: WORKING GROUP REPORT

Chair: G. Ehlers (ORNL)

Other Participants: M. Bleuel (ANL), F. Klose (ORNL), W.-T. Lee (ORNL), M. Ohl (FZ Jülich), C. Pappas (HMI), M. Rheinstädter (U. Missouri)

7.1 Scientific Case

NSE is the spectroscopic method with the highest resolution in quasielastic and inelastic neutron scattering, with energy resolution values typically better than 10^{-5} of the incident neutron energy. Hence NSE spectroscopy is mainly used to study slow motions and relaxation phenomena in hard and soft condensed matter [1,2].

NSE is thus perfectly suited to investigate slow motions in soft matter, biophysics, and biology. The large length scales involved usually require small Q-values. While the spin-echo technique is routinely used for these investigations, some examples shall be given in this report where instrumental development would create a huge scientific impact and open up the technique for new user communities. Inelastic/quasielastic neutron scattering is a unique tool for the investigation of dynamics because it gives a wave vector resolved access to the dynamics, which is essential to associate relaxation rates and excitation frequencies to specific motions and molecular components.

When thinking about science to be done 10–20 years from now, it is instructive to look at current limitations of the technique in order to see which areas need the most development.

1. With the notable exception of the hybrid triple-axis and (resonance) NSE spectrometers, TAS-(R)NSE, NSE is almost exclusively used for quasielastic scattering. Since NSE is a Fourier technique, essentially all scattered neutrons (energy-wise) enter the spin analyzer and detector and therefore only processes that contribute more than about ~5 % to the scattering intensity may be successfully analyzed. Inelastic scattering is usually much weaker than the elastic and quasi-elastic contributions and hence disappears in the counting statistics unless the instrument discriminates among neutrons according to energy transfer, as it is the case in TAS-(R)NSE. NSE was developed at reactor sources and was never combined with a dedicated TOF instrument. At spallation sources, however, NSE will obviously be combined with TOF. This combination will open up new possibilities, as a dedicated TOF NSE spectrometer would also allow for inelastic spin echo and studies of excitation lifetimes with much greater resolution than is currently possible. Presently this is relevant for superconductors and quantum liquids, but in 10–20 years, one may want to study such processes in complex organic molecules. The impact here is to study propagating modes in biophysics and biology and their importance for biological key functions and, on the other hand, expand the range of energy resolution from triple-axis and TOF instruments. The wavelength spread $\delta\lambda$ must be flexible to adapt the Q-resolution for the study of single-crystal experiments.
2. Neutron reflectometry has recently made a quantum leap forward by going beyond the usual specular geometry. The investigation of off-specular scattering opens up a whole new field of

phenomena. Furthermore, first experimental results show that a whole new field of surface excitations will open up if the capability to discriminate between elastic and quasielastic scattering is added to a reflectometer. Such an NSE-reflectometer could also be seen as a very low Q-range traditional NSE, offering new opportunities in the studies of the dynamics on liquid surfaces or of the membranes at very low Q. The access to the smallest Q-values in the order of 10^{-4} Å^{-1} would allow inelastic reflectometry and inelastic SANS. Because of the large structures involved in biophysics and biology, this range of length and time scales is extremely interesting. Information about dynamics on these long length scales up to now mainly stems from analysis of diffuse scattering, with the inherent drawback that underlying Q-information is lost. A small-angle NSE with a horizontal sample stage would innovate the investigation of liquids and allow dynamic investigation of liquid surfaces and interfaces. To adapt the Q-resolution to the particular experiment, a variable wavelength spread $\delta\lambda$ is necessary.

3. Standard NSE measurements become very difficult, if not impossible, when the sample dramatically reduces the beam polarization. This is the case for superconductors and ferromagnets (unless one has a monodomain single crystal) because the internal fields depolarize the beam. In soft matter research, it is common practice to use hydrogen/deuterium contrast methods to "highlight" certain features in the sample; but in most cases, the scattered polarization suffers too much to use this technique in routine NSE operation. Thus large numbers of potentially very interesting systems are excluded from current research with NSE. There are ideas for getting around this problem (see below) and the scientific benefit is evident.
4. A wide-angle spin-echo instrument with a high flux to allow short counting times is necessary to study reaction kinetics and kinetics of biological processes.
5. There will always be samples in which the dynamics are so slow that one needs to go beyond the present technical limits of NSE. Complex systems such as polymers and biological molecules are typical examples of systems requiring very long Fourier times. The NSE project at the FTS addresses this need.

7.2 Instrumental Details

The high energy resolution is reached because in NSE the precession of neutron spins in a magnetic field measures directly the energy transfer at the sample and decouples the resolution from beam monochromatization and collimation. NSE is a Fourier method which measures the intermediate scattering function $I(Q,t) = S(Q,t)/S(Q)$ in the limit $\hbar\omega \ll k_B T$. The relevant parameter is the Fourier time, $t \propto H\,\ell\,\lambda^3$, where H is the magnetic field ("effective" magnetic field in resonance spin echo), ℓ the length over which the precession takes place, and λ the mean incident wavelength.

Concerning chopper operation, an NSE spectrometer will essentially be run like a reflectometer or diffractometer. The inelasticity of the scattering will be detected by the N(R)SE measurement, not by the difference of the neutron TOF from the elastic TOF.

A TOF NSE spectrometer operating in the ranges (λ_{min}, λ_{max}), ($2\theta_{min}$, $2\theta_{max}$), ($H\ell_{min}$, $H\ell_{min}$) will cover a parameter range as schematically shown in Fig. 7.1.

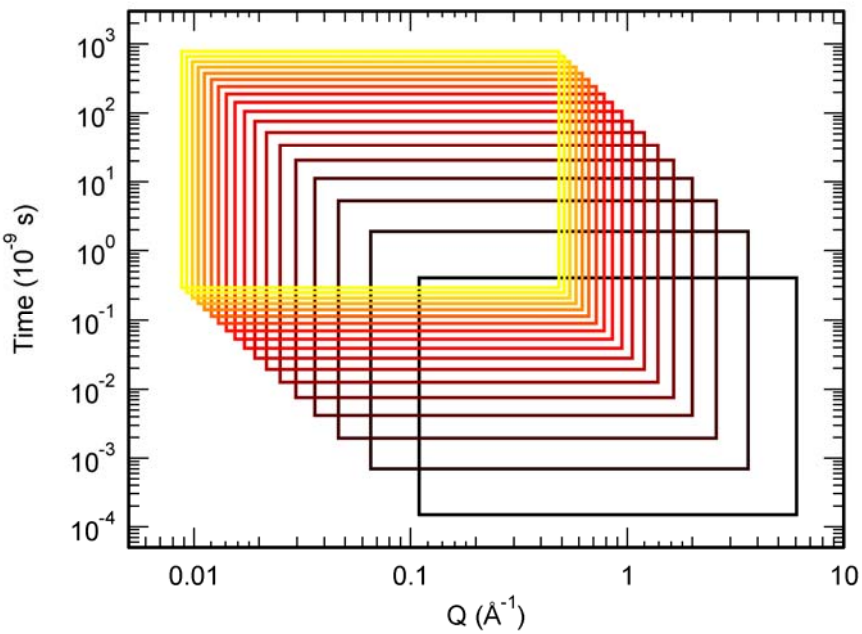

Fig. 7.1. Range covered in a TOF NSE spectrometer. Here λ_{min}=2 Å (black), λ_{max}=25 Å (yellow), $2\theta_{min}$=2°, $2\theta_{max}$=150°, $H\ell_{min}$=100 Oe·cm, $H\ell_{max}$=270,000 Oe·cm. A time of 10^{-3} ns corresponds via Fourier transform to an energy transfer of 1 meV.

When comparing a location at different types of sources (reactor vs spallation source, long vs short pulse) one can omit the wavelength dependence of the intensity in the first approximation because sources will be sufficiently similar in this respect. An FOM will be proportional to the number of data points collected in unit time, divided by their squared errors. In the first approximation, this would be given by the simple relation FOM ~ $I \cdot P^2/B^2$, where *I* is the total intensity at the sample, *B* the background, and *P* the polarization of the incident beam. The data points can be assumed to be equidistant on log scales in both Fourier time and Q vector. Hence the FOM will be proportional to the area of the covered range in Fig. 7.1, multiplied by the time-averaged intensity in each "pixel," which itself is proportional to the accepted wavelength spread δλ in each pixel. At a spallation source, this monochromaticity is given by the length of the incident beam line via δλ (Å) = 4 δt (ms)/L (m), where *δt* is the initial length of the pulse; at a reactor source, δλ is in the 10–20 % range, depending on the velocity selector used. For a reasonable length of the spectrometer at a spallation source, δλ can never be coarser than 5%; hence TOF resolution is virtually meaningless for NSE.

The optimal length of a spectrometer is determined by a combination of considerations for monochromaticity δλ, simultaneously covered wavelength range Δλ (Å) = 4000/L (m)/f (Hz), and instrument background. A large Δλ implies a large area per instrument setting in Fig. 7.1; this is obviously preferred but has the drawback of vastly different counting statistics across the area, which one tries to avoid. Ultimately, the best length of a primary spectrometer can be determined only by considering all aspects of the source, the influence of neighboring instruments, and the intended use of the spectrometer.

Concerning neutron performance, there is a need to expand instrumental capabilities of operating NSE spectrometers at other facilities in the following areas:

1. extend Fourier time range to longer times
2. extend Fourier time range to shorter times
3. increase area with detector coverage
4. extend angular coverage toward low angles
5. become independent from polarization-related limitations to the NSE technique

Discussion of the listed points:

1. This goal is covered by the Spin Echo Spectrometer Project at FTS, led by F. Z. Jülich. There is no need to push this with high priority at STS.
2. Established technologies require a few precessions per spectrometer arm, setting a lower limit to the Fourier times obtainable at a given wavelength. The innovative concept of longitudinal resonance spin echo [3] may provide a workable solution but requires expert R&D efforts. Adding a conventional TOF option to any NSE spectrometer will also significantly increase the dynamic range.
3. This is simply a matter of intensity and funding, as it might require thousands of square meters of supermirrors. To a lesser extent this is also a matter of space, although it is anticipated that at an average distance of ~40 meters from the target there will be enough floor space available.
4. With conventional beam delivery approaches, NSE spectrometers run into high-background issues around scattering angles of ~5° and below. It requires a dedicated setup comparable to a reflectometer to significantly improve and extend the low angle coverage.
5. Standard NSE measurements become very difficult, if not impossible, when the sample reduces the beam polarization too much (see science case). Intensity-modulated NSE [4] is a way out of these limitations, but it uses additional polarizers and analyzers before and after the sample, respectively, implying intensity losses. The MIEZE principle [5] is also an alternative but implies time-resolved measurements. Development in both these directions requires expert R&D efforts.

7.3 Conclusions: High-Level Findings

I. Spin echo spectrometers clearly perform best at a long-pulse source, as long as the number of neutrons emitted *per pulse* is higher than at a short-pulse source. An instrument FOM is proportional to the power of the source.

II. Anticipated working ranges for neutron wavelength are from $\lambda_{min} = 2$ Å to $\lambda_{max} = 25$ Å with peak use around 10 Å. NSE spectrometers would greatly benefit from the long wavelength spectrum of a "very cold" moderator, which would boost the intensity at around 10 Å and make possible NSE measurements at very high resolution with small samples or weakly scattering systems.

III. To provide continuous coverage of a very large dynamic range of 6–7 orders of magnitude, a spin echo mode of operation ($\pi/2$ flippers ON) should be combined with a conventional inelastic scattering option at medium TOF resolution ($\pi/2$ flippers OFF). The NSE spectrometer at HMI has very good experience with this [6]. This combination

would extend the dynamic range by 1.5–2 orders of magnitude toward the low-resolution side. This option requires a high-speed chopper close to the sample.

IV. High count rate in the detector is essential because nowadays experiments simply take too long (~7 days on average).

V. Instruments should be designed to allow for maximum flexibility.

7.4 Proposed Beam Lines

Innovative design of the NSE instruments on STS would extend the experimental capabilities of NSE beyond the existing limits and allow for maximum flexibility as well as an overlap with other techniques. The needs in dynamic range and Q range, however, are so diverse and broad that they cannot be covered in an optimal way by a single instrument. To access very low scattering angles and large scattering angles in one instrument, a reflectometer-type instrument is needed. Ideally, one would like to build two "reflectometers": One should be designed to meet the requirements for the investigation of liquids and free-standing surfaces with a horizontal sample and a vertical scattering plane, while the other would have a horizontal scattering plane with a vertical sample geometry. Furthermore, there is a need for a dedicated wide-angle NSE spectrometer with a large area detector coverage, which pushes the data acquisition rate to its highest limit.

We are proposing three instruments.

BL-1: Vertical surface "reflectometer" (for lack of a better word) with resonance spin echo setup, which minimizes the weight of the echo components and the length of the spectrometer arms, covering the range $2\theta_{min}$=0.1°, $2\theta_{max}$=120°, $H\ell_{min}$=100 Oe·cm, $H\ell_{max}$=100,000 Oe·cm, with a scattered flight path length ~1.5–2 meters.

BL-2: Horizontal surface "reflectometer" with resonance spin echo setup, incident beam line length similar to BL-1, covering the range $2\theta_{min}$=0.1°, $2\theta_{max}$=90°, $H\ell_{min}$=100 Oe·cm, $H\ell_{max}$=100,000 Oe·cm.

BL-3: Wide-angle NSE spectrometer, covering the range $2\theta_{min}$=5°, $2\theta_{max}$=150°, $H\ell_{min}$=100 Oe·cm, $H\ell_{max}$=270,000 Oe·cm.

None of these numbers limiting the ranges is pushing current instrumental limits. BL-1 and 2 need resonance spin echo to minimize the weight of the echo components. Also, field integral correction elements used in conventional NSE must be placed in the beam and are unwelcome. Moreover, the spectrometer arms of BL-1 and 2 can be made shorter in the RNSE configuration.

7.5 Anticipated Performance

Figure 7.2 shows the Q-t range spanned by each of these three instruments.

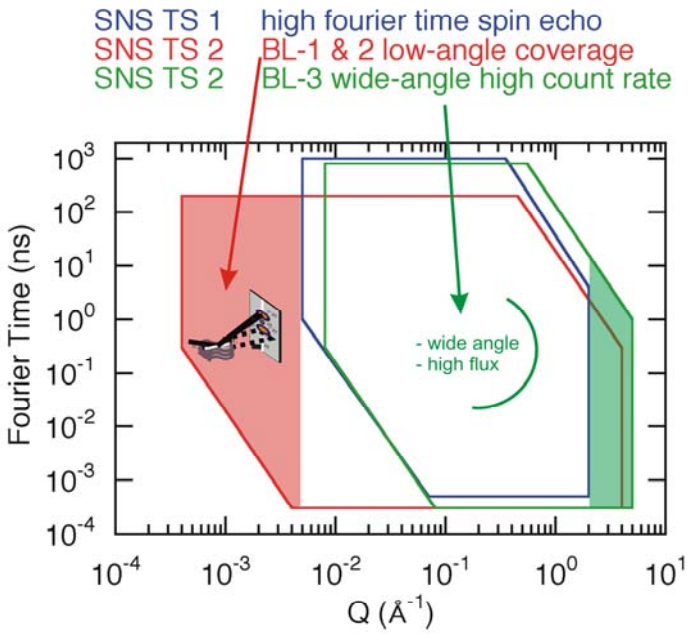

Fig.7.2. Ranges in the spatial and temporal variables covered by the three proposed instruments. Note the gain in low Q-values as compared with existing NSE instruments.

With a target to sample distance *L*~40 meters, which is a reasonable estimate for all three incident beam lines; *f*=20 Hz; 3 MW source power; initial pulse length 1 ms; and an STS cold-coupled moderator spectrum, the following estimates were obtained:

monochromaticity $\delta\lambda \sim 0.1$Å

simultaneously covered wavelength range $\Delta\lambda \sim 5$Å

BL-1 & 2 neutron flux at sample in the band 2Å – 7Å: ~ 2×10^9 n·cm^{-2}·s^{-1}

BL-1 & 2 neutron flux at sample in the band 7Å – 12Å: ~ 4×10^8 n·cm^{-2}·s^{-1}

BL-3 neutron flux at sample in the band 2Å – 7Å: ~ 7×10^8 n·cm^{-2}·s^{-1}

BL-3 neutron flux at sample in the band 7Å – 12Å: ~ 4×10^7 n·cm^{-2}·s^{-1}

BL-1 and 2 are very similar. BL-3 is likely to have a guide with a much larger cross section and a much larger distance (~2.5-3 m) from the guide exit to the sample position. The values quoted above were obtained by scaling from the reflectometer and spin echo beam lines at FTS.

7.6 References

1. D. Richter, M. Monkenbusch, A. Arbe, and J. Colmenero, *Neutron Spin Echo in Polymer Systems,* Springer, Berlin, 2005.
2. C. Pappas, G. Ehlers, and F. Mezei, "Neutron-spin-echo spectroscopy and magnetism," in T. Chatterji, ed., *Neutron Scattering from Magnetic Materials*, chapter 11, p. 521, Elsevier, Amsterdam, 2006.
3. W. Häussler, U. Schmidt, G. Ehlers, and F. Mezei, *Chem. Phys.* **292**, 501 (2003).
4. B. Farago, F. Mezei, Physica B+C **136** p. 100 (1986).
5. M. Bleuel, M. Bröll, E. Lang, K. Littrell, R. Gähler, and J. Lal, *Physica B* **371**, 297 (2006).
6. C. Pappas, A. Triolo, R. Kischnik, and F. Mezei, *Applied Physics A: Materials Science & Processing* **274**, 286 (2002).

8.0 CONVENTIONAL SPECTROMETRY: WORKING GROUP REPORT

Chair: G. Granroth (ORNL)

Other Participants: D. Abernathy (ORNL), G. Bauer (FZ Jülich), C. Brown (NIST), J. Carpenter (ANL), M. Hagen (ORNL), K. Herwig (ORNL), M. Lumsden (ORNL), E. Mamontov (ORNL), R. McGreevy (RAL), F. Mezei (HMI), B. Micklich (ANL), H. Mook, ORNL), S. Nagler (ORNL), M. Rowe (NIST), A. Taylor (RAL), C. Tulk (ORNL), U. Wildgruber (ORNL)

8.1 Scientific Case

The group started by outlining the science that we expect to do with these new instruments and grouping the science together according to similar required properties. The following bulleted list summarizes the discussion.

- Interfacial dynamics in biological samples; absorbent behavior, confinement, tunneling in glassy systems; diffusive processes in ionic and proton conductors
    - Variable energy resolution < 1–100 μeV
    - Maximum Q = 3.5 $Å^{-1}$
    - Q resolution 0.1 $Å^{-1}$
    - Polarized beam
- Quantum magnetism, molecular magnetism, frustrated magnets, relaxor ferroelectrics
    - Variable energy resolution ~ 1–100 μeV
    - Maximum energy transfer 50 meV
    - Maximum Q = 3 $Å^{-1}$
    - Q resolution 0.01 $Å^{-1}$
    - Polarized beam
- Energy storage
    - Variable energy resolution < 1–100 μeV
    - Maximum Q = 3.5 $Å^{-1}$
    - Maximum energy transfer 50 meV
    - Q resolution 0.01 $Å^{-1}$
    - Polarized beam
- Dynamic critical scattering in ferroelectrics
    - Energy resolution < 1 μeV
    - Maximum Q = 2-3 $Å^{-1}$
    - Q resolution 0.005 $Å^{-1}$
    - Polarized beam
- Membrane protein collective dynamics, ferro-elastic modes, shape memory alloys
    - Energy resolution 10-50 μeV
    - Energy transfer range 5-20 meV
    - Maximum Q = 4.0 $Å^{-1}$

- Kinetic experiments, stroboscopic measurements
    - Large numbers of neutrons on sample at expense of Q and energy resolution.
    - Multiple perturbations to excited states, such as electric field, magnetic field, optical pumping, and ultrasound
- Extreme sample environments, parametric studies
    - Sufficient flux to enable enough parameters in a reasonable time
    - Focused beams
    - High magnetic fields
    - Levitated samples
    - High pressure advancements to reduce material in incoming or scattered beam
    - Low temperature in combination with other sample environments such as magnetic field and pressure.

8.2 General Comments

In the discussion, a general point relevant for all instrument designs was mentioned: since protons are incident on the target of a long-pulse source for a longer time than for a short-pulse source, the resulting distribution of high-energy neutrons is also broader in time. If this aspect of a long-pulse source is not considered in instrument design, elevated backgrounds could result. However, appropriate use of long, curved guides and the emphasis on long-wavelength neutrons at STS should make this aspect of a long-pulse source irrelevant.

8.3 Backscattering Spectrometers

The working group has identified two instruments that would be world-class backscattering spectrometers at STS. Nevertheless, we feel that with a detailed design effort, including time focusing techniques [1], pulse shaping techniques [2], and exploration of other analyzer crystals besides silicon and mica, a further optimized instrument will result. The main goals of this design effort should be sub-microvolt resolution, a maximum Q value of 2 $Å^{-1}$, and maximized signal intensity.

8.3.1 Fine-resolution backscattering spectrometer

We reviewed the fine-resolution backscattering spectrometer proposed in the ESS design [3] and felt the design would work well for STS. This design would have a 200 m moderator-to-sample distance and a 4 m sample-to-detector distance. Stressed Si(111) analyzer crystals in exact backscattering would provide 800 neV resolution at zero energy transfer. This instrument would have an energy transfer range of ± 100 μeV around the elastic line and a maximum Q of 1.9 $Å^{-1}$. Pulse-shaping choppers are used to control the moderator contribution to the resolution function. These choppers can also be used to relax the resolution to 4 μeV resolution if more flux is required. At 1 MW on STS we expect 3×10^6 n/cm^2/s on sample; and if the power is increased to 3 MW, we expect 1×10^7 n/cm^2/s on sample. An additional set of analyzer crystals would provide an additional resolution choice.

8.3.2 Ultra-fine-resolution backscattering spectrometer

Another route to sub-microvolt resolution is to use unstressed analyzer crystals to reduce the δd/d contribution to the resolution. To balance the resolution function, the incident beam line would then be approximately 30 m and pulse-shaping choppers would control the pulse shape. This instrument would have 500 neV resolution. The flux on sample would be 1×10^5 n/cm^2/s at 1 MW.

8.4 Chopper Spectrometers

8.4.1 High-resolution cold chopper spectrometer

On a coupled hydrogen moderator at STS, there is an initial question as to the neutron pulse length required to optimize the flux on sample for such an instrument. This question may be answered before specific instrument configurations are considered by keeping in mind the principles of repetition rate multiplication (RRM) [2]. This was illustrated at this workshop [4] where the key parameter is peak neutron flux. This leads to a strong preference for a chopper spectrometer to be on a short-proton-pulse source if equal power is provided by the long-proton-pulse counterpart. From interpretation of calculated beam profiles [5], we estimate that there would be a preference for the long-proton-pulse version if it produces three times the number of neutrons per pulse compared with the short-proton-pulse version. We do not address the technical feasibility of attaining such a short, powerful pulse, but we understand that it is technically challenging and may be an unobtainable goal.

If we consider the case of the CNCS currently located at FTS, with an elastic resolution of 1% of the incident energy, the main gains at STS arise from a two-fold increase in peak flux compared with FTS and the possible use of RRM. This relies on the flight paths remaining fairly long to avoid frame-overlap issues. We estimate that a moderator-to-chopper distance of 30 m would allow RRM gains of approximately 3 to 5. Total gains are between 6 and 15 times the CNCS at FTS.

A simple timing diagram for the case of three incident energies E_i of 2, 1.36, and 0.94 meV (solid green lines) is given in Fig. 8.1. With the moderator at the origin, the sample located 36 m downstream (dotted black line) and with a 4 m final flight path to the detectors (dashed black line), a final energy of 0.15 times E_i (red lines) and 2 times E_i (blue lines) this figure shows small amounts of frame overlap. Therefore, it illustrates the limits of energy transfer range possible with the RRM technique for these values of E_i.

An increased duty cycle may be described by a case of E_i = 10.0, 6.6, 4.4, 2.9, and 1.9 meV where approximately five independent experiments (in terms of resolution and dynamics range) could be performed simultaneously (Fig. 8.2). New concepts in data reduction must also be broached in cases such as these where the interesting scientific features are simultaneously measured at multiple resolutions.

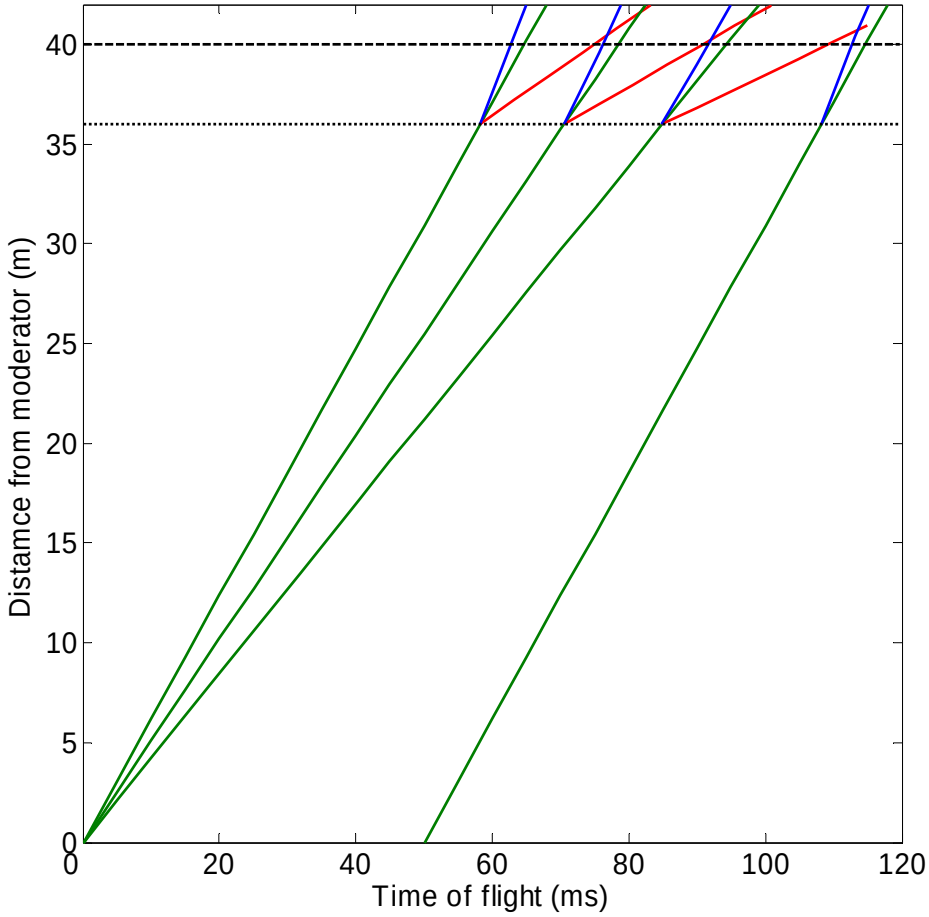

Fig. 8.1. Timing diagram showing possible RRM scheme for a cold neutron chopper spectrometer with E_i = 2, 1.36, and 0.94 meV.

While this is a cold neutron spectrometer, experience indicates that there is sometimes a need to access higher-energy transfers. Therefore, an effort to provide sufficient flux out to 80 meV should be pursued by the moderator designers. This should not detract from optimizing the instrument for incident energies of less than 25 meV. Additionally, the usefulness of a polarized beam in many areas of neutron scattering should be kept in mind in designing this type of instrument and allowing sufficient flexibility for ancillary equipment around the sample position.

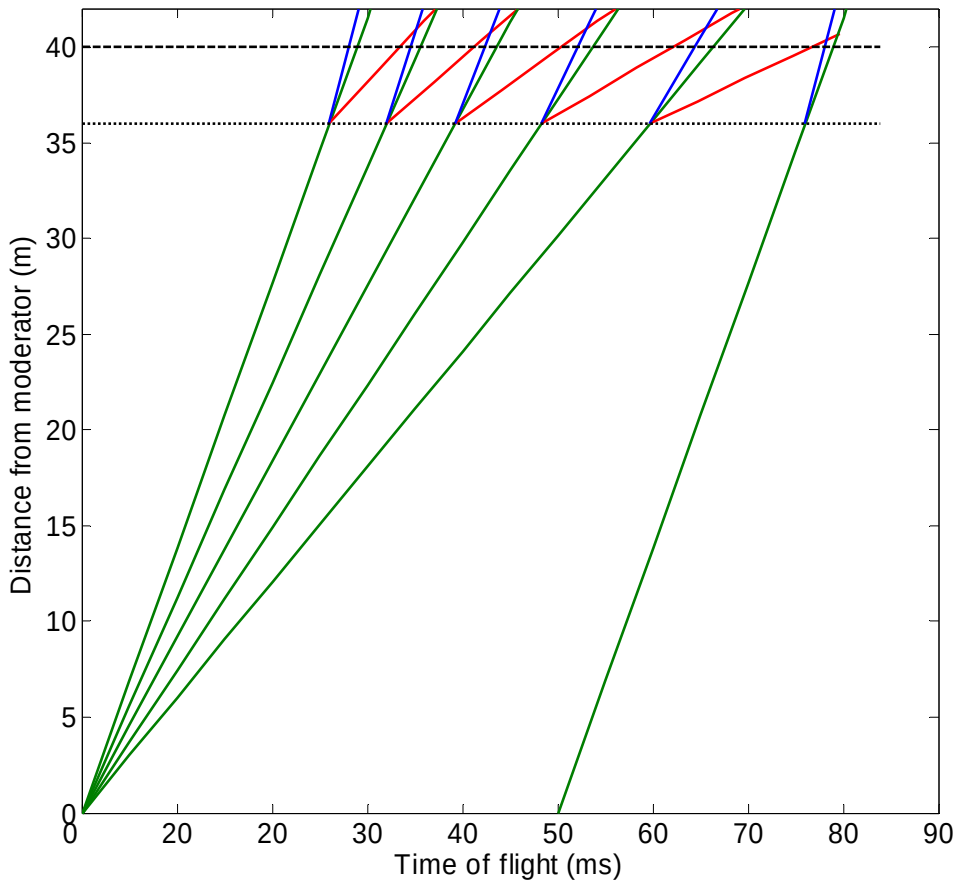

Fig. 8.2. Timing diagram showing possible RRM scheme for a cold neutron chopper spectrometer with E_i = 10, 6.6, 4.4, 2.9, and 1.9 meV.

8.4.2 High-intensity chopper spectrometer

To take advantage of the full source spectrum and relax the requirements for a short-proton-pulse source, one could consider designing an instrument similar in size to the one described above but relaxing the resolution requirements to ~5% of the incident energy. In this case, no pulse shaping is required, and a gain in flux ~1 order of magnitude over the low-resolution CNCS is possible. To break new ground in science, one should consider that an additional order of magnitude in flux can be achieved using focusing techniques (for instance K-B mirrors) to enable the use of 2 mm by 2 mm samples. The combined two orders of magnitude in flux are significant improvements over the CNCS and could benefit areas of science where small sample volumes are predominant.

8.4.3 Extreme sample environment spectrometer

A natural progression from the High Intensity Chopper Spectrometer described is to take that concept and make it more applied. Extreme sample environments are notorious for constricting

sample volumes and/or restricting the available solid angle to detect the scattered neutrons. The use of a micron-size, focused beam (K-B mirrors or equivalent) could effectively allow for inelastic scattering to be measured from samples under giga-Pascal pressures, under relatively fast changing stimulus, or even under high magnetic fields.

The key to this spectrometer is building the sample environment into the spectrometer design. For instance, the retroactive insertion of a focusing K-B mirror is a difficult task for a chopper spectrometer in which one typically wishes to maximize the resolution by having a short final chopper-to-sample distance, yet one needs a few meters of space to allow the insertion of a focusing device.

Significant economy over a traditional spectrometer could be achieved by tailoring the detector layout to be suitable for the sample geometry. Additional gains may be achieved by attempting to multiplex (via monochromators or such) to a dedicated sample environment instrument. Further discussion would be needed to improve understanding of this possibility.

8.5 Crystal Monochromator Instrument

The possibility of building a cold neutron triple-axis spectrometer at STS was also discussed. These instruments are traditionally very productive scientifically and are in short supply in North America—the only such instrument currently accessible to general users is the SPINS spectrometer at NIST. As the time-integrated flux for STS will be comparable to a medium-flux reactor, proper optimization of such an instrument could result in a monochromatic peak flux on sample of about 10^7 n/cm^2/s. This would make such an instrument competitive with most equivalent instruments in the world. In addition, an optimized instrument at STS (at 1 MW) could also be built with very low background, resulting in a very good signal-to–noise ratio. As with any cold triple-axis spectrometer, polarization is easily achievable.

However, if this instrument were located on the new cold source at HFIR, it would perform even better. The new cold source at HFIR will yield a much higher time-integrated flux on sample compared with STS at SNS. In addition, the CG1 guide at HFIR has been well optimized for a cold triple-axis spectrometer and preliminary estimates of flux on sample suggest a peak flux of almost 10^8 n/cm^2/s (at about 9 meV incident energy) making it a world class instrument. For reference, IN14 at ILL is currently one of the best cold triple-axis spectrometer instruments in the world. It is currently undergoing an upgrade, and the projected flux on sample of this upgraded instrument will be about the same as the projected flux for CG1. Both of these instruments would have 4 to 5 times more flux than a similar instrument at STS.

In recent years, several improvements on the traditional triple-axis instrument have been implemented, focusing on the addition of analyzer crystal coverage on the back end. This began with RITA/RITA II/SPINS (individually tunable multi-blade analyzer coupled with a PSD option) and has been extended with new back end concepts such as MACS (multiple double-bounce analyzers), MAD (multi-analyzer detector), and EIGER/CAMERA (continuous angular coverage with multiple vertically scattering analyzers). These concepts are designed to increase the flexibility of the traditional triple-axis spectrometer and bridge the gap between traditional point-by-point triple-axis measurements and broad survey instruments like direct-geometry TOF machines. An optimized back end coupled with the very high flux on sample could make a cold triple-axis at HFIR one of the best instruments of this type in the world.

In summary, the need for such an instrument in North America is clear and we strongly endorse having such an instrument at ORNL. Such an instrument would perform well at STS. However, the instrument would perform better and be a world-class instrument if it were located at the CG1 guide position at HFIR.

8.6 Needed Technical Development

In consideration of the instruments mentioned, several needed technical developments were identified.

First, as mentioned in the section on backscattering spectrometers, high-quality single crystals of a material with a d-spacing in the range between silicon and mica would provide added flexibility in the design of crystal analyzer spectrometers. The technical development is in identifying an appropriate material that can be made a production item or one already in production that would fit the instrument requirements. Diamond films and silicon carbide were mentioned in this discussion, as carbon has a larger scattering cross section than silicon.

Second, focusing optic techniques, which are largely employed on diffraction instruments on FTS, should be developed for the inelastic instruments on STS. This is crucial for the high-flux chopper spectrometer and the special sample environment spectrometer. For the high-flux chopper spectrometer, a significant gain over existing spectrometers arises from the focusing contribution. The final spot size does not necessarily need to be small, but we want gains similar to those currently obtained with K-B mirrors [6] but scaled up to bigger beams. For the special sample environment spectrometer, fine focusing to spot sizes similar to those realized with K-B mirrors for the SNAP instrument is required. [6]

Third, phase-space-transformation devices may prove useful to trade Q resolution for energy resolution and increased flux. Research into appropriate devices for the instruments proposed may provide further paths for optimization.

Fourth, several aspects of chopper capabilities and operation need further development. The wide time profiles of all moderator/target configurations presented mean that pulse-shaping choppers and RRM will be significantly used for these instruments. Further optimizations of chopper systems for RRM are required to ensure that such methods are beyond the prototyping phase. Flexibility in instrument design is always gained by pushing choppers to higher speeds; the current state of the art disk chopper is 333 HZ. The carbon fiber technologies employed on the high-speed discs for the CNCS should allow systems to be designed at higher speeds. Any further increase would be useful. Neutron-absorbing coatings have proved to be difficult for the current 60 Hz bandwidth choppers; advances to make the coating process simpler and more uniform should be investigated.

Fifth, beam multiplexing may be a way to allow several novel sample environment devices to be used at once. The traditional, and current, method of multiplexing uses monochromator crystals. A research effort to examine other ways of multiplexing the beam line might be beneficial.

Finally, combined extreme sample environments would open new areas of science. Therefore, development of equipment that allows low temperature, high magnetic field, and high pressure simultaneously should be pursued.

8.7 References

1. G. Zsigmond and J. M. Carpenter, *Nucl. Instr. Meth. A.* **550**, 359 (2005) .
2. F. Mezei, M. Russina, and S. Schorr, *Physica B* **276**, 128 (2000).
3. K. Clausen et al., *The European Spallation Source Project Report*, Vol. IV, p. 2-26 (2002).
4. G. Bauer, *Report on the STS-2 Neutronics Workshop Held at SNS on Dec. 15 and 16, 2006*, presentation at the SNS Second Target Station Workshop, February 20-22, 2007.
5. F. X. Gallmeier and E. B. Iverson, *A First Effort towards a Target Moderator Reflector Assembly for a SNS Second Target Station*, draft report, Spallation Neutron Source.
6. C. Tulk, private communication.

9.0 IMAGING, TOMOGRAPHY, MICROPROBES, MICROSCOPY, AND SPECIAL TOPICS: WORKING GROUP REPORT

Chair: L. Robertson (ORNL)

Participants: M. Arif (NIST), H. Bilheux (ORNL), T. Cremer (Adelphi Tech.), P. Ferguson (ORNL), F. Gallmeier (ORNL), E. Iverson (ORNL), B. Khaykovich (MIT), W.-T. Lee (ORNL), W. Lu (ORNL), D. Mildner (NIST), D. Penumadu (U. Tennessee), U. Wildgruber (ORNL)

9.1 Specific Instruments

The goal of this working group was to recommend a representative set of instruments for STS. This scope of this recommendation includes considerations such as relocating existing instruments from FTS, identifying instruments that would perform as well or better at HFIR, as well as other uses for STS beam lines. The instruments were evaluated with regard to their use of the unique source characteristics of STS and their potential for significant scientific productivity. The working group evaluated five instrument types and the results are summarized below.

9.1.1 Neutron imaging beam line

The consensus of the group was to consider a configurable multipurpose beam line that combines direct imaging, phase contrast methods, radiography, residual stress, and microscopy into a single "instrument." The optical requirements for these measurements are sufficiently similar without significant compromise to any particular capability. The common geometry that would define such a beam line is a long flight path (> 30 m) and the use of pinhole optics. With such a beam line, there is the potential for significant advances in 3-dimensional and time-resolved imaging. Incorporating simultaneous prompt gamma and x-ray imaging (image fusion), light and electron microscopy and spectroscopy, x-ray fluorescence, x-ray diffraction, polarimetry, rheometry, or ultrasound would further enhance the science that could be done.

There was considerable discussion of whether this instrument would perform better at STS or at HFIR. We concluded that at the reactor source, there is potential for advancement of the field with the use of higher neutron energies for deeper penetration (thicker materials), longer-wavelength neutrons for better sensitivity to composition and thickness and for attaining much higher spatial resolution than is currently available. If this beam line were located at STS, it could realize all the advances described for a reactor source with the additional capabilities of using TOF to separate the contribution from different wavelengths to get sharper images, using epithermal neutrons for imaging very large (thick) materials, and developing Bragg edge imaging techniques.

9.1.2 Three-dimensional imaging of large objects

The layout of the beam line described is not conducive to the study of very large objects simply because of the logistical challenges involved. A dedicated instrument with sample handling capabilities similar to those of the VULCAN instrument on FTS would be required but

with similar optical requirements to the beam line described in Sect. 9.1.1. However, the geometry could be better optimized for maximum throughput with a $\delta\lambda/\lambda < 1\%$ for extremely high spatial resolution. The design of this instrument should include the capability for large field tomography with the ability to "zoom in" and do more discrete measurements at higher resolution.

9.1.3 Research and development beam line

We identified an almost desperate need for a R&D beam line dedicated to instrument development and testing. The need for increased R&D was noted as a universal theme during the summary presentations of the other working groups as well. Neutron detectors, in particular, were identified as an area where the limitations of current technology are inhibiting the performance of next-generation neutron scattering instruments. New neutron optical concepts need to be tested and optimized during all stages of instrument development. In addition, there is a clear need for low-energy cross section measurements for more accurate computer modeling of instrument performance, as well as moderator and beam line characterization to get the largest gains in performance possible. Novel concepts and configurations of targets, moderators and reflectors will also require experimental development. Finally, this beam line will serve as an invaluable tool for education and training.

9.1.4 Microprobe instrument

Small-gage volumes on the order of 100 microns at ~1 Å to 10 microns at ~4 Å are used to achieve the extremely high spatial resolution required to study, for example, interfaces, inclusions, precipitants, grain boundaries, and intra-granular strain. This emphasizes the need for high neutron flux at long wavelengths. Such an instrument would be best suited for a "cool" source because of the inherent tradeoff between better optics performance at long wavelengths and the Q range accessible. It was also noted that better performance is expected at a reactor source, where Kirkpatrick-Baez optics are more effective.

9.1.5 Holography instrument

A neutron holography instrument would use a novel technique based on recording the interference of neutron waves coherently scattered by atoms located within a material with a suitable reference wave. That is, a point source of spherical neutron waves within a material can be realized as a result of the extremely large value of the incoherent neutron scattering cross section of the proton. Hydrogen atoms embedded in a sample will emit spherical neutron waves as a result of incoherent scattering when the sample is placed in a monochromatic beam of cold neutrons. The interference between the undisturbed wave field and that part of the wave which is scattered by neighboring atoms can be recorded to produce a hologram. No one in the working group had much experience with this technique but we did produce a few comments and recommendations:

- This technique may be limited to the study of artificial structures and crystals that are not overly complex.
- Long-wavelength neutrons are needed to image engineered nanophase materials.
- Shorter-wavelength neutrons are needed to image atomic-level structure surrounding strong incoherent scatterers such as hydrogen (proteins).

- Neutron holography needs flux; there is no obvious advantage from using TOF methods.
- There is possibly an advantage to using a spallation source because of the ability to access nuclear resonances.

10.0 FUNDAMENTAL NEUTRON PHYSICS: WORKING GROUP REPORT

Chair: G. Greene (ORNL)

Participants: M. Arif (NIST), P. Ferguson (ORNL), P. Huffman, B. Micklich (ANL), M. Snow (Indiana U.)

10.1 Introduction

Cold neutrons and UCN have been employed in a wide variety of investigations that shed light on important issues in nuclear, particle, and astrophysics in the determination of fundamental constants and in the study of the fundamental symmetries of nature. In many cases, these experiments provide information that is not available from existing accelerator-based facilities and provide an important scientific opportunity. In recognition of this opportunity, the SNS allocated Flight Path 13 for the Fundamental Neutron Physics Beamline (FNPB). The initial proposals for experiments on the FNPB include a search for the neutron electric dipole moment, precision measurements of neutron beta decay, and studies of the hadronic weak interaction. These proposals represent efforts by more than 100 researchers at more than 30 institutions. This opportunity has also been identified in numerous programmatic planning documents [1], most recently in the Nuclear Sciences Advisory Committees Long Range Plan white paper [2] that explicitly highlights the search for both the neutron electric dipole moment and the elucidation of the parameters which describe neutron beta decay.

An intense pulsed source such as the SNS offers a particular opportunity for fundamental neutron physics. Measurements in this field are almost always significantly limited by statistical and systematic effects. A pulsed source offers a particular advantage in the identification of systematic errors, and the FNPB has been specifically designed with the reduction of such errors in mind. In general, the advantages of the SNS in reducing systematic errors lie in four main areas:

1. Utilizing the time structure of the beam to analyze background and to separate the signal from parasitic effects that have different velocity dependence *(important for the experiments that study the weak NN interaction via gamma asymmetry measurements and neutron spin rotation).*
2. Utilizing the time structure of the beam to make both precise and accurate determinations of neutron beam polarization with polarized ^{3}He gas cells *(important for the beta asymmetry measurements of the A and B correlation coefficients in neutron decay).*
3. Utilizing developments in neutron guide technology, particularly curved "benders" to transport the beam far away from other equipment and experiments without significant loss of flux, thereby reducing gamma-ray and neutron backgrounds. The proposed external UCN facility will be far from other instruments.
4. The design of an independent external experimental facility allows the opportunity to address seismic/vibration noise that is particularly important for some experiments with UCN.

10.2 Science Program at the Fundamental Neutron Physics Beamline

Because it is extremely difficult to predict the outstanding scientific opportunities 8–10 years hence, it is not possible to define, in detail, the beam characteristics required for fundamental neutron physics at STS. In the absence of such guidance, the best way to describe the beam line needs at STS is to review the current FNPB research program. This program represents nearly a projected decade's worth of activities that provide the best current "snapshot" of the opportunities for fundamental neutron physics.

For the purposes of beam line requirements, it is convenient to consider three classes of fundamental neutron physics experiments proposed for the FNPB:

1. "High integrated flux" experiments

   Experiments in this class are capable of accepting a large cross section beam (on the order of 10 cm) with relatively high divergence. Examples of this type of experiment include the $n+p \rightarrow d+\gamma$ experiment, the $n+p \rightarrow d+\gamma$ experiment, and the n+He spin rotation experiment.

2. "High brightness" experiments

   Experiments in this class are optimized with a small (on the order of ~2 cm) well-collimated beam. In many cases, the FOM for such experiments is given by the neutron capture flux; thus these experiments favor a colder beam. Examples of this type of experiment include abBA, Nab, and PANDA

3. "Ultracold" beam experiments.

   While the SNS does not have the capability to produce beams of UCN, there are several proposed experiments which accept neutrons with a wavelength of ~8.9 Å and convert them to UCN in the experimental apparatus. Such experiments benefit from a large–cross-section, large-divergence beam. The long wavelength also implies that the coldest available moderator would be preferred. Experiments of this type include the search for a neutron electric dipole moment and the measurement of the neutron lifetime.

10.3 Opportunities at STS

The opportunities for fundamental neutron physics at STS will depend heavily on the beam intensity and character of the source moderator system. For experiments that can accept a broad spectrum, the effect of a lower repetition rate will, to some extent, be compensated by the fact that the reduction of frame overlap problems will allow broader wavelength acceptance. Without consideration of detailed experiments, it is reasonable to assume that, for broad-wavelength experiments, STS will have a roughly similar capability to the FNPB.

However, for ultracold neutron experiments, there would appear to be a significant opportunity STS. If a fully optimized ballistic guide were installed and used exclusively for an experiment such as the current nEDM experiment, one could expect an increase in beam intensity of nearly an order of magnitude from improved optics alone [3]. If a fully optimized cold source were employed, an additional factor of ×4 could possibly be realized.[4] Such a 40-fold increase in flux would qualitatively change the science that is attainable at the SNS.

10.4 Summary

The detailed opportunities for fundamental neutron physics at STS will have to await the results from, and the evolution of, experiments now under way. However it seems likely that there will be emerging opportunities, and the scientific case for a pulsed cold beam for fundamental neutron physics should be considered as planning for STS is refined.

There appears to be a significant opportunity for an UCN beam line at STS. Such a beam line could provide significantly more than an order of magnitude higher flux at 8.9Å than is available at the FNPB and could transform the science at the SNS. This opportunity should be taken into consideration in the detailed design of STS.

10.5 References

1. R. Tribble, et al., *Report to the Nuclear Sciences Advisory Committee on Fundamental Physics with Neutrons* (2003).
2. M. Ramsey-Musolf, et al., *NSAC Long Range Plan, Fundamental Symmetries White Paper* (2007).
3. P. Huffman, private communication (2006).
4. P. Ferguson, private communication (2007).

APPENDIX: WORKSHOP PARTICIPANTS

Participant	Institution
Abernathy, Douglas	ORNL
Anderson, Ian	ORNL
Ankner, John	ORNL
Arif, Muhammad	NIST
Bauer, Günter	FZ Jülich
Bilheux, Hassina	ORNL
Bleuel, Markus	ANL
Brown, Craig	NIST
Carpenter, John	ANL
Chakoumakos, Bryan	ORNL
Coates, Leighton	LANL/ORNL
Crawford, R. Kent	ORNL
Cremer, Jay	Adelphi Techn.
Ehlers, Georg	ORNL
Ferguson, Phillip	ORNL
Galambos, John	ORNL
Gallmeier, Franz	ORNL
Granroth, Garrett	ORNL
Greene, Geoffrey	ORNL
Hagen, Mark	ORNL
Haines, John	ORNL
Herwig, Kenneth	ORNL
Hodges, Jason	ORNL
Hoffmann, Christina	ORNL
Huffman, Paul	N.C. State U.
Huq, Ashfia	ORNL
Iverson, Erik	ORNL
Khaykovich, Boris	MIT
Klose, Frank	ORNL
Lee, Wai-Tung (Hal)	ORNL
Littrell, Ken	ORNL
Lu, Wei	ORNL
Lumsden, Mark	ORNL
Majewski, Jarek	LANL
Majkrzak, Charles	NIST
Mamontov, Eugene	ORNL
Mason, Thom	ORNL
McGreevy, Robert	RAL
McManamy, Thomas	ORNL
Mezei, Ferenc	HMI
Micklich, Bradley	ANL
Mildner, David	NIST
Mook, Herb	ORNL
Myles, Dean	ORNL
Nagler, Stephen	ORNL
Neuefeind, Jörg	ORNL
Ohl, Michael	FZ Jülich
Pappas, Catherine	HMI
Penumadu, Dayakar	U. Tennessee
Popova, Irina	ORNL
Proffen, Thomas	LANL
Pynn, Roger	Indiana U.
Rekveldt, Matheus	TU Delft
Rheinstädter, Maikel	U. Missouri
Richardson, James	ANL
Robertson, Lee	ORNL
Rowe, John M.	NIST
Schultz, Arthur	ANL
Smith, Gregory	ORNL
Snow, William M.	Indiana U.
Stoica, Alexandre	ORNL
Taylor, Andrew	RAL
Thiyagarajan, Pappannan	ANL
Tulk, Chris	ORNL
van Vuure, Thorwald	ITU Karlsruhe
Wang, Xun-Li	ORNL
Wildgruber, Christoph	ORNL
Wilkinson, Angus	Georgia Tech
Zhao, Jinkui	ORNL